Award Number: W81XWH-12-2-0106

TITLE: "Characterization and Expression of Drug Resistance Genes in MDROs Originating from Combat Wound Infections"

PRINCIPAL INVESTIGATOR: Dr. Derrick E. Fouts, Ph.D.

CONTRACTING ORGANIZATION: J Craig Venter Institute
Rockville, MD 20850

REPORT DATE: September 2016

TYPE OF REPORT: Final

PREPARED FOR: U.S. Army Medical Research and Materiel Command
Fort Detrick, Maryland 21702-5012

DISTRIBUTION STATEMENT: Approved for Public Release;
Distribution Unlimited

The views, opinions and/or findings contained in this report are those of the author(s) and should not be construed as an official Department of the Army position, policy or decision unless so designated by other documentation.

REPORT DOCUMENTATION PAGE

Form Approved
OMB No. 0704-0188

1. REPORT DATE	2. REPORT TYPE	3. DATES COVERED
September 2016	Final	13Sep2012 - 12Jun2016

4. TITLE AND SUBTITLE
Characterization and Expression of Drug Resistance Genes in MDROs Originating from Combat Wound Infections

5a. CONTRACT NUMBER

5b. GRANT NUMBER
W81XWH-12-2-0106

5c. PROGRAM ELEMENT NUMBER

6. AUTHOR(S)
Dr. Derrick E. Fouts, Ph.D.
Dr. Agnes Chan, Ph.D.

email: dfouts@jcvi.org

5d. PROJECT NUMBER

5e. TASK NUMBER

5f. WORK UNIT NUMBER

7. PERFORMING ORGANIZATION NAME(S) AND ADDRESS(ES)

J. Craig Venter Institute
9714 Medical Center Dr.
Rockville, MD 20850

8. PERFORMING ORGANIZATION REPORT NUMBER

9. SPONSORING / MONITORING AGENCY NAME(S) AND ADDRESS(ES)
U.S. Army Medical Research and Materiel Command
Fort Detrick, Maryland 21702-5012

10. SPONSOR/MONITOR'S ACRONYM(S)

11. SPONSOR/MONITOR'S REPORT NUMBER(S)

12. DISTRIBUTION / AVAILABILITY STATEMENT
Approved for Public Release; Distribution Unlimited

13. SUPPLEMENTARY NOTES

14. ABSTRACT
Twenty-five multi-drug resistant organisms (MDROs) of high military importance were sequenced using the Illumina HiSeq platform to identify drug resistance and virulence mechanism contributing to their success as pathogens in the wound environment. A novel bioinformatics pipeline was used to incorporate genomic sequencing data obtained from multiple sequencing platforms with optical restriction map data to assemble the genomes into sequence contigs. Bioinformatics processes for the automated identification and classification of antibiotic resistance mechanisms and IS elements were developed to enable mapping of these features onto the genomes of the 25 selected MDROs. Preliminary investigations of IS element content showed considerable diversity and abundance levels across a collection of *Acinetobacter* genomes. Three top priority MDROs and three commensal microbes were chosen and obtained from WRAIR MRSN for *in vitro* co-culturing in confrontation assays aimed at investigating alterations in gene expression, particularly antibiotic resistance genes and virulence factors. Mock confrontations using *E. coli* and *S. aureus* controls have been conducted for the development of a new solid-media based confluent lawn co-culturing assay, and an RNA extraction protocol that is biologically reproducible. Human cell cultures to be used in bacterial-human cell confrontations have been received and grown successfully in the lab.

15. SUBJECT TERMS
Antibiotic resistance, whole genome sequencing, bacterial confrontation assays, qPCR, MDROs

16. SECURITY CLASSIFICATION OF:

a. REPORT	b. ABSTRACT	c. THIS PAGE	17. LIMITATION OF ABSTRACT	18. NUMBER OF PAGES	19a. NAME OF RESPONSIBLE PERSON USAMRMC
U	U	U	UU	57	19b. TELEPHONE NUMBER *(include area code)*

Table of Contents

INTRODUCTION

Antimicrobial resistance in bacterial pathogens is steadily increasing and recognized as one of the greatest threats to global public health. This is of particular concern to the Military Health System since recent wars in Afghanistan and Iraq resulted in a major spike in the number of wound and healthcare-acquired infections by bacteria resistant to three or more antibiotics (i.e., multi-drug resistant organisms, or MDROs). This study uses advanced genomic and bioinformatics approaches coupled to cell culturing to identify and characterize factors that influence virulence (including antibiotic resistance, and biofilm formation) in multidrug-resistant organisms (MDROs). This objective will be accomplished through experiments focusing on the regulatory responses of both target and challenger organisms in bacterial-bacterial and bacterial-eukaryotic interactions likely to occur in the wound environment. Deep next-generation cDNA sequencing is being used as a tool to dissect the regulatory networks altered during these organismal-level confrontations. Cell-cell challenges include: MDROs versus human microbiome organisms, MDROs versus other MDROs and MDROs versus the human host via cell culture. It is anticipated that there will be specific interacting partners that have a negative effect on MDRO virulence, while other interactors will induce the expression of genes involved in virulence. This project is being carried out in collaboration with the Walter Reed Army Institute of Research Multidrug-resistant Organism Repository and Surveillance Network (WRAIR MRSN), who have provided isolates of highest clinical importance collected from military health care facilities. The research outcome may lead to novel treatment of combat wound infections in the future.

BODY

We have fulfilled the deliverables as outlined in the proposed scope of work by 1) working closely with MRSN to establish the list of 25 MDRO isolates for genome sequencing; 2) sequencing the genomes of these isolates; 3) incorporating genomic sequence data and optical maps provided by MRSN in addition to our sequence data to generate the best possible assemblies (i.e., contiguous pieces of genomic sequence) and making the data publicly available; 4) selecting and obtaining three representative MDROs and three commensal bacterial isolates to be used in confrontation assays; 5) conducting bacteria:bacteria confrontation assays and analyzing the RNA-Seq results; 6) conducting MDRO:human dermal fibroblast (HDF) co-culture confrontation assays and analyzing the RNA-Seq results; and 7) submission of all raw RNA-Seq sequence reads to NCBI SRA public repository. The fulfillment of these deliverables resulted in the development of new bioinformatics tools that were applied to understand the diversity of Acinetobacter baumannii isolated from the military health system and the evolution of antimicrobial resistance of A. baumannii as presented in a publication in Genome Biology [1](**Appendix I**).

Aim 1. Months 1-6. Sequence characterization of 25 MDROs from WRAIR MRSN

Task 1a. MDRO bacterial isolate selection. Select 25 high priority clinically relevant MDRO isolates for genome sequencing. Selection will be based on recommendations by the WRAIR MRSN. Criteria include drug resistance profiles, prevalence in the military environment of care and/or wound infections, and novel phylogenetic patterns. WRAIR MRSN will provide to JCVI purified bacterial genomic DNA for whole genome sequencing for this task, and bacterial stock culture for co-culture assays in Tasks 2 and 3. **[Task COMPLETED]**

The MRSN specifically collects, characterizes and archives unique strains in order to avoid overlap or redundancy with other agencies such as the CDC, or SENTRY of JMI labs. From the MRSN collection, the strains that have been selected for this study have the highest clinical and military relevance as determined by active duty military physicians, infection preventionists, and microbiologists. Specifically, strains were selected on the basis of one or more or all of the following characteristics: 1) they were isolated in military medical treatment facilities (MTFs) in Afghanistan and Iraq, 2) they were obtained from fatal infections, 3) they were involved in serious outbreaks, 4) they were collected from wound infections, 5) they were paired isolates obtained from both wound and bloodstream or respiratory sites within the same patient, 6) and they were either extremely or pan-drug resistant (XDR/PDR), and/or they were resistant to the agent of 'last hope' for PDR infections. MTFs of origin include Combat Health Supports (CHSs) or Coalition Force Hospitals (CFHs) in

Afghanistan (AFG) and Iraq (IRQ); Level or Role IV referral centers in Europe, and Level or Role V MEDCENS in the Continental United States (CONUS). Genomic DNA samples of acceptable quantity and quality for all 25 MDROs were received by JCVI on December 18, 2012. The list of isolates as well as database accession numbers is listed in **Table 1**.

Table 1. List of High-Priority MDRO Isolates Sequenced in this Study

#	Sample ID	MTF	SITES	ISOLATION DATE	BIOPROJECT	BIOSAMPLE	WGS Master	ORGANISM	SOURCE	Comment
1	MRSN 3405	DC-Baltimore metro#2	LVL 5	3/29/12	PRJNA223610	SAMN02906922	JPIA00000000	*Acinetobacter baumannii*	WOUND	CO-S
2	MRSN 3527	DC-Baltimore metro#2	LVL 5	Apr-11	PRJNA223611	SAMN02906923	JPHZ00000000	*Acinetobacter baumannii*	WOUND	CO-S
3	MRSN 3942	DC-Baltimore metro#2	LVL 5	Jul-11	PRJNA223612	SAMN02906926	JPHY00000000	*Acinetobacter baumannii*	WOUND	CO-R
4	MRSN 4106	DC-Baltimore metro#2	LVL 5	Jul-11	PRJNA223613	SAMN02906927	JPHX00000000	*Acinetobacter baumannii*	WOUND	CO-R
5	MRSN 58	DC-Baltimore metro	LVL 5	Jun-10	PRJNA223614	SAMN02906928	JPHW00000000	*Acinetobacter baumannii*	WOUND	
6	MRSN 7339	DC-Baltimore metro	LVL 5	Sep-04	PRJNA223615	SAMN02906929	JPHV00000000	*Acinetobacter baumannii*	WOUND	respiratory-wound pair (MRSN 7341) from same patient
7	MRSN 7341	DC-Baltimore metro	LVL 5	Sep-04	PRJNA223616	SAMN02906930	JPIB00000000	*Acinetobacter baumannii*	RESPIRATORY	respiratory-wound pair (MRSN 7339) from same patient
8	MRSN 11489	SW US	LVL 5	8/30/12	PRJNA223617	SAMN03160298	JTEP00000000	*Enterobacter hormaechei*	WOUND	KPC+
9	MRSN 11248	SW US	LVL 5	8/6/12	PRJNA223618	SAMN03486506	LBLX00000000	*Enterobacter hormaechei*	WOUND	
10	MRSN 10204	SW US/San Antontio	LVL 5	7/18/12	PRJNA223619	SAMN03486507	LBLW00000000	*Escherichia coli*	WOUND	KPC+
11	MRSN 11639	DC-Baltimore metro#3	LVL 5	7/14/12	PRJNA223620	SAMN03486508	LBIN00000000	*Enterococcus*	WOUND	
12	MRSN 3418	DC-Baltimore metro#2	LVL 5	4/29/11	PRJNA223621	SAMN03486509	LBIM00000000	*Enterococcus*	WOUND	Vancomycin-resistant *Enterococcus* (VRE)
13	MRSN 4777	DC-Baltimore metro#2	LVL 5	10/9/11	PRJNA223622	SAMN03486510	LBIL00000000	*Enterococcus faecium*	WOUND	Sent as ACB but confirmed as *E. faecium*
14	MRSN 12230 (HE12)	Central America/Honduras	LVL 3	7/19/12	PRJNA223623	SAMN03486511	LBLV00000000	*Klebsiella pneumoniae*	WOUND	
15	MRSN 1319	DC-Baltimore metro	LVL 5	2/11/09	PRJNA223624	SAMN03160297	JSVB00000000	*Klebsiella pneumoniae*	WOUND	
16	MRSN 2404	DC-Baltimore metro	LVL 5	7/27/09	PRJNA223625	SAMN03486512	LBIK00000000	*Klebsiella pneumoniae*	WOUND	
17	MRSN 6902	SW US/San Antonio	LVL 5	2/21/12	PRJNA223626	SAMN03486513	LBLU00000000	*Klebsiella pneumoniae*	WOUND	KPC+
18	MRSN 8611	DC-Baltimore metro	LVL 5	2/7/04	PRJNA223627	SAMN03486514	LBIJ00000000	*Staphylococcus aureus*	BLOOD	blood-wound pair (MRSN 8613) from same patient
19	MRSN 8613	DC-Baltimore metro	LVL 5	2/12/04	PRJNA223628	SAMN03486515	LBII00000000	*Staphylococcus aureus*	WOUND	blood-wound pair (MRSN 8611) from same patient
20	MRSN 317	DC-Baltimore metro	LVL 5	6/9/10	PRJNA223629	SAMN03486516	LBIH00000000	*Pseudomonas aeruginosa*	WOUND	
21	MRSN 321	DC-Baltimore metro	LVL 5	7/29/10	PRJNA223630	SAMN03486517	LBIG00000000	*Pseudomonas aeruginosa*	WOUND	
22	MRSN 2154*	COALITION AFG-South	LVL 3	3/4/11	N.A.	N.A.	N.A.	*Providencia stuartii*	BLOOD	
23	MRSN 2761	DC-Baltimore metro	LVL 5	2/19/03	PRJNA223633	SAMN03486518	LBIF00000000	*Staphylococcus aureus*	WOUND	
24	MRSN 3562	DC-Baltimore metro	LVL 5	4/22/11	PRJNA223634	SAMN03486519	LBIE00000000	*Klebsiella pneumoniae*	BLOOD	blood-tissue pair (MRSN 3852) from same patient
25	MRSN 3852	DC-Baltimore metro	LVL 5	4/24/11	PRJNA223635	SAMN03486520	LBID00000000	*Klebsiella pneumoniae*	TISSUE	blood-tissue pair (MRSN 3562) from same patient

*Note, the finished genome was sequenced by WRAIR MRSN and deposited in GenBank separately.

Task 1b. Genomic library construction and whole genome sequencing. Construct barcoded standard Illumina libraries from bacterial genomic DNA and carry out library QC. Pool libraries and perform sequencing using the Illumina HiSeq sequencing platform. **[Task COMPLETED]**

We successfully completed library construction, and QC validation for all 25 isolates (**Figure 1, Table 2**). These results indicated that the libraries were of expected DNA insert size (~300-400 bp) and quantity (2,000 pM minimum) required for Illumina sequencing. Genomic DNA was submitted to the JTC (the JCVI sequencing facility) on January 7, 2013 with libraries completed on March 5, 2013. **This delay in library construction was due to a backlog of library construction requests in our sequencing facility.**
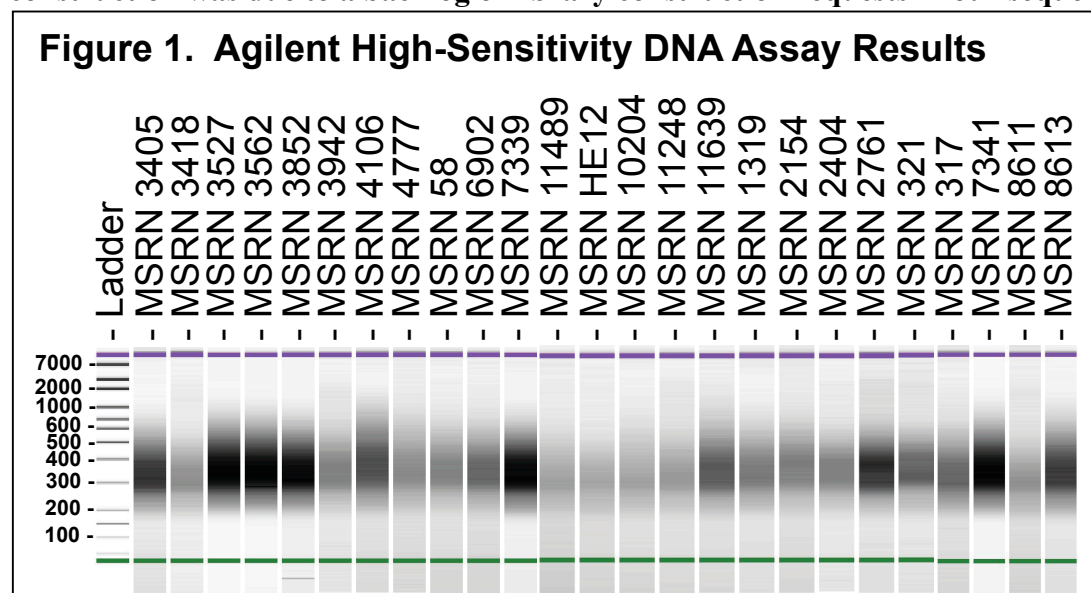

Figure 1. Agilent High-Sensitivity DNA Assay Results

Table 2. MDRO Library QC Summary

Sample ID	Library Name	Lib BC	Lib Size	Lib vol (uL)	Conc (pM)
MRSN 11489	11489-PE-IL1-1	2ZSYA	360	13.9	12,903
MRSN 10204	10204-PE-IL3-1	2ZSYC	381	13	17,821
MRSN 11248	11248-PE-IL4-1	2ZSYD	376	14.5	13,806
MRSN 11639	11639-PE-IL5-1	2ZSYE	436	11.8	33,103
MRSN 1319	1319-PE-IL6-1	2ZSYF	390	13.1	15,321
MRSN 2154	2154-PE-IL7-1	2ZSYG	421	16.9	14,156
MRSN 2404	2404-PE-IL8-1	2ZSYH	373	16	10,768
MRSN 2761	2761-PE-IL9-1	2ZSYI	392	18.7	22,170
MRSN 317	317-PE-IL10-1	2ZSYJ	392	14.7	12,959
MRSN 321	321-PE-IL11-1	2ZSYK	408	14.4	9,989
MRSN 3405	3405-PE-IL12-1	2ZSYL	349	12.6	29,267
MRSN 3418	3418-PE-IL15-1	2ZSYM	331	15.8	21,850
MRSN 3527	3527-PE-IL16-1	2ZSYN	365	15.1	37,619
MRSN 3562	3562-PE-IL20-1	2ZSYO	365	14.9	60,433
MRSN 3852	3852-PE-IL21-1	2ZSYP	360	14.7	27,448
MRSN 3942	3942-PE-IL23-1	2ZSYQ	361	13.1	13,922
MRSN 4106	4106-PE-IL24-1	2ZSYR	395	13	23,512
MRSN 4777	4777-PE-IL26-1	2ZSYS	372	13.8	13,501
MRSN 58	58-PE-IL27-1	2ZSYT	372	11.2	16,076
MRSN 6902	6902-PE-IL28-1	2ZSYU	365	17.2	15,256
MRSN 7339	7339-PE-IL29-1	2ZSYV	356	16.6	56,048
MRSN 7341	7341-PE-IL30-1	2ZSYW	419	17.6	55,981
MRSN 8611	8611-PE-IL40-1	2ZSYX	362	15.5	13,318
MRSN 8613	8613-PE-IL41-1	2ZSYY	395	18	27,301
MRSN HE12	HE12-PE-IL2-1	2ZSYB	350	10.4	11,164

Task 1c. Sequence assembly and mapping. *De-multiplex Illumina reads and carry out de novo assembly and reference-based assembly to obtain genome contigs for the MDRO bacterial isolates.*

We successfully obtained high-quality genomic sequence data from the Illumina HiSeq 2000 platform for the 25 selected MDRO bacterial isolates. The samples were loaded onto the HiSeq machine on April 1, 2013 and completed on April 13, 2013. **The delay getting the completed libraries loaded onto the sequencing machine was due to a backlog of sequencing requests in the JTC.** Raw reads were binned (de-multiplexed) by and trimmed of their corresponding Illumina MID, and reads were assembled into contigs initially using the Celera Assembler. We found that ~ 90-fold sequence coverage works best to produce high-quality assemblies from short-read Illumina data; therefore, a sampling of reads sufficient to produce 90-fold coverage (based on the predicted genome size) was used for genome assembly.

Genome quality of our sequencing data was monitored in two ways: read-based genome QC and assembly based metrics. The JCVI Genome QC pipeline samples sequence reads and performs BLAST-based protein and nucleotide searches against comprehensive non-redundant NCBI sequence databases. The results for all but 2 of the isolates matched their predicted bacterial species. The two that deviated from the predicted organism identity were MRSN 2761 and MRSN 4777. For MRSN 2761, it was originally determined to be *Staphylococcus haemolyticus*; however, BLAST analysis suggested that it was *S. aureus*. COL Lesho's group at MRSN subsequently confirmed that MRSN 2761 was indeed *S. aureus* based on the presence of a *S. aureus* (MRSA)-specific gene, *qacB* [2]. For MRSN 4777, it was originally identified as *Enterococcus faecium*, but BLAST results suggest that it is more likely a *Ralstonia* species. Analysis of the genome assembly metrics (total contig span and GC%) showed that only one genome, MRSN 4777, varied from expected values (Table 3). For *E. faecium*, the genome size should be ~ 3 Mbp with a GC% of ~ 33%; however, our assembly results indicated a predicted genome size (i.e., total contig span) to be ~5 Mbp with a GC% of ~65%, which matches closely with *Ralstonia* sp. (5.2 Mbp, 65% GC). MRSN 4777 was later confirmed by COL Lesho's group to be *E. faecium* by sub-culturing from the freezer stock archive on blood and McKonkey agar plates and taxonomic identification by the BD Phoenix Automated Microbiology System (Becton Dickinson), Vitek 2 (Biomerieux) and Microscan Walkaway 96 (Siemens) sytems. In addition, we have subsequently determined that the genomic sequence data was a mixture of a *Ralstonia* sp. and *E. faecium*. Complete GenBank reference genomes

were used to separate reads into bins belonging to these two distantly related microorganisms, one containing reads matching the *Ralstonia* reference (NCBI BioProject #PRJNA50545) and one containing reads matching the *Enterococcus* reference (NCBI BioProject #PRJNA87025). Reads from each bin plus reads that did not map either reference genome were *de novo* assembled using the Celera Assembler [3]. Even though the resulting MRSN 4777 *Enterococcus* assembly generated contigs with just 9.14-fold average sequence coverage, most of the reference genome was covered (red diagonal line, **Figure 2**).

Figure 2. Mapping of MRSN 4777 Contigs to *E. faecium* Reference

Enterococcus faecium Aus0004
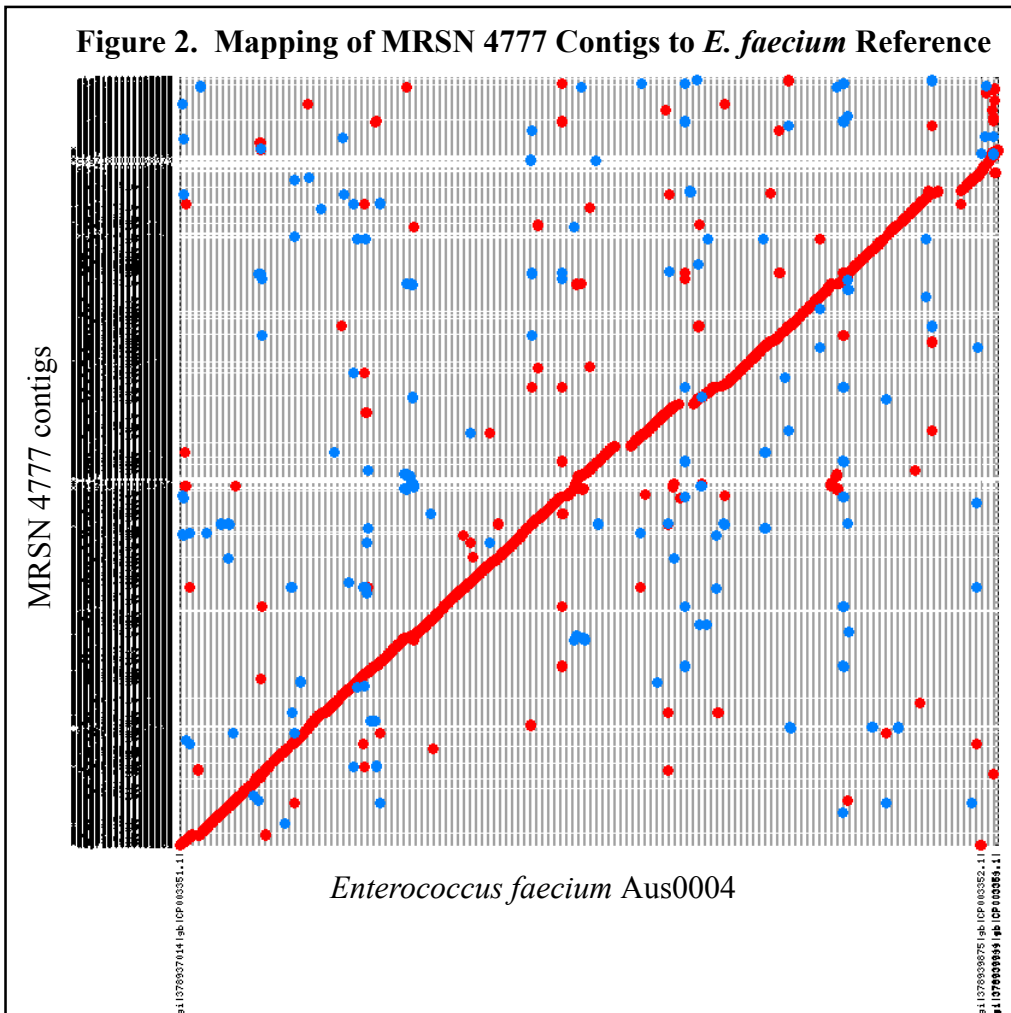
Though the assembly results were of good quality for Illumina-only data, we worked to improve upon these results by incorporating raw sequence data and optical maps that were generated by MRSN as described in our proposal. We had to establish an MTA in the form of a CRADA (fully executed on June 13, 2013) in order to obtain genomic sequence and OpGen optical restriction map data from WRAIR MRSN. **The CRADA with WRAIR took ~ 2 months to get established, delaying progress towards fulfilling this aim.** JCVI received a hard-drive from MRSN, containing genomic sequence reads and optical maps, on July 9, 2013. A JCVI in-house NextGen Sequence Assembly pipeline integrated the JCVI Illumina HiSeq data generated from this project (2x100 bp reads), the WRAIR MRSN reads generated from various platforms (Ion Torrent, Illumina MiSeq, and 454), and OpGen optical restriction maps. Overall, Auto Gap Closure improved the genome assemblies of all isolates by reducing the number of contigs, increasing the contig N50 and increasing the genome span. Optical maps improved assemblies by reducing the number of contigs by 1-7 contigs per genome. Nine of the fourteen genomes with optical map data had 75% or more of contigs placed on the restriction map. 454 Junior data supplied by MRSN contributed the most to gap closure; however, for at least one of the strains, MRSN 11489, the Ion Torrent 200bp reads aided automated closure of plasmids. This pipeline was described in our Genome Biology publication [1], **Appendix I**.

Task 1d. Months 4-6. Genome annotation and analysis. Run JCVI prokaryotic genome annotation pipeline to identify gene coding regions in the bacterial genome assembly. Identify genomic features associated with antibiotic resistance and generate multilocus sequence typing data. Submit Illumina reads, genomic sequence contig, gene annotation to the public NCBI databases. Share sequence and analyzed data with WRAIR. **[Task COMPLETED]** – MANUSCRIPT PUBLISHED IN GENOME BIOLOGY July 20, 2015 [1], Appendix I.

UPDATE: In a separate analysis funded by the NIAID Genome Centers for Infectious Diseases (GCID), we performed a large scale phylogenetic analysis of 379 *Enterobacter cloacae* complex strains (**Figure 3**). Data collected included the average nucleotide identity (ANI) of core genes, historical *hsp60* typing, and core single nucleotide polymorphisms (SNPs). From this analysis it was determined that the WRAIR would isolates MRSN 11248 and MRSN 11489 sequenced in this study originally thought to be *E. cloacae* should now be classified as *E. hormaechei* subsp. *oharae*. In addition, a third WRAIR isolate, MRSN 17626, not sequenced in this study also appears misclassified and now belonging to an unclassified *E. hormaechei* sp.

Figure 3: Phylogenetic SNP tree of *Enterobacter cloacae* complex genomes. A whole genome core SNP tree was constructed for 379 *Enterobacter cloacae* complex genomes using kSNP and RaXM). The asterisk indicates the *Enterobacter* genome used in confrontation assays.

Aim 1b. Months 6-12. Perform bacterial-bacterial confrontation assays to monitor bacterial cell interactions between MDROs and the human skin microbiome, and interactions between MDROs.

Task 2a. Months 6-9. Bacterial-bacterial confrontation assay. Select 3 MDRO isolates from Aim 1a and 3 common skin microbes. Propagate bacterial isolates on solid media. Set up biological replicates representing pairwise bacterial-bacterial co-culture between individual MDROs and skin microbes and between individual MDROs. Set up controls for self-self interactions for each bacterial species. Harvest bacterial cells from the co-culture assays. Repeat Task 2a for experimental replicates. **[Task COMPLETED]**

Three MDROs (*Acinetobacter baumannii* MRSN 7339, *Klebsiella pneumoniae* MRSN 1319, and *Enterobacter hormaechei* MRSN 11489) and three commensal organisms (*Staphylococcus epidermidis* SK-135, *Lactobacillus reuteri* SD2112 ATCC 55730 and *Corynebacterium jeikeium* ATCC 43734) were used in pair-wise confrontation assays as depicted in **Table 3**. We choose *L. reuteri* over *Propionibacterium acnes* because *P. acnes* is anaerobic, which is incompatible with growth requirements of the MDROs and remaining commensals.

Prior to commencing with confrontation assays, it was necessary to determine accurate growth curves of each organism so that equal numbers of actively dividing cells will be used in the co-culture assays. Growth curves for each organism were conducted in triplicate. *S. epidermidis* SK-135, *C. jeikeium*, *L. reuteri*, *A. baumannii* MRSN 7339 and *A. baumannii* MRSN58 were cultured in BHI broth. *L. reuteri* was cultured in MRS broth (**Figure 4**).
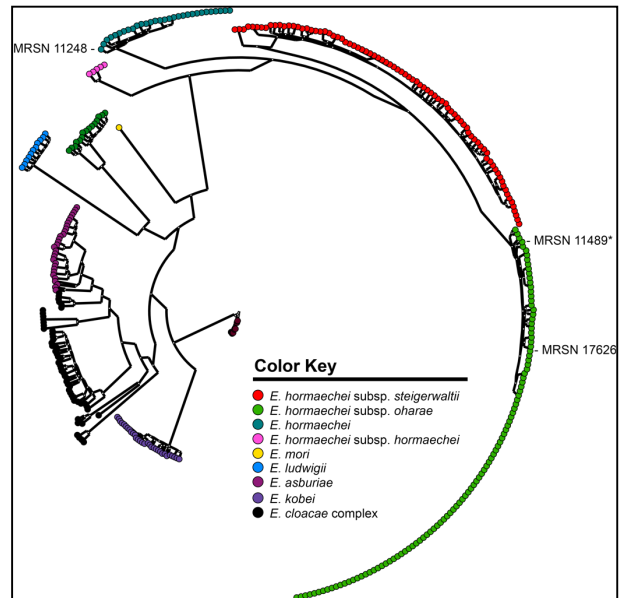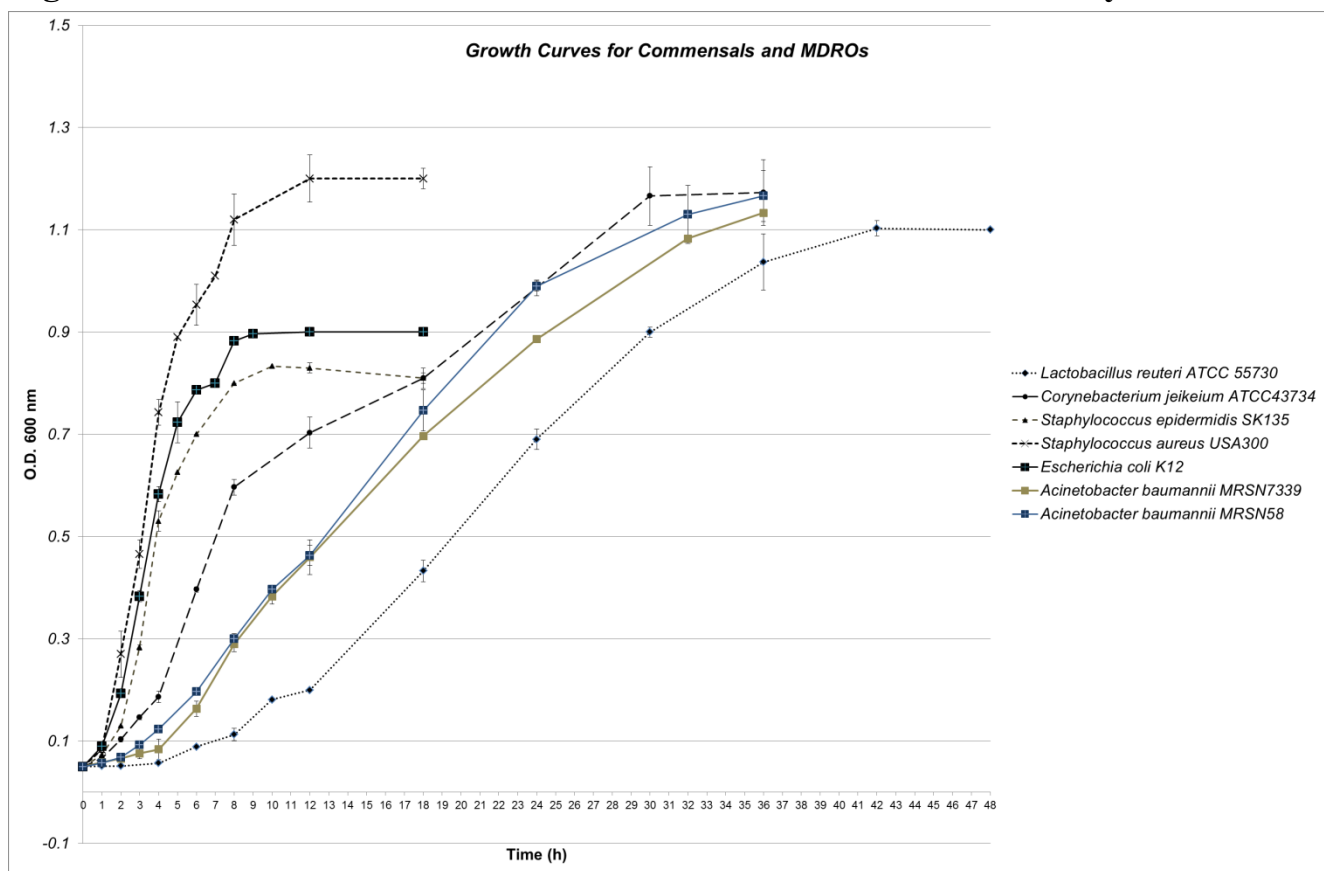
Figure 4. Growth Curves of selected microbes for confrontation assays

We have also established and validated our co-culturing plate method, and RNA extraction procedures. Our results showed that plate confrontations using previously proposed interlocking stamps for inoculation resulted in poor biological reproducibility. We have therefore developed a new approach by first mixing two bacterial liquid cultures to homogeneity prior to inoculation on a plate to produce a confluent lawn of growth. *E. coli* K-12 and *S. aureus* USA300 (Figure 3) were used in a control experiments to validate our co-culturing and RNA extraction methods since we already have gene expression data and complete genome sequences available for comparison. Quantitative PCR (qPCR) was used to measure relative gene expression of *S. aureus* USA300 genes that were up or down regulated in the presence of *E. coli* K-12, using *gyrB* as a constitutively expressed reference gene. Preliminary results showed that the new co-culture technique was reproducible across experimental replicates.

Table 3. Bacteria-Bacteria Confrontation Assays

Target Species		Commensal Controls	Challenger species		
			E. hormaechei	*K. pneumoniae*	*A. baumannii*
			EC	KP	AB
S. epidermidis	SE	SE:SE	EC:SE	KP:SE	AB:SE
L. reuteri	LR	LR:LR	EC:LR	KP:LR	AB:LR
C. jeikeium	CJ	CJ:CJ	EC:CJ	KP:CJ	AB:CJ
E. hormaechei	EC		EC:EC	KP:EC	AB:EC
K. pneumoniae	KP			KP:KP	AB:KP
A. baumannii	AB				AB:AB

Bacteria-bacteria confrontations. Commensal bacteria were obtained from ATCC/BEI Resources. *A. baumannii, K. pneumoniae, E. hormaechei*, and *S. epidermidis* were grown in BHI broth (BD) to a

9

concentration of 1 x 10^8 CFU/ml in log phase growth. *C. jeikeium* was grown to the same concentrations in BHI supplemented with 1% (vol/vol) Tween-80 (Fisher). For confrontations, equal amounts of cells from the cultures were combined and shaken at 37°C for 5 min at 200 RPM. 1 x 10^7 CFU of each confrontation were plated on to a BHI agar plate, each in triplicate. Plates were incubated at 37°C for 6 hours, at which point approximately 1 x 10^8 CFU from each triplicate plate were combined and treated with RNAprotect bacteria reagent (Qiagen) according to the manufacturer's instructions. Bacterial cells were spun down and the RNAprotect bacterial reagent removed after treatment. Cell pellets were stored at -80°C until RNA extraction.

Task 2b. Months 9-12. Bacterial RNA-Seq and gene expression analysis. Isolate total RNA and deplete bacterial ribosomal RNA from sample. Construct barcoded ssRNA-Seq libraries for Illumina sequencing. De-multiplex Illumina reads and carry out *de novo* and reference-based transcript assembly to reconstruct gene expression levels in the bacterial transcriptome during co-culture of the target and challenger species. **[Task COMPLETED]. *NOTE: A manuscript describing this work is being edited for submission*.**

RNA isolation. RNA was extracted using RNeasy Mini Kit (Qiagen). The manufacturer's protocol was followed with a few additional steps. Enzymatic lysis was performed on cell pellets when resuspended in TE with 15 mg/ml lysozyme (Fisher) and 3 mg/ml Proteinase K (NEB) and incubated for 10 min at room temperature with vortexing for 10 s every 2 min. After enzymatic lysis, mechanical lysis was performed by adding buffer RLT with 1% vol/vol 2-mercaptoethanol and transferring the lysate to a Lysis Matrix B bead beating tube (MP bio). Samples were homogenized for 45 s at 6.5 m/s on a FastPrep120 Cell Disrupter System. On-column DNAse treatment (Qiagen) was used according to the manufacture's protocol. Isolated RNA was treated with TURBO DNase (Ambion) following the manufacture's protocol.

Library preparation for Illumina sequencing. Enrichment for mRNA was done using the RiboZero rRNA Removal Kit for bacteria (Epicentre). Libraries were constructed from up to 10 ng of mRNA using the NEBNext Ultra Directional RNA Library Prep Kit (NEB) following the manufacturer's protocol. Libraries were normalized for sequencing using qPCR (Kapa Biosystems Library Quantification Kit). The resulting libraries were sequenced on the Illumina HiSeq platform (2x100 bp).

RNA-Seq data analysis. Illumina sequencing reads in FASTQ format were analyzed using CLC Genomics Workbench version 6.5 (http://www.clcbio.com) after trimming for low quality reads (CLC quality score limit = 0.05, maximum of 2 ambiguities), reads less than 50 bp and adaptors. Known 4,692 distinct rRNA sequences were collected from SILVA database (http://www.arb-silva.de/) for all five species of bacteria used in confrontations and mapped using BWA [4] allowing up to three mismatches. Reference files for RNA-Seq analysis were prepared from Genbank files imported into CLC (Table 1). All rRNA reads were removed from further analysis, leaving only non-rRNA reads for normalization and analysis. For each control and co-culture experiment, the expected genomes were selected and reads were mapped using the following setting: maximum number of mismatches = 2, minimum length fraction = 0.8, minimum similarity fraction = 0.98, maximum number of hits for a read = 10, minimum and maximum distances for paired reads =1,1000 and counting scheme of "include broken pairs". The expression values were measured in RPKM (Reads Per Kilobase Per Million mapped reads). For confrontations, RPKM values must be adjusted since the denominator for the normalization is the sum of reads mapped to any of the two genomes. The adjustment formula for the RPKM value for a gene in species A is: (RPKM_adjusted_in_A = RPKM_in_A * (N_A+N_B) / N_A) where N_A = total number of reads mapped to genome A, and N_B = total number of reads mapped to genome B. The total gene reads were used as raw read count to determine up or down regulated genes using default settings in EdgeR ((http://bioconductor.org) [5].

All raw Illumina sequence read data was deposited into the NCBI SRA (Table 4). NCBI enables Biosamples to be linked to more than one Bioproject so that if a researcher is interested in, for example *L. reuteri*, they will have access to every Biosample (i.e., experiment involving *L. reuteri*), by selecting the *L. reuteri* Bioproject. Confrontations (i.e., Biosamples) between *L. reuteri* and other bacteria will also be linked via the Bioprojects of

the confronting organism. We have linked Biosamples to multiple Bioprojects, which are now neatly housed under one "umbrella" Bioproject (**Table 4**).

Table 4. Confrontation Raw Reads Deposited in the NCBI SRA

	Biosample_id	Experiment_id	Confrontations	Biological Replicate	BioProject id
Bacterial - Bacterial Confrontation Expe	SAMN04532757	ABABA	*A. baumannii* only	1	292770
	SAMN04532758	ABABD	*A. baumannii* only	2	292770
	SAMN04532759	ABCJA	*A. baumannii* vs. *C. jeikeium*	1	292770
	SAMN04532760	ABCJD	*A. baumannii* vs. *C. jeikeium*	2	292770
	SAMN04532761	ABECA	*A. baumannii* vs. *E. hormaechei**	1	292770
	SAMN04532762	ABECD	*A. baumannii* vs. *E. hormaechei**	2	292770
	SAMN04532763	ABKPA	*A. baumannii* vs. *K. pneumoniae*	1	292770
	SAMN04532764	ABKPD	*A. baumannii* vs. *K. pneumoniae*	2	292770
	SAMN04532765	ABLRA	*A. baumannii* vs. *L. reuteri*	1	292770
	SAMN04532766	ABLRD	*A. baumannii* vs. *L. reuteri*	2	292770
	SAMN04532767	ABSEA	*A. baumannii* vs. *S. epidermidis*	1	292770
	SAMN04532768	ABSEG	*A. baumannii* vs. *S. epidermidis*	2	292770
	SAMN04532769	CJCJA	*C. jeikeium* only	1	294781
	SAMN04532770	CJCJD	*C. jeikeium* only	2	294781
	SAMN04532771	CJECA	*C. jeikeium* vs. *E. hormaechei*	1	294781
	SAMN04532772	CJECD	*C. jeikeium* vs. *E. hormaechei*	2	294781
	SAMN04532773	CJKPA	*C. jeikeium* vs. *K. pneumoniae*	1	294781
	SAMN04532774	CJKPE	*C. jeikeium* vs. *K. pneumoniae*	2	294781
	SAMN04532775	ECECA	*E. hormaechei** only	1	292777
	SAMN04532776	ECECD	*E. hormaechei** only	2	292777
	SAMN04532777	ECKPA	*E. hormaechei** vs. *K. pneumoniae*	1	292777
	SAMN04532778	ECKPD	*E. hormaechei** vs. *K. pneumoniae*	2	292777
	SAMN04532779	ECLRA	*E. hormaechei** vs. *L. reuteri*	1	292777
	SAMN04532780	ECLRD	*E. hormaechei** vs. *L. reuteri*	2	292777
	SAMN04532781	ECSEA	*E. hormaechei** vs. *S. epidermidis*	1	292777
	SAMN04532782	ECSEG	*E. hormaechei** vs. *S. epidermidis*	2	292777
	SAMN04532783	KPKPA	*K. pneumoniae* only	1	292776
	SAMN04532784	KPKPD	*K. pneumoniae* only	2	292776
	SAMN04532785	KPLRA	*K. pneumoniae* vs. *L. reuteri*	1	292776
	SAMN04532786	KPLRD	*K. pneumoniae* vs. *L. reuteri*	2	292776
	SAMN04532787	KPSEA	*K. pneumoniae* vs. *S. epidermidis*	1	292776
	SAMN04532788	KPSEG	*K. pneumoniae* vs. *S. epidermidis*	2	292776
	SAMN04532789	LRLRA	*L. reuteri* only	1	294773
	SAMN04532790	LRLRD	*L. reuteri* only	2	294773
	SAMN04532791	SESEI	*S. epidermidis* only	1	294780
	SAMN04532792	SESEJ	*S. epidermidis* only	2	294780
Bacteria - HDF Cell Confrontati	SAMN04532793	AB3	*A. baumannii* no human cells	1	292770
	SAMN04532794	AB8	*A. baumannii* no human cells	2	292770
	SAMN04532795	EC3	*E. hormaechei** no human cells	1	292777
	SAMN04532796	EC8	*E. hormaechei** no human cells	2	292777
	SAMN04532797	KP3	*K. pneumoniae* no human cells	1	292776
	SAMN04532798	KP8	*K. pneumoniae* no human cells	2	292776
	SAMN04534817	HDF1	HDF cells only	1	314266
	SAMN04534818	HDF4	HDF cells only	2	314266
	SAMN04534819	ABHDF1	*A. baumannii* vs HDF cells	1	314266
	SAMN04534820	ABHDF6	*A. baumannii* vs HDF cells	2	314266
	SAMN04534821	ECHDF1	*E. hormaechei* vs HDF cells	1	314266
	SAMN04534822	ECHDF6	*E. hormaechei* vs HDF cells	2	314266
	SAMN04534823	KPHDF1	*K. pneumoniae* vs HDF cells	1	314266
	SAMN04534824	KPHDF6	*K. pneumoniae* vs HDF cells	2	314266

* MRSN 11489, originally named E. cloacae, has been renamed to *E. hormaechei* subsp. *oharae*

Reverse Transcription and qRT-PCR. Reverse transcription (RT) was performed to generate cDNA from both biological replicates to be used in qRT-PCR for validation of RNA-Seq data. RNA concentrations were determined with an Agilent 2100 Bioanalyzer and 1.5 µg of total RNA were used in each reaction. RNA was incubated in 18.5 µl with 6 µg of random hexamers (Invitrogen) and 40 U of RNaseOUT (Invitrogen) at 70°C for 10 min, followed by snap cooling on ice. Then the reaction was brought to 1X First Strand Buffer, 10 mM DTT, 0.5 mM dNTPs (Invitrogen), and 400 U SuperScript® III Reverse Transcriptase (Invitrogen) in 30 µl. The reaction was incubated in a 42°C water bath for 16 h. and then reaction was stopped and RNA was hydrolyzed with 0.1 M EDTA and 0.2 M NaOH at 65°C for 12 min. Tris-HCl (pH 7.0) was added to neutralize the pH. Purification of cDNA was achieved by using QIAquick PCR Purification kit (Qiagen) following the manufacturer's protocol and quantitated by fluorometric assays using SYBR Gold (Invitrogen).

qRT-PCR reactions were performed with 10 ng of template cDNA in 10 µl triplicated reactions with SYBR Green Master Mix (Roche) in 384-well plates on the LightCycler480 qPCR instrument (Roche). Cycling conditions were 95°C for 10 min followed by 50 cycles of 95°C for 20 s, 58°C for 30 s, and 72°C for 15 s. A melting curve analysis was performed after all cycles were completed to verify the Tm of amplified products. No-RT controls and qPCR control reactions were performed as well. To determine the CP for each reaction, the 'Fit Point Method' was performed in the LightCycler480 software 1.5.0 (Roche Diagnostics). Efficiency for each primer was optimized by adjusting primer concentration and was determined for the reaction conditions. Efficiency and CP values were used to calculate the gene expression with normalization to *gyrB*. Relative expression ratios were determined by comparing co-culture samples with monoculture samples using the method described previously [6]. Primer sequences and concentrations used are in **Table 5**.

Table 5. Sequence and concentration of qPCR primers used

Target Gene	Primer Name	Primer Sequence	Concentration of primer in qPCR reactions
A. baumannii primers			
DNA gyrase, B subunit	T634_0013 Fwd	TGAGCTTGCTTTACATATTAGTGCT	0.2 uM
	T634_0013 Rvs	ACTTCGAGTAATGCATCCAGTAAG	
conserved hypothetical protein	T634_0987 Fwd	GCGAGCCATACCGTTTACTAT	1 uM
	T634_0987 Rvs	AAGTGTACCCGCACCATAATTT	
ethylmalonate-semialdehyde dehydrogenase	T634_0140 Fwd	TGAAGAAGTCGACGCTGCTA	0.5 uM
	T634_0140 Rvs	TCAGCCGTCAATACTTGTGC	
aldehyde dehydrogenase (NAD) family protein	T634_2358 Fwd	AAAGCTTCATGGAATAAATCTTCAC	0.2 uM
	T634_2358 Rvs	AAGGTCAGCTGCTAAAGTTTCAC	
PapD pilus/flagellar-assembly chaperone N-terminal domain	T634_2490 Fwd	CCAAATGCGTTACTCAATTCC	0.5 uM
	T634_2490 Rvs	AGCTCAGACTGGCCTTGTTG	
Hpt domain protein	T634_3235 Fwd	ATCTTAATATTTGGGTAGGTGAGCA	0.2 uM
	T634_3235 Rvs	AACGCTCATAGATGCTTTCTAATTC	
EamA-like transporter family protein	T634_3500 Fwd	GCAATATGTGACTGCGGTTG	0.5 uM
	T634_3500 Rvs	TCTCCACTGACCACCAACAC	
fimbrial assembly protein PilN	T634_3585 Fwd	CGTCCAGTAGTGGTAAGACTTG	0.2 uM
	T634_3585 Rvs	GGAGTAGTTCGGCTACTGTATTT	
K. pneumoniae primers			
PTS system fructose IIA component	T643_A0079 Fwd	TTTGCCGGTAGCGTGAATA	1 uM
	T643_A0079 Rvs	CGTTTGTTAATGCCTCGGTAAT	
SIS domain protein	T643_A0084 Fwd	CAGGACGAGTACCTGACCAGT	1 uM
	T643_A0084 Rvs	CAAATTCATTAATTGCCATCATC	
citrate/malate transporter	T643_A0191 Fwd	AGCTGGCTAACGTGGTGTCT	1 uM
	T643_A0191 Rvs	TGAAGGCGTTTACCAGTTCC	
aconitate hydratase 2	T643_A0266 Fwd	ATAGCCACAAAGGCCAACTG	1 uM
	T643_A0266 Rvs	ACCCATACACAGGGAACAGC	
nitrite extrusion protein 1	T643_A2635 Fwd	GCCTTATTACGCGTGCCTTA	1 uM
	T643_A2635 Rvs	GATGCTAAACGGCGTAGAGG	
4-aminobutyrate transaminase	T643_A4354 Fwd	CATCTGCAGGAAGTGCTCAA	1 uM
	T643_A4354 Rvs	GTTCTCCTGCGCTTTCTGTT	
DNA gyrase, B subunit	T643_A4645 Fwd	CTGTTGACCTTCTTCTATCGTCAG	1 uM
	T643_A4645 Rvs	GATGGAGATCTGATACTGATCCA	

Response of A. baumannii

The response of *A. baumannii* co-cultured with *K. pneumoniae*, *E. hormaechei* or *C. jeikeium* is illustrated in Figure 5, panel A-C.

Upregulated genes. There are only 28 commonly upregulated genes when *A. baumannii* was in co-culture with *K. pneumoniae, E. hormaechei* or *C. jeikeium*. We also observed the differential regulation of some genes common to all confrontations suggesting a general stress response or growth phase associated gene expression.

In co-culture with *K. pneumoniae*, of the 190 *A. baumannii* genes upregulated, only 49 of these were specific to this confrontation (see **Figure 5, Panel A**). Among the 49 uniquely upregulated genes specific to the confrontation with *K. pneumoniae*, 8 flexible Genomic Island (fGI) classified genes were identified of which three are phage associated, one is fGI, *comM* [1] and the remaining of unknown function, with one protein identified as the carbon starvation protein CstA. Other uniquely upregulated genes include genes associated cell envelope, other cellular processes, energy metabolism and one Ton-B-dependent siderophore receptor, efflux and ABC type transporters and some hypotheticals.

With the *E. hormaechei* co-culture, 160 *A. baumannii* genes were upregulated, of which only 35 were specific to this bacterial confrontation. The 35 uniquely upregulated genes specific in confrontation with *E. hormaechei* include: two fGI genes that appear to be involved in energy metabolism (succinylornithine transaminase/acetylornithine aminotransferase domain protein and arginine N-succinyltransferase), eight transport and binding family proteins that include Ton-B dependent receptors, ABC transporters and some iron-chelate and siderophore interacting proteins.

Figure 5. Genes differentially expressed (DE) in bacterial confrontations. DE is defined as a FDR of < 0.05. Left panels are counts of *A. baumannii* DE genes when confronted with *C. jeikeium* (pink circle), *E. hormaechei* (yellow circle), or K. pneumoniae (red circle). Right panels are counts of *K. pneumoniae* DE genes when confronted with *C. jeikeium* (pink circle), *E. hormaechei* (yellow circle), or A. baumannii (blue circle). The lower figure legend classifies the genes in the pie charts. Pie charts show the breakdown of DE gene types that are uniquely regulate in the confrontations. Cellular processes- Biosynthesis of cofactors, prosthetic groups and carriers, Fatty acid and phospholipid metabolism, Amino acid biosynthesis, DNA metabolism, Central intermediary metabolism, Purines, pyrimidines, nucleosides, and nucleotides, Transcription; Unknown function- Hypothetical proteins, Unclassified, Null; Non-coding RNAs-tRNA, ncRNA, tmRNA.

The most number of differentially regulated genes in any confrontation was observed when *A. baumannii* was co-cultured with the commensal *C. jeikeium* and in this confrontation, 185 genes were differentially expressed of which 141 genes were unique to this confrontation. About half of these are categorized as hypotheticals or unknown function, but in contrast to the MDRO-MDRO confrontations, we observed specific upregulation of regulatory functions and cell envelope related functions. More fGI and fGI phage genes were also differentially expressed in this particular co-culture. Most of these (12) are hypothetical proteins, but also includes a cold shock protein CspE and CRISPR associated proteins. One distinct phenomenon was the upregulation of Type IV pili genes only observed in the AB-CJ confrontation.

Of the highest upregulated genes (> 1.5 log FC), 20 were in specific response to *E. hormaechei* (**Figure 5, panel B**) There are genes of transport and binding category, including some TonB –dependent receptors and ABC transporters, and the remaining appear to be involved in energy metabolism and other cellular processes. No acquired antibiotic resistance genes were induced. In contrast to the strong response of *K. pneumoniae* to *A. baumannii*, the response of *Acinetobacter* towards *Klebsiella* appears to be mild with only 10 highly upregulated
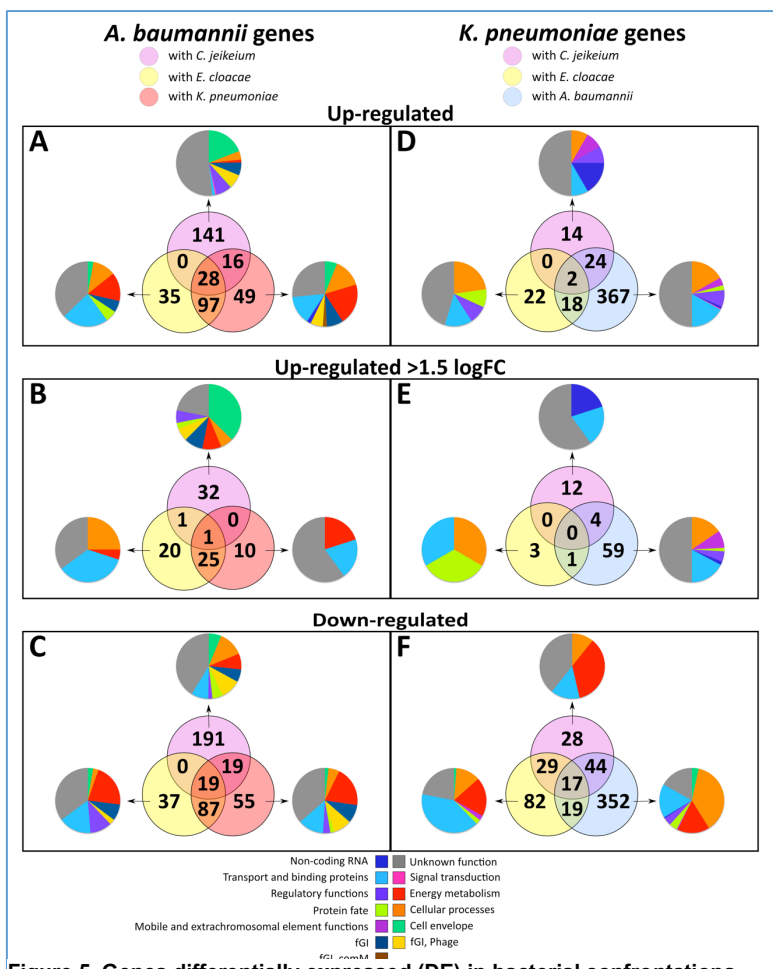
genes. These include proteins of unknown function, ABC transporter family, and one protein annotated as a spore coat protein (T634_2491). A BLASTp search and protein threading (using Phyre v2.0) [7] of this sequence shows that it is has a cell adhesion or protein binding domain, but its function remains unknown. Of the 32 genes highly upregulated in AB-CJ confrontation, one interesting trend is the upregulation of a number of genes related to pili and fimbrial assembly. Also induced are three genes belonging to the same fGI, of which two can also be linked with a cell envelope related role.

We observed differential regulation of the siderophore cluster 3, Acinetobactocin biosynthesis and transport including the Fur regulated the *bau* genes occur in both *A. baumannii-E. hormaechei* and *A. baumannii-K. pneumoniae* confrontation, but the fold induction was 1.5-2 fold, specifically in the *A. baumannii-E. hormaechei* confrontation (**Appendix II**). From previous studies it is evident that Acinetobactin (high-affinity iron chelator) synthesis is essential for growth *in vitro* in iron-limiting conditions as well as for persistence in the human host and for successful virulence in model *in vivo* infection systems [8]. In the *A. baumannii-E. hormaechei* co-culture we also observed upregulation of the Aerobactin biosynthesis proteins and TonB siderophore receptor, suggesting that these organisms were creating iron-limiting conditions in the co-culture requiring the production of iron uptake systems for survival, similar to conditions that may occur during infection in the host.

Two of the most highly upregulated genes we observed in *A. baumannii* are aldehyde dehydrogenase and an-iron dependent alcohol dehydrogenase. These genes were upregulated 3.6 fold against both MDROs and 1-fold against *C. jeikeium* although the induction in this case is not specific to the presence of ethanol in the medium, unless it was produced by the co-culture participant. Presence of low concentrations of ethanol favors growth of *A. baumannii* and induces *ompA*, and also elicits a global stress response, increasing salt tolerance, increasing virulence against potential competitors or predators in the environment, induction of proteins to protect against oxidative stress, and molecular chaperones to prevent protein misfolding. This is similar to the response seen from presence of reactive oxygen species and presence of antibiotics. Ethanol also induces lipid biosynthesis genes that may correlate with membrane biogenesis and the formation of biofilm structures as another environmental stress response [9].

Downregulated genes. Only 19 genes are commonly downregulated when AB confronts each of the other MDROs and the commensal (**Figure 5 Panel C**). Of the 180 genes downregulated in response to *K. pneumoniae*, only 55 are specific to this co-culture. There was no striking functional class of genes that was downregulated and included some fGI genes, but also unknown function, energy metabolism, transport and binding and genes in categories that were also upregulated. When in co-culture with *E. hormaechei*, only 37 of the 143 genes downregulated were specific to this confrontation, and there was no distinctive pattern of downregulation of a particular functional category. In both these cases, the energy metabolism genes that were downregulated appear to be those that would not be beneficial to the particular environment, unlike the metabolic pathways that could be induced for competitive growth and survival against competing bacteria under limited nutrient conditions.

Similar to the trend of upregulated genes of *A. baumannii* in response to *C. jeikeium*, 229 genes were downregulated, of which almost all (191) were specific to this confrontation. Several of these are of unknown function, but we also observed an increased number of protein transport and processing, cell envelope related genes, transport and binding proteins, and those categorized as involved in cellular processes. In the latter category are genes like CsuE, universal stress proteins, and a β-lactamase. Genes associated with iron scavenging were distinctly downregulated in the *A. baumannii-C. jeikeium* confrontation.

The Csu chaperone system associated with Type I pili formation was upregulated only in the *A. baumannii-K. pneumoniae* confrontation about 1.5 fold, while distinctly downregulated almost 3 fold when co-cultured with *C. jeikeium*. The *csu* operon is thought to be relevant for adherence and formation of biofilm on abiotic surfaces in *A. baumannii* ATCC 19606T, but not for human respiratory cells [10]. Biofilm formation in *A. baumannii* has been extensively studied and several factors critical for this phenomenon have been identified-Csu encoding genes, *ompA* (homologous to *bap* in Staphylococcus), autoinducer synthase AbaI, a part of the quorum sensing system [11], and *pgaABCD* operon responsible for production of PNAG (poly-β-1,6-N-acetylglucosamine) have been proposed as critical for biofilm formation [12]. Type IV pili (TFP) genes were upregulated only in the *A. baumannii-C. jeikeium* confrontation. These pili are associated with natural transformation, twitching mobility, and biofilm formation [13]. The deletion of TFP retraction gene *pilU* and *pilT*

leads to reduction in biofilm formation, indicating that fully functional TFP are required for biofilm production in strain *A. baumannii* ATCC 17978 [14]. Suggesting that *A. baumannii* may form biofilms with *C. jeikeium*.

Response of *K. pneumoniae*
Many of the differentially regulated genes in *K. pneumoniae* indicate a general stress response- induction of phage and transposon genes, universal stress proteins, DNA damage repair, and stationary phase stress response [15-17] (**Appendix III**). Studies also implicate a connection between environmental stressors, phage induction and biofilm formation [18], [19]. The induction of BhsA (putative multiple stress resistance protein) may be another indication of stress in the growth environment. In *Escherichia coli* it is also annotated as YcfR and is known to encode a putative outer membrane protein, and induced in *E. coli* biofilms and during stress conditions. The deletions of this multiple stress resistance protein can make the cell more sensitive to acid, heat, H_2O_2, and cadmium. YcfR was observed to be involved in the regulation of *E. coli* K-12 biofilm formation and hence it has been proposed that that this locus be named *bhsA*, for influencing biofilm through hydrophobicity and stress response [20]. Some of the responses might confer K. pneumoniae with some growth advantage like the upregulation of PQQ may allow participation in diverse carbon utilization pathways. The anti-restriction protein ArdA upregulated against *A. baumannii* may prime the organism for DNA uptake. These ArdA proteins and type I R-M systems are more frequently discovered through genome sequencing in several bacteria and is hypothesized to be involved in the regulation of gene transfer among bacterial genomes [21].

Upregulated genes. *K. pneumoniae* appears to respond strongly to *A. baumannii* and this is evident from the number of genes that were upregulated (411) (**Figure 5, panel D**). Of these, 367 genes are unique to the *A. baumannii* confrontation. We identified biofilm regulatory proteins BssS (T643_A0534), LuxR family transcriptional regulators, an inhibitor of vertebrate lysozyme, toxin RelE, plasmid stabilization protein RelE/ParE family, universal stress family proteins, a multiple stress resistance protein BhsA, a protein that provides DNA protection during starvation, the cell division inhibitor protein SulA, MarR associated with drug resistance [22], competence/damage inducible protein CinA, Ton-B associated receptors, hemin binding proteins and iron chelate associated proteins, a protein associated with toxin-antitoxin system, a conjugal transfer entry exclusion protein of the TraS family, quaternary ammonium compound-resistance protein SugE, a DDE domain protein [23]. In the co-culture with *E. hormaechei*, *Klebsiella* showed a moderate response compared with its response to *Acinetobacter* and upregulates only 42 genes. Of the 22 genes that are uniquely upregulated there is a component of a toxin-antitoxin system, universal stress proteins, Fe SOD, hemolysin expression modulating protein, an O-antigen biosynthesis protein WbnF. The response to *C. jeikeium* was also comparably mild; only 40 genes were upregulated, of which 14 were unique to this confrontation and include transport and binding proteins, some proteins of unknown function, DNA repair UmuD and a Type I restriction enzyme like domain protein.

There are 59 genes induced specifically (> 1.5 log FC) in response to *A. baumannii* (**Figure 5, panel E**). Most of these were of unknown function. Other categories represented include metabolism, general cellular processes, transport and binding, mobile and extra-chromosomal elements, some factors associated with regulatory functions and protein fate. Some phage related proteins were also upregulated. *K. pneumoniae* also induces the multiple stress resistance protein BhsA when in contact with the MDRO *Acinetobacter* and upregulates the expression of PQQ, and the anti-restriction protein ArdA. Pyrroquinoline quinone is a low molecular weight redox active cofactor for bacterial dehydrogenases not required for bacterial survival, but can enhance the rate of cell growth by participating in carbon utilization pathways. *K. pneumoniae* has a demonstrated ability to produce PQQ and this is accomplished by the *pqq* operon comprising of six genes *pqqA-F* [24] [25]. The TonB dependent and heme transport systems are also significantly upregulated (3-5 fold). *K. pneumoniae* showed a milder response to *C. jeikeium* compared with its reaction to *A. baumannii* with only 12 specifically induced genes- tRNAs, hypotheticals and few categorized as transport and binding proteins (phosphate transport system/ PTS components). Only three genes were uniquely upregulated in response to *E. hormaechei* - a sodium transporter, universal stress protein and Hsp20 related to proteins fate.

Downregulated genes. The downregulation of *K. pneumoniae* genes is shown in **Figure 5, panel F**. In response to the MDRO *E. hormaechei*, 147 genes were downregulated, of which 82 were specific to this confrontation. More than a third of these are involved in transport and binding, especially a number siderophores and iron

transporter related proteins are downregulated 1.5-2 fold. The response to the commensal *C. jeikeium* was relatively mild; only 28 of the 118 genes were specific to this confrontation and mostly involved in basic cellular processes and energy metabolism. The response to *A. baumannii* was more dramatic, with 432 genes downregulated and of these 352 genes is specific to this confrontation. Over 50 of these are involved in transport and binding and energy metabolism and 132 in basic cellular processes, primarily protein synthesis and central intermediary metabolism, transport and binding- ABC type transporters mostly for amino acid, di-and oligo-peptides transport.

Many of the differentially regulated genes in *K. pneumoniae* indicate a general stress response- induction of phage and transposon genes, universal stress proteins, DNA damage repair, and stationary phase stress response [15-17]. Studies have also shown a connection between environmental stressors, phage induction and biofilm formation [18], [19]. The induction of BhsA (putative multiple stress resistance protein) may be another indication of stress in the growth environment. In *E. coli* it is also annotated as YcfR and is known to encode a putative outer membrane protein, and induced in *E. coli* biofilms and during stress conditions. The deletions of this multiple stress resistance protein can make the cell more sensitive to acid, heat, H_2O_2, and cadmium. YcfR was observed to be involved in the regulation of *E. coli* K-12 biofilm formation and hence it has been proposed that that this locus be named *bhsA*, for influencing biofilm through hydrophobicity and stress response [20]. Some of the responses might confer *K. pneumoniae* with some growth advantage like the upregulation of PQQ may allow participation in diverse carbon utilization pathways. The anti-restriction protein ArdA upregulated against *A. baumannii* may prime the organism for DNA uptake. These ArdA proteins and type I R-M systems are more

Figure 6. Regulation of siderophore gene cluster expression in *K. pneumoniae* (enterobactin) and *A. baumannii* (acinetobactin) when in confrontation with a challenger species. Siderophore gene expression response of *K. pneumoniae* (KP), *A. baumannii* (AB), *E. hormaechei* (EH), and *C. jeikeium* (CJ). The MDROs were individually co-cultured and confronted with a different MDRO or the commensal CJ. Differentially regulated genes shown with EdgeR false discovery rate (FDR): <0.05 (pink circle) and <0.01 (yellow circle). Log base 2 fold changes (FC) with reference to monoculture were shown as bar graphs. Gene expression level was shown as log base 2 counts per million (CPM) averaged across all experiments.

frequently discovered through genome sequencing in several bacteria and is hypothesized to be involved in the regulation of gene transfer among bacterial genomes [21].

Differential expression of siderophores

Siderophores are molecules used by cells for iron acquisition and are critical tools for survival of bacterial pathogens in eukaryotic hosts where free iron is extremely limiting. Siderophore gene clusters were upregulated when MDRO species were individually co-cultured with another MDRO, except for *K. pneumoniae* Enterobactin-producing genes when confronted with *E. hormaechei* (**Figure 6**). In general, an up regulation of siderophore expression was observed across 5 out of 6 of the MDRO-MDRO pairwise co-culture assays performed (**Figure 6**). An opposite response was only observed whereby the *K. pneumoniae* siderophore gene cluster was strongly

down regulated by close to 8-fold when *K. pneumoniae* was co-cultured with *E. hormaechei*. Down regulation of *K. pneumoniae* and *A. baumannii* siderophore gene clusters was also observed when these MDROs were individually co-cultured with the commensal *C. jeikeium*. It would be very exciting if lowering siderophore production is a mechanism whereby a commensal microorganism can out compete invading pathogens in/on the human host. Also of note, both *K. pneumoniae* and *E. hormaechei* encode Enterobactin, but only *K. pneumoniae* shuts down transcription of Enterobactin in the presence of *E. hormaechei* and not vice versa. It is conceivable that *K. pneumoniae* may have evolved feedback mechanisms, in terms of iron utilization, and is therefore capable of re-using the enterobactin produced by *Enterobacter*; however, *Enterobacter* is not able to do the same. In contrast, the expression of the *A. baumannii* siderophore Acinetobactin was always upregulated regardless if the challenger organism was *K. pneumoniae* or *E. hormaechei*.

Table 6. Reads mapped by reference genomes

Confronting Bacteria		MDRO										
		A. baumannii				*K. pneumoniae*				*E. hormaechei*			
		Reads mapped to *A. baumannii* genome		Reads mapped to confronting bacteria		Reads mapped to *K. pneumoniae* genome		Reads mapped to confronting bacteria		Reads mapped to *E. hormaechei* genome		Reads mapped to confronting bacteria	
S. epidermidis	Replicate 1	32,234,355	82.5%	509,081	1.3%	25,025,649	77.5%	42,914	0.1%	34,150,078	81.7%	37,189	0.1%
	Replicate 2	32,579,207	78.7%	211,461	0.5%	23,568,809	82.1%	39,305	0.1%	21,403,908	81.2%	8,916	0.03%
L. reuteri	Replicate 1	28,473,822	84.9%	18,964	0.1%	33,577,168	84.5%	1,719	0.004%	15,585,890	72.4%	15,034	0.1%
	Replicate 2	27,295,015	82.4%	3,144	0.01%	25,241,273	80.2%	23,909	0.1%	23,719,926	84.0%	5,225	0.02%
C. jeikeium	Replicate 1	41,378,734	80.2%	16,330	0.03%	22,517,239	78.3%	1,350	0.005%	30,987,505	77.8%	1,183	0.003%
	Replicate 2	24,022,732	81.7%	1,358	0.005%	31,012,045	80.1%	2,385	0.01%	29,476,237	71.1%	1,091	0.003%
E. hormaechei	Replicate 1	9,468,615	44.9%	8,592,602	40.7%	7,696,986	32.4%	10,578,989	44.6%	33,613,582	86.3%		
	Replicate 2	13,758,555	49.4%	9,568,925	34.3%	13,908,025	35.0%	17,650,831	44.5%	19,182,465	83.3%		
K. pneumoniae	Replicate 1	16,455,140	45.8%	13,503,059	37.6%	13,603,176	84.4%						
	Replicate 2	14,591,964	53.0%	8,352,266	30.3%	23,242,160	81.5%						
A. baumannii	Replicate 1	34,351,880	86.6%										
	Replicate 2	30,045,911	85.9%										

Response of Commensals

Confrontations of MDROs to commensals had a low number of readings belonging to the commensals therefore preventing EdgeR analysis of commensal genes (**Table 6**). When EdgeR analysis was performed for MDRO genes when confronted with *S. epidermidis* very few genes had a FDR of <0.05 (**Table 7**). For *A. baumannii* confronted with *S. epidermidis* there were 12 differentially expressed genes, and *K. pneumoniae* when confronted with *S. epidermidis* there were 112 differentially expressed genes. These numbers were very small compared to the other confrontations and therefore it was concluded that the expression profile of the MDRO at the six-hour time point did not differ from monoculture expression. The response by each organism is likely to vary depending on the growth phase. Studies in *A. baumannii* strain ATCC 17978 showed a significant change in protein production when cells transition from log phase to stationary phase [26]. Although there were differences in the growth rates of the commensals and the MDROs, the fact that we still noticed differential expression of genes by MDROs in response to some of the commensals, like *S. epidermidis*, shows that these studies are still valuable due to the inherent internal control nature of these experiments. In *K. pneumoniae*, more than 90% of the differentially regulated genes are downregulated and none are specific to *S. epidermidis*, and are classified as cellular processes, energy metabolism, transport and binding. Only four were uniquely upregulated, and were proteins of either unknown function, regulatory or cell envelope categories. None of the eight upregulated genes (primarily energy metabolism) in *A. baumannii* were unique to *S. epidermidis,* but of the three genes (all chaperones, GroL, GroS and DnaK) downregulated, GroL and DnaK were specific for *S. epidermidis*.

Table 7. Number of differentially expressed gene in *E. hormaechei*, *K. pneumoniae*, and *A. baumannii* when confronted with other bacteria. Differentially expressed genes are defined as genes with an FDR <0.05 from EdgeR analysis.

	Confronting Bacteria					
	A. baumannii	*K. pneumoniae*	*E. hormaechei*	*C. jeikeium*	*S. epidermidis*	*L. reuteri*
A. baumannii genes	---	388	322	424	11	1
K. pneumoniae genes	909	---	212	164	95	14

E. hormaechei genes	78	15	---	0	4	1

Confirmation of differential expression by qPCR

RNA-Seq data for the bacterial confrontations was validated by qPCR of select differentially expressed genes. Genes were chosen for analysis based on the ability to design unique primers and their logFC values. Biological replicates were both tested and qPCR was performed on cDNA from reverse transcription of total RNA. For *K. pneumoniae*, 2 downregulated (*acnB*, T643_A0266; *gabT*_2, T643_A4354) and 3 upregulated (SIS domain protein, T643_A0084; *cimH*, T643_A0191; hypothetical protein, T643_A0079) genes were tested. For *A. baumannii*, 3 downregulated (PapD, T634_2490; *mmsA*_1, T634_0140; EamA-like transporter, T634_3500) and 4 upregulated (PilN, T634_3585; NAD
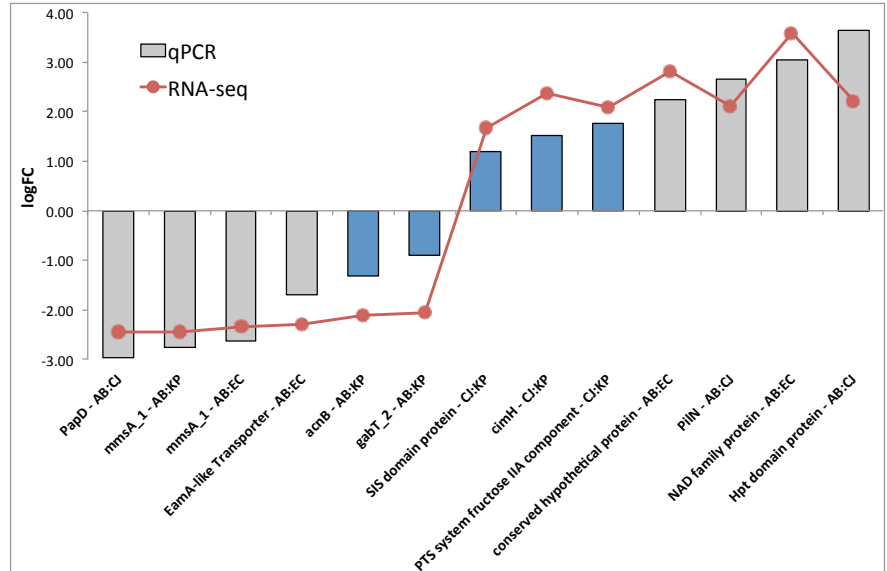

Figure 7. Validation of DE genes. Lines indicated logFC expression from EdgeR analysis of RNA-Seq data and bars indicate logFC expression as measured by qPCR where blue bars are *K. pneumoniae* genes and gray bars are *A. baumannii* genes.

family protein, T634_2358; Hpt domain protein, T634_3235; hypothetical protein, T634_0987) genes were tested. Gene expression was normalized to *gyrB* and relative expression ratios were determined by comparing co-culture samples with monoculture samples. Relative expression ratios were converted to logFC and compared to the logFC from RNA-Seq data. All genes tested showed the same direction of logFC in both RNA-Seq and qPCR analysis (**Figure 7**), confirming the trends observed in the RNA-Seq analysis.

Conclusions for bacteria-bacteria confrontations

The most prominent results from this study were- 1) The response of *A. baumannii* to the two MDROs *(E. hormaechei* and *K. pneumoniae*) and the commensal *C. jeikeium* was significantly stronger compared with the response to *S. epidermidis*, 2) *K. pneumoniae* raised a more robust response to *A. baumannii* than vice versa and responds in a comparable manner to the three other organisms. The unique reactions, depending on the type of organism in the co-culture, clearly shows the importance of confrontation type experiments to understand response and regulation of organisms during infections. It is evidence towards our hypothesis that no single genetic response by an organism would be an effective means for dealing with every possible microbial encounter.

In our targeted analysis of the RNA-Seq of the MDROs response to other MDROs and the commensals, we found some differential regulation of factors associated with virulence and upregulation of genes that might confer a growth advantage over the confronting species, indicating that these types of interactions can influence the pathogen's response during infection. Upregulation of some genes in response to other organisms in the microbiome might also prime the pathogen to be prepared for antibiotic treatment through global regulation of some stress response.

This work is one of the few studies of bacterial-bacterial confrontation observing differential transcriptional regulation via RNA-Seq analysis. Using RNA-Seq we were able to identify unique matches in each participant and simultaneously map both upregulated and downregulated genes. Many proteins of unknown function and non-coding RNAs were differentially regulated, suggesting a need for deeper genomics analysis to unravel the yet unknown factors influencing infection process and drug resistance. This study highlights the fact that an organism responds differently to each source of stimulus in the environment, and knowing this response can help comprehend the influence of surrounding stimuli on a pathogen's ability to cause disease. This type of analysis will have extensive value in studying pathogenesis in terms of both host-pathogen and pathogen-

microbiome interactions, and can be particularly beneficial to observe infections where the pathogen is not in isolation such as in wound infections.

Aim 2. Months 12-24. Perform bacterial-eukaryotic confrontation assays to monitor bacterial-host cell interactions between MDROs and human skin cell cultures.

Task 3a. Months 12-13. Primary human skin cell culture. Obtain commercially available cryo-preserved cell culture stock and establish primary culture for adult human skin cells. **[Task COMPLETED]**

Frozen cell lines for adult human dermal fibroblasts (HDFa) and adult human epidermal keratinocytes (HEKa) were obtained from Invitrogen, catalog numbers C0135C and C0055C, respectively. Cells were expanded and frozen, but consistent recovery of human dermal fibroblasts was the best and deemed most suited to conduct confrontation experiments.

Task 3b. Months 13-19. Bacterial-eukaryotic confrontation assay. Propagate bacterial isolates on solid media. Set up biological replicates representing pairwise bacterial-eukaryotic co-culture between individual MDROs and primary human skin cell cultures. Set up controls with MDROs under the same tissue culture conditions in the absence of human skin culture. Harvest bacterial and human skin cells from co-culture assays. Repeat Task 3b for experimental replicates. **[Task COMPLETED]**

Subtask. Carry out pilot experiments to determine sub-lethal infection (multiplicity) ratio of bacterial and human cells for co-culture experiments. **[Subtask COMPLETED]**

HDF cell cultures were set-up to test multiplicity of infection (MOI) as well as incubation times for individual MDROs. The MOIs for all three MDROs with HDF cells was determined to be optimal at 100:1 (MDRO:HDF). The length of confrontation was tested whereby one-hour duration was determined to be optimal. Prolonged confrontation times resulted in acidification of the cell culture media, which was avoided to eliminate interference with gene expression due to pH changes and direct interactions among the MDROs.

Subtask. Determine that bacterial isolates adhere to human cells prior to isolation of RNA. **[Subtask COMPLETED]**

Bacterial retention control experiments were repeated and the MDROs were observed via light microscopy to be adherent to the HDF cells, even after 3 rinses with PBS (data not shown). Cells were isolated for RNA extraction from confrontations after removing excess culture media so only adherent/close proximity bacterial cells were harvested. Cells were then treated with RNAprotect Cell Reagent (Qiagen) to immediately stabilize RNA transcripts before further processing.

Bacterial-HDF confrontations
Three MDROs (*Acinetobacter baumannii* MRSN 7339, *Klebsiella pneumoniae* MRSN 1319, and *Enterobacter hormaechei* MRSN 11489) were confronted with Human Dermal Fibroblasts, adult (HDFa) (C-013-5C, Gibco).

HDFa Culture Growth
Primary HDFa were expanded in 4 x 25 cm^2 flasks in Medium 106 (M-106-500, Gibco) supplemented with Low Serum Growth Supplement (LSGS) (S-003-10, Gibco) and Gentamicin/Amphotericin B (50-0640, Gibco). Cells were incubated at 37°C, 5% CO_2, 90% RH. Media was changed every 2 days until cells reached 80% confluence (6 days), at which point they were harvest with 0.05% Trypsin-EDTA (25300-054, Gibco). Trypsin was neutralized with Trypsin Neutralizer Solution 1X (R-002-100, Gibco) and media. Cells were split into 4 x 75 cm^2 flasks and incubated at 37°C, 5% CO_2, 90% RH for their second passage. Media was changed at 24 h and then every 48 hours until at 90% confluence (6 days) at which point they were harvested with Trypsin again. Cells were then spun down at 180x g for 10 min and the media removed and cells resuspended in Synth-

a-freeze (A12542-01, LifeTechnologies). Resuspended cells were at a concentration of 9.6 x 10^5 viable cells/ml and split into 1 ml aliquots were gradually cooled to -80°C and stored in liquid nitrogen (vapor phase) storage.

For confrontations an aliquot of twice passaged HDFa cells were thawed in 37°C water bath and expanded in a 75 cm^2 flask with Medium 106 (M-106-500, Gibco) supplemented with Low Serum Growth Supplement (LSGS) (S-003-10, Gibco) at 37°C, 5% CO_2, 90% RH. Media was changed at 24 h and then every 48 h until cells reached 80% confluence at which point cells were harvested with trypsin as described above and split into 25 cm^2 flasks. Media was changed at 24 h and every 48 hours after that. When cells were 80% confluent media was changed 16 h before being confronted with the MDROs.

A. baumannii, *K. pneumonia*, and *E. hormaechei* cells were grown in BHI broth (BD) to a concentration of 1 x 10^8 CFU/ml in log phase growth. 0.5 ml of each culture was spun down for 3 min at 10k x RCF, BHI was removed and cells were resuspended in Media 106 + LSGS. Bacteria was added at an MOI of 100:1 (bacteria:HDF) to the 25 cm^2 flask of HDFa and incubated for 1 h at 37°C, 5% CO_2, 90% RH. Bacteria only controls were also added to empty 25 cm^2 flasks in cell culture media and incubated for the same time in the same conditions.

RNA Isolation. Total RNA was isolated using Proteinase K in conjunction with lysozyme to lyse cells instead of bead beating, followed by Trizol/chloroform extraction. RNA was cleaned using a Qiagen RNeasy Kit and then residual gDNA was removed by TURBO DNase treatment as was done previously for bacteria-bacteria confrontation RNA preparations.

Task 3c. Months 19-24. Bacterial-host RNA-Seq and gene expression analysis. Isolate human polyA mRNA from samples to collect transcripts derived from human skin cells. Isolate bacterial mRNA from samples by depletion of human mRNA and bacterial and eukaryotic rRNAs to collect transcripts derived from the MDRO isolates. Combine bacterial and human mRNA, and construct barcoded ssRNA-Seq libraries for Illumina sequencing. **[Task COMPLETED]**

rRNA Depletion and Library Construction. Prokaryotic and Eukaryotic rRNAs were depleted prior to library construction using the Ribo-Zero Gold rRNA Removal Kit (Epicentre). Fourteen directional RNA-Seq Illumina libraries were generated using NEBNext Ultra RNA Directional Library Preparation Kit. Libraries were run on a total of 4 lanes of Illumina HiSeq 2000 Paired End Sequencing (2x100bp). Sequencing reads were binned and mapped to human and bacterial references genomes as described for bacteria-bacteria confrontations except where noted in the results.

Bacterial responses to HDFa cells

Transcriptome-wide gene responses were studied in confrontation assays when MDROs were individually co-cultured with cultured HDFa cells. Two gene clusters in *K. pneumoniae* were specifically down regulated when *K. pneumoniae* was co-cultured with HDFa cells. The down regulated *K. pneumoniae* gene clusters were involved in fimbriae production and capsule synthesis (**Figure 8**). Both of these bacterial products carry Pathogen-Associated Molecular Patterns (PAMPs), which are bacterial products that are recognized by the human innate immune system [27, 28]. We observed similar downregulations in the *A. baumannii* Csu and Type IV pili gene clusters and an *E. hormaechei* fimbrial operon, but the results were not below the 0.05 FDR significance cutoff (data not shown).
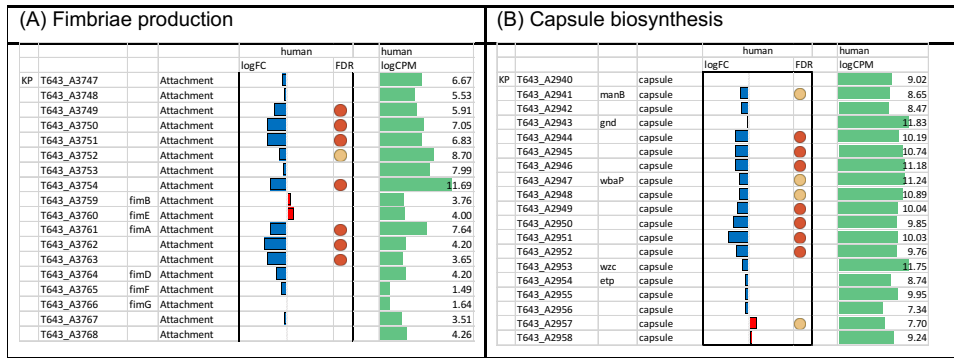
Figure 8

(A) Fimbriae production

Gene	Label		logFC	FDR	human logCPM
KP T643_A3747		Attachment			6.67
T643_A3748		Attachment			5.53
T643_A3749		Attachment		●	5.91
T643_A3750		Attachment		●	7.05
T643_A3751		Attachment			6.83
T643_A3752		Attachment		○	8.70
T643_A3753		Attachment			7.99
T643_A3754		Attachment		●	11.69
T643_A3759	fimB	Attachment			3.76
T643_A3760	fimE	Attachment			4.00
T643_A3761	fimA	Attachment		●	7.64
T643_A3762		Attachment		●	4.20
T643_A3763		Attachment			3.65
T643_A3764	fimD	Attachment			4.20
T643_A3765	fimF	Attachment			1.49
T643_A3766	fimG	Attachment			1.64
T643_A3767		Attachment			3.51
T643_A3768		Attachment			4.26

(B) Capsule biosynthesis

Gene	Label		logFC	FDR	human logCPM
KP T643_A2940		capsule			9.02
T643_A2941	manB	capsule		○	8.65
T643_A2942		capsule			8.47
T643_A2943	gnd	capsule			11.83
T643_A2944		capsule		●	10.19
T643_A2945		capsule		●	10.74
T643_A2946		capsule		●	11.18
T643_A2947	wbaP	capsule		○	11.24
T643_A2948		capsule		○	10.89
T643_A2949		capsule			10.04
T643_A2950		capsule		●	9.85
T643_A2951		capsule		●	10.03
T643_A2952		capsule		●	9.76
T643_A2953	wzc	capsule			11.75
T643_A2954	etp	capsule			8.74
T643_A2955		capsule			9.95
T643_A2956		capsule			7.34
T643_A2957		capsule		○	7.70
T643_A2958		capsule			9.24

Figure 8. *K. pneumoniae* (KP) differentially expressed genes when confronted with HDF cells. Expression of KP fimbriae production (A) and capsule biosynthesis (B) gene clusters in response to co-cultured HDF cells. Differentially regulated genes shown with EdgeR false discovery rate (FDR): <0.05 (pink circle) and <0.01 (yellow circle). Log base 2 fold changes (FC) with reference to monoculture were shown as bar graphs. Gene expression level was shown as log base 2 counts per million (CPM) averaged across all experiments.

HDFa responses to MDROs

Analysis of HDFa-derived reads revealed a set of 21 human genes that were up-regulated and shared across all three MDRO-skin co-culture assays. Pathway and GO term enrichment analyses of the gene list using the DAVID Bioinformatics Resources Database [29, 30] showed that the shared gene set was enriched in cytokine and chemokine signaling pathways, and inflammatory responses (**Table 8**). Out of the 21 upregulated genes, a total of 9 genes can be mapped to the NOD-like receptor signaling pathway in KEGG (**Figure 9**).

Table 8. Pathway and GO enrichment analysis of a shared human gene set upregulated by MDROs *K. pneumoniae*, *A. baumannii*, and *E. hormaechei*.

(A) Top 3 enriched pathways

Pathway	p-value	Gene matches
NOD-like receptor signaling pathway	1.018200e-13	9
Cytokine-cytokine receptor interaction	5.642554e-6	8
Chemokine signaling pathway	1.831407e-5	7

(B) Top 3 enriched GO terms (biological processes)

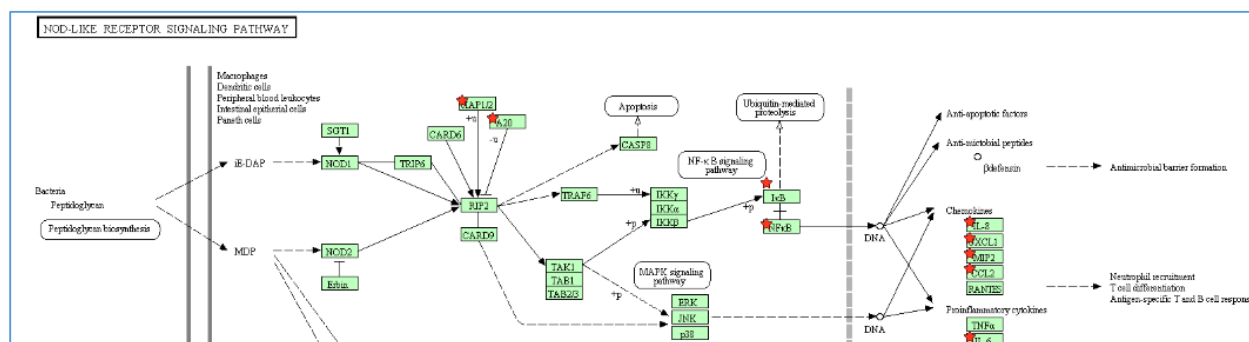| GO term	p-value	Gene matches
response to lipopolysaccharide [GO:0032496]	1.949874e-10	11
response to molecule of bacterial origin [GO:0002237]	3.102596e-10	11
inflammatory response [GO:0006954]	9.053733e-9	12

Figure 9. Mapping of human upregulated genes in MDRO-HDFa confrontation assays. The KEGG NOD-like receptor signaling pathway is illustrated with the nine cytokine and chemokine genes that were up regulated during bacterial confrontations (red star).

KEY RESEARCH ACCOMPLISHMENTS

- Generated high quality Illumina HiSeq genome reference assemblies and annotations for 25 MDROs of highest military importance.
- Developed a novel graph-based algorithm and used it to assemble the first consensus pan-chromosome of *A. baumannii*, identifying both the order and orientation of core genes and flexible genomic regions, enabling us to identify gene clusters responsible for carbon utilization, siderophore production, and pilus assembly demonstrating frequent gain or loss among isolates.
- Demonstrated the existence of novel resistance islands and isolates with increased numbers of resistance island insertions over time, from single insertions in the 1950s to triple insertions in 2011.
- Conducted MDRO-MDRO and MDRO-commensal confrontation assays that demonstrated differential expression of genes involved in cell surface attachment/biofilm (e.g., pili), iron scavenging (e.g., siderophore) and stress response pathways (e.g., universal stress family proteins, BhsA).
- Conducted MDRO-human cell confrontation assays that showed down regulation of bacterial attachment proteins and an increase in the expression of human innate defenses.

REPORTABLE OUTCOMES

- A set of annotated genomes of 25 MDROs of military importance submitted to NCBI GenBank and shared with MRSN collaborators.
- A set of highly variable genomic regions including K and O antigen loci, which control virulence and antigenicity, were identified based on analysis across over 240 military and civilian *A. baumannii* isolates.
- A comprehensive catalog of genomic features representing antibiotic resistance islands (RIs) and virulence factors (e.g. siderophores, cell surface attachments/biofilm, etc.) for seven *A. baumannii* strains isolated from US military personnel and provided by WRAIR MRSN.
- A group of differentially regulated genes when MDROs are in confrontation with other MDROs, commensal bacteria, or adult human dermal fibroblasts.
- A database of antibiotic resistance genes based on manually curated sets of proteins described in the literature. This enabled the identification of several antibiotic resistance genes previously missed by the public CARD database.
- Based on our pan-chromosome and variable region gene content identification algorithms supported by this award, we applied for the Department of Energy Joint Genome Institute (DOE JGI) Emerging Technologies Opportunity Program (ETOP) 2015 award.
- We also sought funding from NIAID to study the spread of AMR genes within the microbiome, leveraging databases of AMR genes generated based on work supported by this award.
- Both Jessica DePew and Radha Krishnakumar received employment opportunities based on experience and training in part supported by this award.

CONCLUSION

Our project goal was to identify and characterize factors that influence virulence (including antibiotic resistance, and biofilm formation) in multidrug-resistant organisms (MDROs), specifically microbial or host-derived signals that induce the expression of virulence-associated genes. We were able to demonstrate that two critical pathways for pathogenesis, siderophores (for iron sequestration) and pili (for attachment and biofilm formation) are reduced in expression in MDROs by a commensal organism and by cultured HDFa cells. We also showed that these same factors vary among *A. baumannii* isolates, especially military isolates, indicating high importance and perhaps selection in this pathogen. The tools and knowledge gained from pan-genome analysis and co-culture expression data will enhance the detection, characterization, and reporting of multidrug-resistant organisms in the Military Health System. This research will ultimately enhance the knowledge products the MRSN provides to its customers and stakeholders, and may lead to future drugs to be used in conjunction with antibiotic therapies that prevent the expression of drug resistance genes. Importantly, we have provided evidence that the expression of siderophores and pili/fimbriae can be regulated by factors expressed by a commensal microorganism or HDFa cells. Future efforts should be focused on identifying these factors so that a potential therapeutic can be developed that will weaken the pathogens ability to obtain iron and to colonize the wound. Likewise, future studies should investigate *C. jeikeium* as a potential probiotic to prevent wound infections.

REFERENCES

1. Chan AP, Sutton G, DePew J, Krishnakumar R, Choi Y, Huang XZ, Beck E, Harkins DM, Kim M, Lesho EP, et al: **A novel method of consensus pan-chromosome assembly and large-scale comparative analysis reveal the highly flexible pan-genome of *Acinetobacter baumannii*.** *Genome Biol* 2015, **16:**143.
2. McGann P, Kwak YI, Summers A, Cummings JF, Waterman PE, Lesho EP: **Detection of *qacA/B* in clinical isolates of methicillin-resistant *Staphylococcus aureus* from a regional healthcare network in the eastern United States.** *Infection control and hospital epidemiology : the official journal of the Society of Hospital Epidemiologists of America* 2011, **32:**1116-1119.
3. Myers EW, Sutton GG, Delcher AL, Dew IM, Fasulo DP, Flanigan MJ, Kravitz SA, Mobarry CM, Reinert KH, Remington KA, et al: **A whole-genome assembly of *Drosophila*.** *Science* 2000, **287:**2196-2204.
4. Li H, Durbin R: **Fast and accurate short read alignment with Burrows-Wheeler transform.** *Bioinformatics* 2009, **25:**1754-1760.
5. Gentleman RC, Carey VJ, Bates DM, Bolstad B, Dettling M, Dudoit S, Ellis B, Gautier L, Ge Y, Gentry J, et al: **Bioconductor: open software development for computational biology and bioinformatics.** *Genome Biol* 2004, **5:**R80.
6. Pfaffl MW: **A new mathematical model for relative quantification in real-time RT-PCR.** *Nucleic Acids Res* 2001, **29:**e45.
7. Kelley LA, Sternberg MJ: **Protein structure prediction on the Web: a case study using the Phyre server.** *Nat Protoc* 2009, **4:**363-371.
8. Gaddy JA, Arivett BA, McConnell MJ, Lopez-Rojas R, Pachon J, Actis LA: **Role of acinetobactin-mediated iron acquisition functions in the interaction of Acinetobacter baumannii strain ATCC 19606T with human lung epithelial cells, Galleria mellonella caterpillars, and mice.** *Infect Immun* 2012, **80:**1015-1024.
9. Camarena L, Bruno V, Euskirchen G, Poggio S, Snyder M: **Molecular mechanisms of ethanol-induced pathogenesis revealed by RNA-sequencing.** *PLoS Pathog* 2010, **6:**e1000834.
10. de Breij A, Gaddy J, van der Meer J, Koning R, Koster A, van den Broek P, Actis L, Nibbering P, Dijkshoorn L: **CsuA/BABCDE-dependent pili are not involved in the adherence of *Acinetobacter baumannii* ATCC19606(T) to human airway epithelial cells and their inflammatory response.** *Res Microbiol* 2009, **160:**213-218.
11. Niu C, Clemmer KM, Bonomo RA, Rather PN: **Isolation and characterization of an autoinducer synthase from Acinetobacter baumannii.** *J Bacteriol* 2008, **190:**3386-3392.
12. Choi AH, Slamti L, Avci FY, Pier GB, Maira-Litran T: **The pgaABCD locus of Acinetobacter baumannii encodes the production of poly-beta-1-6-N-acetylglucosamine, which is critical for biofilm formation.** *J Bacteriol* 2009, **191:**5953-5963.
13. Harding CM, Tracy EN, Carruthers MD, Rather PN, Actis LA, Munson RS, Jr.: **Acinetobacter baumannii strain M2 produces type IV pili which play a role in natural transformation and twitching motility but not surface-associated motility.** *MBio* 2013, **4**.
14. Tucker AT, Nowicki EM, Boll JM, Knauf GA, Burdis NC, Trent MS, Davies BW: **Defining gene-phenotype relationships in Acinetobacter baumannii through one-step chromosomal gene inactivation.** *MBio* 2014, **5:**e01313-01314.
15. Capy P, Gasperi G, Biemont C, Bazin C: **Stress and transposable elements: co-evolution or useful parasites?** *Heredity (Edinb)* 2000, **85 (Pt 2):**101-106.
16. Piacentini L, Fanti L, Specchia V, Bozzetti MP, Berloco M, Palumbo G, Pimpinelli S: **Transposons, environmental changes, and heritable induced phenotypic variability.** *Chromosoma* 2014, **123:**345-354.
17. McClintock B: **The significance of responses of the genome to challenge.** *Science* 1984, **226:**792-801.
18. Binnenkade L, Teichmann L, Thormann KM: **Iron Triggers lambdaSo Prophage Induction and Release of Extracellular DNA in Shewanella oneidensis MR-1 Biofilms.** *Appl Environ Microbiol* 2014, **80:**5304-5316.

19. Whiteley M, Bangera MG, Bumgarner RE, Parsek MR, Teitzel GM, Lory S, Greenberg EP: **Gene expression in Pseudomonas aeruginosa biofilms.** *Nature* 2001, **413:**860-864.
20. Zhang XS, Garcia-Contreras R, Wood TK: **YcfR (BhsA) influences Escherichia coli biofilm formation through stress response and surface hydrophobicity.** *J Bacteriol* 2007, **189:**3051-3062.
21. Nekrasov SV, Agafonova OV, Belogurova NG, Delver EP, Belogurov AA: **Plasmid-encoded antirestriction protein ArdA can discriminate between type I methyltransferase and complete restriction-modification system.** *J Mol Biol* 2007, **365:**284-297.
22. Randall LP, Woodward MJ: **The multiple antibiotic resistance (mar) locus and its significance.** *Res Vet Sci* 2002, **72:**87-93.
23. Guerillot R, Siguier P, Gourbeyre E, Chandler M, Glaser P: **The diversity of prokaryotic DDE transposases of the mutator superfamily, insertion specificity, and association with conjugation machineries.** *Genome Biol Evol* 2014, **6:**260-272.
24. Shen YQ, Bonnot F, Imsand EM, RoseFigura JM, Sjolander K, Klinman JP: **Distribution and properties of the genes encoding the biosynthesis of the bacterial cofactor, pyrroloquinoline quinone.** *Biochemistry* 2012, **51:**2265-2275.
25. Meulenberg JJ, Sellink E, Riegman NH, Postma PW: **Nucleotide sequence and structure of the Klebsiella pneumoniae pqq operon.** *Mol Gen Genet* 1992, **232:**284-294.
26. Fiester SE, Actis LA: **Stress responses in the opportunistic pathogen Acinetobacter baumannii.** *Future Microbiol* 2013, **8:**353-365.
27. Mogensen TH: **Pathogen recognition and inflammatory signaling in innate immune defenses.** *Clin Microbiol Rev* 2009, **22:**240-273, Table of Contents.
28. Hajishengallis G, Sojar H, Genco RJ, DeNardin E: **Intracellular signaling and cytokine induction upon interactions of *Porphyromonas gingivalis* fimbriae with pattern-recognition receptors.** *Immunol Invest* 2004, **33:**157-172.
29. Huang da W, Sherman BT, Lempicki RA: **Systematic and integrative analysis of large gene lists using DAVID bioinformatics resources.** *Nat Protoc* 2009, **4:**44-57.
30. Huang da W, Sherman BT, Lempicki RA: **Bioinformatics enrichment tools: paths toward the comprehensive functional analysis of large gene lists.** *Nucleic Acids Res* 2009, **37:**1-13.

Genome **Biology**

RESEARCH   **Open Access**

CrossMark

A novel method of consensus pan-chromosome assembly and large-scale comparative analysis reveal the highly flexible pan-genome of *Acinetobacter baumannii*

Agnes P. Chan[1†], Granger Sutton[1†], Jessica DePew[1], Radha Krishnakumar[1], Yongwook Choi[1], Xiao-Zhe Huang[2^], Erin Beck[1], Derek M. Harkins[1], Maria Kim[1], Emil P. Lesho[3], Mikeljon P. Nikolich[2] and Derrick E. Fouts[1*]

Abstract

Background: Infections by pan-drug resistant *Acinetobacter baumannii* plague military and civilian healthcare systems. Previous *A. baumannii* pan-genomic studies used modest sample sizes of low diversity and comparisons to a single reference genome, limiting our understanding of gene order and content. A consensus representation of multiple genomes will provide a better framework for comparison. A large-scale comparative study will identify genomic determinants associated with their diversity and adaptation as a successful pathogen.

Results: We determine draft-level genomic sequence of 50 diverse military isolates and conduct the largest bacterial pan-genome analysis of 249 genomes. The pan-genome of *A. baumannii* is open when the input genomes are normalized for diversity with 1867 core proteins and a paralog-collapsed pan-genome size of 11,694 proteins. We developed a novel graph-based algorithm and use it to assemble the first consensus pan-chromosome, identifying both the order and orientation of core genes and flexible genomic regions. Comparative genome analyses demonstrate the existence of novel resistance islands and isolates with increased numbers of resistance island insertions over time, from single insertions in the 1950s to triple insertions in 2011. Gene clusters responsible for carbon utilization, siderophore production, and pilus assembly demonstrate frequent gain or loss among isolates.

Conclusions: The highly variable and dynamic nature of the *A. baumannii* genome may be the result of its success in rapidly adapting to both abiotic and biotic environments through the gain and loss of gene clusters controlling fitness. Importantly, some archaic adaptation mechanisms appear to have reemerged among recent isolates.

Background

Acinetobacter baumannii is a Gram-negative, non-fermenting coccobacillus that can be found in soil and water, but in recent decades has been recognized as an emerging multidrug-resistant (MDR) nosocomial pathogen causing pneumonia, bacteremia, meningitis, and skin/soft-tissue infection associated with trauma [1–5]. The Centers for Disease Control and Prevention (CDC)

estimates that each year in the US there are 12,000 healthcare-associated *Acinetobacter* infections, 63 % of which are MDR [6]. In 2010 an expert panel deemed MDR organisms one of the top five infectious threats to the US Military [7]. Infections with *A. baumannii* resistant to nearly every available antibiotic complicate the care of many patients [8, 9]. Surveillance for asymptomatic colonization among injured service members reveals *A. baumannii* to be one of the common Gram-negative MDR pathogens isolated along with *Acinetobacter calcoaceticus* and *Klebsiella pneumoniae* [10].

The genetic factors that contribute to the success of *A. baumannii* as a pathogen, such as biofilm formation,

* Correspondence: dfouts@jcvi.org
†Equal contributors
^Deceased
[1]J. Craig Venter Institute (JCVI), Rockville, MD, USA
Full list of author information is available at the end of the article

Chan *et al. Genome Biology* (2015) 16:143

Page 2 of 28

ability to compete for and sequester iron in nutrient-deprived environments, and resistance to multiple broad-spectrum antibiotics, have been areas of intense study. In a recently published study of 97 clinical isolates collected from military treatment facilities, 80 % were found to be MDR with markers known to confer resistance to β-lactams, aminoglycosides, macrolides, tetracycline, phenicol, quaternary amines, streptothricin, sulfonamides, and diaminopyrimidine [11]. Drug resistance is manifested by a number of well-characterized mechanisms, including inactivation of drugs (e.g., β-lactamases, cephalosporinases, carbapenemases), prevention of drug entry through outer membrane alterations, removal of the drugs via efflux pumps, and mutations in drug targets [12–18]. In addition, *A. baumannii* has the capacity to up-regulate expression of resistance mechanisms [19–24] and acquire new determinants on genomic regions called resistance islands (RIs) [25], especially in environments such as hospitals where broad spectrum antibiotics are in use [26].

Previous *A. baumannii* comparative genomics studies used modest sample sizes to study representative strains causing infections worldwide. Di Nocera et al. [27] compared seven *A. baumannii* strains, including three of the most frequent strains responsible for epidemics in Mediterranean hospitals. Sahl et al. [28] compared 23 isolates, including three they sequenced, for the presence/absence of invasion- and colonization-specific genes and conducted a pan-genome analysis of six complete genomes. Whole genome phylogenetic analysis of 136 *Acinetobacter* genomes was used to shed light on the expansion of the genus occurring through the gain and loss of genes and conservation of pathogenesis associated genes in the *Acinetobacter calcoaceticus-baumannii* complex [29]. Recently, pan-genome analysis on 34 [30] and 35 [31] *A. baumannii* isolates was conducted.

Since the use of a single reference genome would limit our understanding of gene order and content to a single isolate, comparisons with all available related genomes would be preferable. Thus, a consensus representation of multiple genomes would provide a better framework for comparison than a single reference genome. Methods for constructing the consensus of bacterial strains do not yet exist as far as we know; however, methods do exist to reconstruct contiguous regions of ancestral eukaryotic genomes based on evolutionary breakpoints or rearrangements [32–34]. These methods would fail to assemble a consensus prokaryotic genome by not capturing variable regions acquired via horizontal gene transfer events that were nonexistent in the ancestor. In addition, methods that rely on rearrangements will not work with draft genomes. These limitations necessitated the development of a new program, *gene_order.pl*, which computes the consensus pan-genome from the output

generated by our pan-genome ortholog clustering tool, PanOCT [35].

Here we compare genomic features from the largest number of *A. baumannii* isolates of clinical and military relevance using a pan-genome analysis of 249 publicly available *A. baumannii* isolates, of which 50 were sequenced at the J. Craig Venter Institute (JCVI) for this study. The 249 isolates were collected over several decades and also represented a global collection obtained from hospitals in the US and around the world. First, using *gene_order.pl* as described above, we assembled the first consensus "pan-chromosome" independent of any pre-assigned genome reference and identified both invariant (core) and variable (flexible) regions within the chromosome, which are key components that define a bacterial strain. Second, we utilized a comparative genomics approach on 249 genomes to analyze the diversity of RIs and virulence factors of *A. baumannii*. Our results revealed that decades-old isolates already encoded a vast collection of genetic determinants and mechanisms to confer antibiotic resistance and survival adaptations. We demonstrated the existence of novel RIs and isolates with increased number of RI insertions over time. Clusters of genes for carbon source utilization, siderophore production, pilus assembly and resistance mechanisms were highly variable, and some of these may have reemerged, sometimes in different genomic locations, among modern isolates. These analyses will provide insight into the evolution of *A. baumannii* as a nosocomial pathogen and directly aid the future efforts for large-scale epidemiological studies of this continuously evolving MDR organism.

Results

Genome sequencing of new *A. baumannii* isolates from the military healthcare system

A total of 50 isolates identified as *A. baumannii* from the US military healthcare system were chosen for whole genome shotgun sequencing based on novel clustering by pulsed-field gel electrophoresis (PFGE; Additional file 1), increased prevalence in the military healthcare system, or pan-drug resistance profiles (e.g., Multidrug-resistant Organism and Surveillance Network (MRSN) isolates; Table 1; Additional file 2). These strains were isolated between 2003 and 2011 and comprised 23 different known sequence types (STs) from multilocus sequence typing (MLST) with one potentially novel predicted ST. Seventeen of the isolates were sequenced with a genome finishing status of "improved high-quality draft" (IHQD) (Table 1; Additional file 2), which included manual finishing through sequence gap closure, PCR to link physical ends, or automated gap closure.The remaining isolates were sequenced to a "high-quality draft" (HQD) status. On average, the genomes assembled into 65 contigs (range 3 to 197), 4,023,048 bp in length (range 3,740,684 to

Chan et al. Genome Biology (2015) 16:143

Page 3 of 28

Table 1 Select genomic features and metadata of *A. baumannii* genomes sequenced in this study

Number	Strain	Accession	G+C %	Finishing status†	Number of contigs	Number of proteins	Length (bp)	MLST ST	MLST allelic profile§	Origin/site	Country	City	Year	Reference
1)	OIFC137	AFDK00000000	36.9	IHQD	4	3871	4,081,420	3	3-3-2-2-3-1-3	Catheter tip	USA	Washington, DC	2003	
2)	OIFC032	AFCZ00000000	40.8	IHQD	4	3718	3,893,886	32	1-1-2-2-3-4-4	Wound	Germany	Landstuhl	2003	[8]
3)	OIFC109	ALAL00000000	38.4	IHQD	13	3945	4,107,121	3	3-3-2-2-3-1-3	Right residual limb wound	USA	Washington, DC	2003	[8]
4)	OIFC143	AFDL00000000	37.3	IHQD	8	4265	4,441,327	25	3-3-2-4-7-2-4	Thigh wound	USA	Washington, DC	2003	
5)	OIFC189	AFDM00000000	44.1	IHQD	10	3849	4,043,115	2	2-2-2-2-2-2-2	Wound	USA	Bethesda, MD	2003	[88]
6)	Canada BC-5	AFDN00000000	38.0	IHQD	3	3787	3,998,016	1	1-1-1-1-5-1-1	Clinical isolate	Canada*	NA	2007	
7)	Naval-17	AFDO00000000	42.9	IHQD	21	3848	4,009,964	2	2-2-2-2-2-2-2	Wound	USA	Bethesda, MD	2006	[87]
8)	Naval-18	AFDA00000000	37.6	IHQD	11	4406	4,454,613	25	3-3-2-4-7-2-4	Wound	USA	Bethesda, MD	2006	[87]
9)	Naval-81	AFDB00000000	36.5	IHQD	5	3981	4,080,872	3	3-3-2-2-3-1-3	Blood	USA	Bethesda, MD	2006	
10)	IS-123	ALII00000000	38.7	IHQD	20	4013	4,063,081	3	3-3-2-2-3-1-3	Wound	Iraq	Baghdad	2009	
11)	OIFC074	AMDE00000000	40.5	HQD	66	3815	3,935,888	19	1-2-1-1-5-1-1	Clinical isolate	Germany	Landstuhl	2003	
12)	OIFC098	AMDF00000000	39.5	HQD	72	3659	3,812,112	10	1-3-2-1-4-4-4	Clinical isolate	Germany	Landstuhl	2003	
13)	OIFC180	AMDQ00000000	40.1	HQD	141	3942	3,986,823	2	2-2-2-2-2-2-2	Clinical isolate	USA	NA	2003	
14)	Naval-13	AMDR00000000	40.6	HQD	64	3948	4,107,737	3	3-3-2-2-3-1-3	Wound	USA	Bethesda, MD	2006	[87]
15)	IS-235	AMEI00000000	41.0	HQD	76	3981	4,060,387	1	1-1-1-1-5-1-1	Blood	Iraq	Baghdad	2008	[88]
16)	IS-251	AMEJ00000000	39.6	HQD	72	3908	4,007,286	1	1-1-1-1-5-1-1	Respiratory tract	Iraq	Baghdad	2008	[88]
17)	OIFC0162	AMFH00000000	39.4	HQD	55	3856	4,078,399	412	1-52-2-2-67-4-5	Trachea	USA	Washington, DC	2003	[8]
18)	Naval-72	AMFI00000000	41.2	HQD	52	3607	3,840,453	405	5-3-16-4-29-1-60	Wound	USA	Bethesda, MD	2006	[87]
19)	Naval-83	AMFK00000000	39.7	HQD	103	4000	4,106,603	20	3-1-1-1-5-1-1	Wound	USA	Bethesda, MD	2006	[87]
20)	OIFC110	AMFL00000000	40.3	HQD	53	3818	3,981,666	515	56-3-2-2-9-4-14	Clinical isolate	Germany	Landstuhl	2003	
21)	IS-143	AMGE00000000	41.1	HQD	93	3883	4,020,019	414	2-2-2-2-2-37-2	Wound	Iraq	Baghdad	2008	
22)	IS-116	AMGF00000000	40.0	HQD	40	3779	3,952,511	136	3-2-19-25-5-2-5	Wound	Iraq	Baghdad	2008	
23)	WC-692	AMGG00000000	39.7	HQD	79	4004	4,183,446	513	56-3-55-2-9-4-14	Intact skin surface	Iraq	NA	2008	
24)	IS-58	AMGH00000000	40.9	HQD	61	3944	4,063,888	1	1-1-1-1-5-1-1	Respiratory tract	Iraq	Baghdad	2008	[88]
25)	WC-487	AMZR00000000	39.5	HQD	121	3994	4,115,076	410	20-26-26-14-26-16-23	Skin	USA	Bethesda, MD	2008	
26)	WC-348	AMZT00000000	39.2	HQD	61	3897	4,108,488	412	1-52-2-2-67-4-5	Intact skin surface	Iraq	NA	2008	
27)	Naval-113	AMZU01000000	49.7	HQD	130	4002	4,095,626	2	2-2-2-2-2-2-2	Wound	USA	Bethesda, MD	2006	[87]
28)	Naval-82	AMSW00000000	38.2	HQD	197	3969	3,908,929	428	3-1-2-3-6-1-16	Blood	USA	Bethesda, MD	2006	[87]
29)	Naval-2	AMSX00000000	39.5	HQD	114	4074	4,126,550	2	2-2-2-2-2-2-2	Blood	USA	Bethesda, MD	2006	[87]
30)	Naval-21	AMSY00000000	40.0	HQD	75	3829	3,923,796	19	1-2-1-1-5-1-1	Wound	USA	Washington, DC	2006	[87]

27

Chan et al. Genome Biology (2015) 16:143

Page 4 of 28

Table 1 Select genomic features and metadata of A. baumannii genomes sequenced in this study (Continued)

Number	Strain	Accession	G+C %	Finishing status‡	Number of contigs	Number of proteins	Length (bp)	MLST ST	MLST allelic profile§	Origin/site	Country	City	Year	Reference
31)	Canada BC1	AMSZ00000000	39.7	HQD	66	3825	3,936,404	1	1-1-1-5-1-1	Nosocomial infection	Canada	NA	2007	
32)	WC-A-694	AMTA00000000	39.7	HQD	82	3830	4,008,103	3	3-3-2-2-3-1-3	Clinical isolate	USA	Washington, DC	2008	
33)	OIFC035	AMTB00000000	43.0	HQD	44	3741	3,972,611	403	3-2-6-1-3-4-59	Groin wound	USA	Washington, DC	2003	
34)	Naval-57	AMFP00000000	40.7	HQD	138	3838	3,953,596	155	3-2-2-2-44-4-4	Wound	USA	Bethesda, MD	2006	
35)	OIFC087	AMFS00000000	39.1	HQD	96	3922	4,004,682	32	1-1-2-2-3-4-4	Perineum	USA	Washington, DC	2003	
36)	OIFC099	AMFT00000000	40.1	HQD	75	3748	3,918,177	32	1-1-2-2-3-4-4	Environmental sample	USA	Washington, DC	2003	[8]
37)	WC-A-92	AMFU00000000	38.1	HQD	151	3802	3,838,812	431	1-4-2-1-70-1-2	Clinical isolate	USA	Washington, DC	2007	
38)	OIFC065	AMFV00000000	39.5	HQD	54	3893	4,029,646	136	3-2-19-25-5-2-5	Left leg	USA	Washington, DC	2003	
39)	OIFC047	AMFW00000000	39.2	HQD	39	3505	3,740,684	Novel	1-75-2-2-67-1-2	Perineum	USA	Washington, DC	2003	
40)	OIFC338	AMFX00000000	40.1	HQD	108	4081	4,155,681	2	2-2-2-2-2-2-2	Clinical isolate	USA	Washington, DC	2003	
41)	OIFC111	AMFY00000000	40.8	HQD	44	3732	3,988,061	49	3-3-6-2-3-1-5	Perineum	USA	Washington, DC	2003	
42)	Naval-78	AMFZ00000000	39.9	HQD	112	3950	4,053,379	2	2-2-2-2-2-2-2	Wound	USA	Bethesda, MD	2006	[87]
43)	AA-014	AMGA00000000	39.4	HQD	61	3618	3,857,932	158	41-42-13-1-5-4-14	Wound	Iraq	Al Anbar	2008	
44)	MRSN 3405	JPIA00000000	38.3	IHQD	64	3958	4,082,715	94	1-2-2-1-5-1-1	Wound	USA	Washington, DC	2011	[15]
45)	MRSN 3527	JPHZ00000000	38.7	IHQD	46	4101	4,206,186	81	1-1-1-1-5-1-2	Wound	USA	Washington, DC	2011	[15]
46)	MRSN 3942	JPHY00000000	38.4	IHQD	69	3849	3,975,719	94	1-2-2-1-5-1-1	Wound	USA	Washington, DC	2011	[15]
47)	MRSN 4106	JPHX00000000	38.6	IHQD	62	3824	3,952,684	94	1-2-2-1-5-1-1	Wound	USA	Washington, DC	2011	[15]
48)	MRSN 58	JPHW00000000	39.8	IHQD	40	3866	3,974,176	1	1-1-1-1-5-1-1	Wound	USA	Washington, DC	2010	[20]
49)	MRSN 7339†	JPHV00000000	39.3	IHQD	34	3787	3,955,466	1	1-1-1-1-5-1-1	Wound	USA	Washington, DC	2004	
50)	MRSN 7341‡	JPIB00000000	39.4	IHQD	52	3766	3,911,280	2	2-2-2-2-2-2-2	Respiratory	USA	Washington, DC	2004	

†Improved high-quality draft (IHQD); high-quality draft (HQD)
§cpn60:fusA:gltA:pyrG:recA:rplB:rpoB
*Sample isolated from a soldier evacuated via Landstuhl Regional Medical Center
‡Isolated from the same individual
MLST multilocus sequence typing, NA not available, NI not identified

Chan *et al. Genome Biology* (2015) 16:143

Page 5 of 28

4,454,613 bp) with 3885 predicted protein-coding sequences (range 3505 to 4406). Antibiotic susceptibility profiles and predicted resistance mechanisms are presented in Additional file 3. For one isolate, Naval-83, an amino acid substitution previously not observed in *Acinetobacter* (Glu88Lys) was identified in *parC*, which was recently shown to confer resistance to levofloxacin in *Haemophilus influenza* [36].

Pan-genome

Despite the intensive effort to characterize *A. baumannii* and the sizable number of whole genome comparisons published in the past decade [26, 29, 37–40], the size of the pan-genome remains unknown. We set out to determine the pan-genome of *A. baumannii*. Using PanOCT [35], a total of 22,281 orthologous protein clusters were identified from a collection of all *A. baumannii* genomes publicly available at the time of the analysis, which included 50 sequenced in this study plus 199 genomes obtained from GenBank, totaling 249 genomes (Additional files 4 and 5).

PanOCT only includes non-paralogs in clusters and uses conserved gene neighborhood to separate duplicated genes. This means that insertion sequence (IS) elements that are in novel contexts will often form singleton clusters even though they are identical in sequence to other IS elements within or between genomes analyzed. When the "core" pan-genome is defined to be all 249 genomes analyzed (100 %), there were 1867 core/universal protein clusters and 10,602 singleton clusters (i.e., clusters with a single member from a single genome) (Fig. 1a). If the core pan-genome were instead defined as clusters having protein members from 95 % or 75 % of the genomes analyzed, the core pan-genome would be 2833 and 3126, respectively.

For the analysis of pan-genome size, we followed the convention of merging clusters of paralogous proteins, which greatly reduced the number of clusters from 22,281 to 11,694. To predict the theoretical maximum pan-genome size (i.e., the total number of genes, including core/universal, novel/unique/strain-specific and periphery/dispensable genes) a pan-genome model was implemented using medians and an exponential decay function [41] (Fig. 1b). The maximum pan-genome size was estimated to be 12,554 ± 65 genes. To determine whether the *A. baumannii* pan-genome is open or closed, the number of new genes identified (i.e., unique or strain-specific genes) for each genome added was determined and fit to a power law function ($n = \kappa N^{-\alpha}$) as described previously [42] (Fig. 1b). Conceptually, a pan-genome is closed when sequencing the genomes of additional isolates fails to expand the pan-genome (i.e., the entire gene repertoire has been discovered) [43]. The exponent 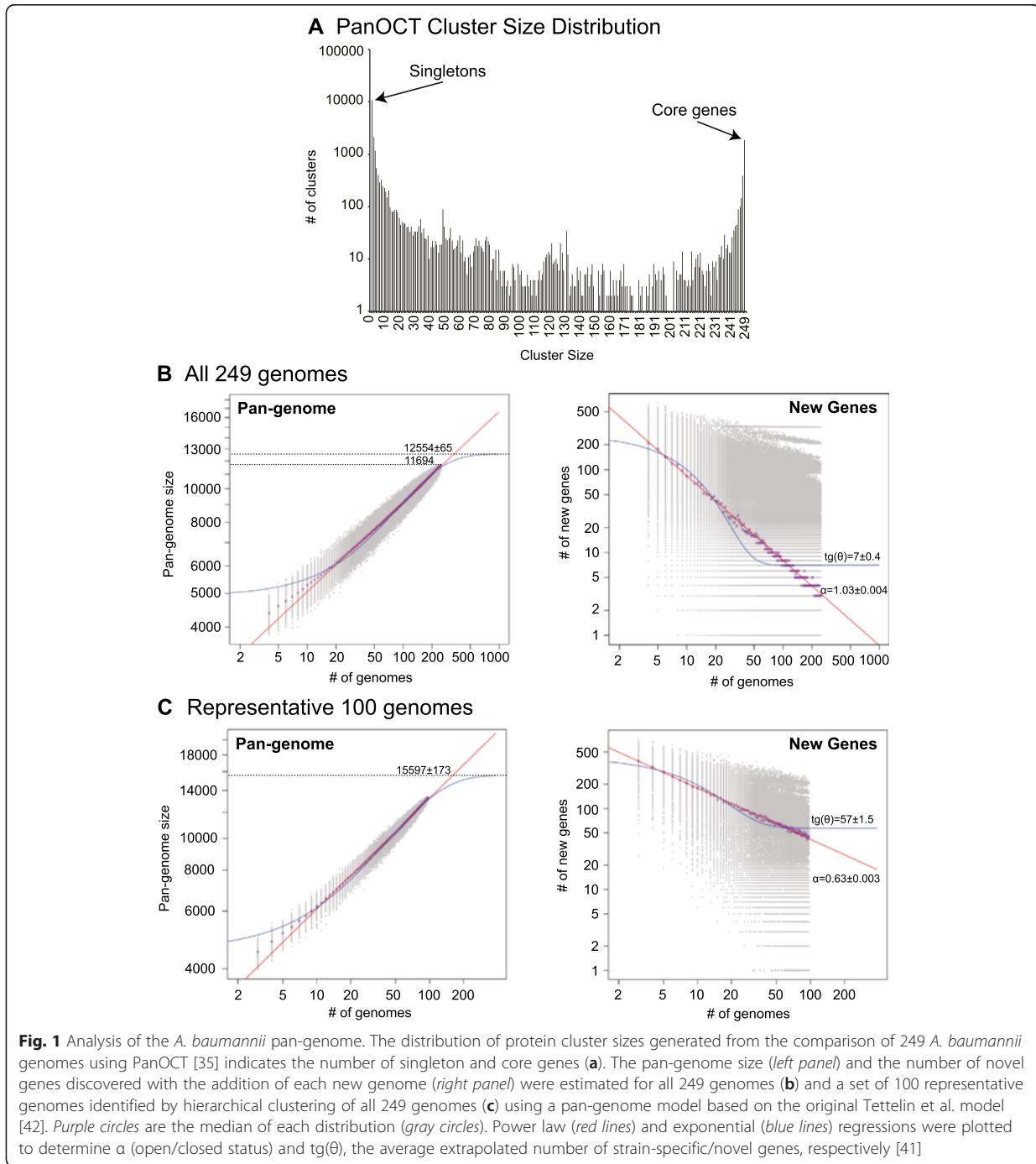(α) indicates whether the pan-genome is open (α ≤ 1) or closed (α > 1) [41]. Using this equation, the pan-genome of *A. baumannii* appears to be barely closed (α = 1.03 ± 0.004; Fig. 1b). For each genome added, the number of new genes was extrapolated by calculating tg(θ) (from an exponential decay function), which was determined to be 7 ± 0.4 (Fig. 1b).

Since a large number of the *A. baumannii* isolates included in this study were of MLST ST 2 (Additional file 4), it is possible the results of the pan-genome state (i.e., open versus closed) were biased toward this dominant ST. Using a phylogenetic tree computed from the BLAST score ratio (BSR) distance matrix generated by PanOCT (Additional file 6), 100 genomes were selected by hierarchical clustering (gold label, Additional file 6). This set of 100 genomes, which represents an even distribution of *A. baumannii* genomic diversity, had a theoretical maximum pan-genome size larger than the combined 249 dataset (by ~3000 genes), with 15,597 ± 173 genes and 57 ± 1.5 new genes discovered for each genome added (Fig. 1c). The pan-genome of the diverse 100 genomes was also open (α = 0.63 ± 0.003; Fig. 1c). In contrast, the theoretical maximum pan-genome size obtained from just the ST 2 genomes decreased to 7980 ± 68 genes and the ST 2 pan-genome was closed (α = 1.08 ± 0.002; Additional file 7).

Flexible genomic islands

Genomic variations among bacterial strains are often found to be mobile elements (e.g., prophage, plasmids, integrated elements), or variable or "flexible" regions that encode genes involved in cell surface structures (e.g., O-antigen, capsular polysaccharides, teichoic acid, S-layer, flagella, pili, and porins) as well as genes for nutrient utilization. All such highly variable regions have been referred to as flexible genomic islands (fGIs) [44–50].

As a prerequisite to identifying fGIs in the pan-genome, a consensus core backbone and fGI assemblies of the pan-genome were computed using *gene_order.pl* (Additional file 8). This algorithm uses output generated by PanOCT to link core gene clusters (cGCs) based on the consensus of the layout of the cGCs in individual genomes (Fig. 2a). The cGCs were defined as containing genes from 75 % or more of the 249 genomes, resulting in a consensus core "pan-chromosome" of *A. baumannii* composed of 3126 genes whose coding regions totaled 2,988,228 bp. When the maximum sizes of all fGIs were inserted into the core backbone, the maximum size of the pan-chromosome increased to 5,070,600 bp, which is 1,047,552 bp (~20 %) larger than the average genome size of 4,023,048 bp. The constructed pan-chromosome had a circular topology (rings 4 and 5 of Fig. 2b), indicating that cGCs were linked together forming a circle as expected, even though the majority of genome assemblies comprising the pan-

Chan *et al. Genome Biology* (2015) 16:143

Page 6 of 28

Fig. 1 Analysis of the *A. baumannii* pan-genome. The distribution of protein cluster sizes generated from the comparison of 249 *A. baumannii* genomes using PanOCT [35] indicates the number of singleton and core genes (**a**). The pan-genome size (*left panel*) and the number of novel genes discovered with the addition of each new genome (*right panel*) were estimated for all 249 genomes (**b**) and a set of 100 representative genomes identified by hierarchical clustering of all 249 genomes (**c**) using a pan-genome model based on the original Tettelin et al. model [42]. *Purple circles* are the median of each distribution (*gray circles*). Power law (*red lines*) and exponential (*blue lines*) regressions were plotted to determine α (open/closed status) and tg(θ), the average extrapolated number of strain-specific/novel genes, respectively [41]

genome are in draft status or possibly incomplete. In addition to the chromosome, seven additional circular "assemblies" were determined that encode between 2 and 120 genes. Five of the circular assemblies were identified as sharing homology to known *A. baumannii* plasmids pABTJ2 [51], pAB2 [52], pRAY [53], and p4ABAYE [54].

Two of these circular assemblies were of bacteriophage and IS element origin.

In addition to generating a consensus core backbone, *gene_order.pl* identified the location of flexible genomic regions (fGRs), which are variable regions between cGCs of the pan-chromosome (Fig. 2a). These fGRs are
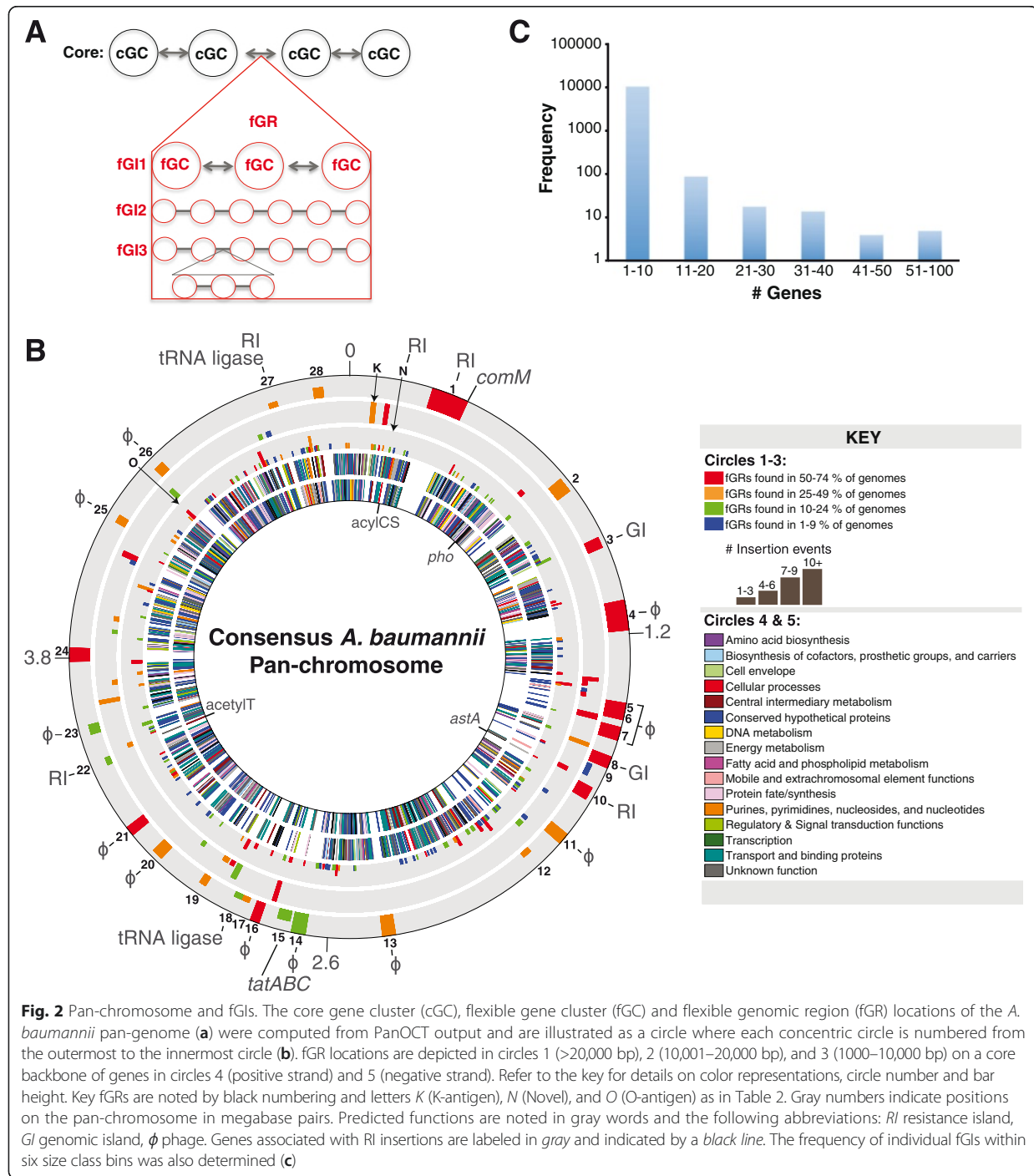
Chan *et al. Genome Biology* (2015) 16:143

Page 7 of 28

Fig. 2 Pan-chromosome and fGIs. The core gene cluster (cGC), flexible gene cluster (fGC) and flexible genomic region (fGR) locations of the *A. baumannii* pan-genome (**a**) were computed from PanOCT output and are illustrated as a circle where each concentric circle is numbered from the outermost to the innermost circle (**b**). fGR locations are depicted in circles 1 (>20,000 bp), 2 (10,001–20,000 bp), and 3 (1000–10,000 bp) on a core backbone of genes in circles 4 (positive strand) and 5 (negative strand). Refer to the key for details on color representations, circle number and bar height. Key fGRs are noted by black numbering and letters *K* (K-antigen), *N* (Novel), and *O* (O-antigen) as in Table 2. Gray numbers indicate positions on the pan-chromosome in megabase pairs. Predicted functions are noted in gray words and the following abbreviations: *RI* resistance island, *GI* genomic island, *ϕ* phage. Genes associated with RI insertions are labeled in *gray* and indicated by a *black line*. The frequency of individual fGIs within six size class bins was also determined (**c**)

composed of a collection of fGIs (Additional file 9). A given fGI is an instance of genomic sequence variation observed at the fGR. Each fGI in turn is made up of individual linear assemblies of flexible genomic clusters (Fig. 2a). In order to avoid and filter out spurious fGIs due to random IS elements or bad gene calls, we required any fGIs carrying less than three genes in length to be present in at least 10 % of the genomes analyzed. To be included within an fGR, we required fGIs of three or more genes in length to be present in at least three genomes. The fGRs are illustrated on the outer rings 1–3 of Fig. 2b. The majority of fGIs contained between one and ten genes (Fig. 2c), which are composed of IS elements, gene duplications, the

31

Chan *et al. Genome Biology* (2015) 16:143

Page 8 of 28

O-antigen biosynthesis cluster (labeled "O" in Fig. 2b) and other small variable biosynthetic gene clusters. There were 89 fGIs encoding 11–20 genes (ring 2, Fig. 2b) and 41 fGIs encoding 21+ genes (ring 1, Fig. 2b). The largest fGI encoded 97 genes, was 79,689 bp in length, similar to phage 3 in ACICU [37], and highly prevalent (present in 151 genomes).

fGIs in the largest fGRs
The largest fGI assemblies within the 20+ kb fGR size class were analyzed for functionality, their potential role in virulence, survival, drug resistance, and evidence of lateral transfer. While many fGRs were targets for insertion of fGIs that encode bacteriophage components (fGRs 4–7, 11, 13, 14, 16, 20, 21, 23, 25, 26), we identified metabolic pathways, drug resistance genes, and potential virulence factors as well as unusual duplications of typical core genes that were inserted within the largest fGRs. Some of these fGRs contained fGIs that were reported previously, such as the putative "alien islands", a.k.a. "pAs", reported in the MDR *A. baumannii* strain ACICU [38] (Table 2).

Virulence genes in fGRs
In *A. baumannii*, the outer membrane protein OmpA is associated with biofilm formation [55], resistance to antibiotics [56] and increased cytotoxicity of outer membrane vesicles in cell cultures [57], where a number of OmpA and OmpA-like proteins were present in outer membrane vesicle preparations. Although several OmpA domain proteins were found in the core pan-genome, we also located SmpA/OmlA family proteins and multiple OmpA domains in some fGIs within fGR 9 (Fig. 2b, Table 2). In addition to OmpA-like adhesins, we identified a YadA-like domain protein in fGR 9, which in *Yersinia* is known to be a major virulence factor functioning in adhesion and complement evasion [58].

fGIs were also identified that encode proteins with putative roles in iron regulation. For example, a homolog of the ferric uptake regulator protein (Fur), which is required for iron homoeostasis and defense against reactive oxygen species [59], was identified in an fGI within fGR 27 (Fig. 2b, Table 2). There is an additional copy of *fur* found in the core pan-genome, which was previously identified as conserved between *Acinetobacter baylyi* and *A. baumannii* strains [54]. Additionally, putative TonB-dependent transporters/receptors were identified in fGR 15 (Fig. 2b, Table 2). TonB-dependent transporters/receptors are outer membrane proteins that bind and transport nutrients for energy metabolism, iron-chelating siderophores, and other metal-containing complexes [60], have been previously shown to be involved in bacterial virulence in some *A. baumannii* strains and were horizontally transferred [61], as is consistent with being within a fGI.

At least four other TonB-like transporter genes were identified within smaller fGIs.

Metabolic pathways within fGIs
Three fGRs (10, 18, and 24; Fig. 2b, Table 2) were identified whose predicted protein functions fell into central metabolism and biosynthetic pathway role categories. A number of enzymes of the aldehyde dehydrogenase family, such as vanillin dehydrogenase, acyl-CoA dehydrogenase, and succinate-semialdehyde dehydrogenase, were identified in fGIs. In bacteria, the action of alcohol dehydrogenase and aldehyde dehydrogenase on alcohol produces organic acids like acetic acid and eventually acetyl-CoA. The acetyl-CoA produced enters fatty acid metabolism and the tricarboxylic acid cycle. It has already been reported that low concentrations of ethanol can stimulate growth of *A. baumannii* and also increase its pathogenicity towards some organisms [62].

Additionally, enzymes for the breakdown of aromatic compounds indicate metabolic versatility in *A. baumannii* to possibly enable survival on alternative carbon, sulfur, and nitrogen sources [63]. For instance, homoprotocatechuate/hydroxyphenylacetate degradation (fGR 18) and phenylpropanoid degradation (fGR 9) pathways can provide intermediates for the tricarboxylic acid cycle. A phenylpropanoid/aromatic degradation pathway (fGR 9) was also previously mentioned as conserved catabolic regions (*pca-qui* genes) in *A. baumannii* strain AYE and *A. baylyi* strain ADP1 [54].

House-keeping genes in fGIs
We also observed two house-keeping genes in fGIs (tRNA ligase genes and *tat*ABC system). tRNA ligases (a.k.a. aminoacyl tRNA synthetases or "aaRSs") are typically single copy essential genes with rare instances of duplications seen in few bacteria, *Escherichia coli* [64] and *Bacillus subtilis* [65, 66] being two such examples. We found that 11 of the 249 sequenced *A. baumannii* genomes contain one or more tRNA synthetase duplications (*tyrS, cysS, thrS*; fGRs 18, 27), with three genomes carrying *cysS* and *thrS* duplications, and one genome with all three duplications. Twin-arginine translocation (Tat) system protein translocases TatA, TatB, and TatC [67] were observed in eight of the sequenced genomes (fGR 15), but we were unable to identify an effector protein with a Tat secretion signal that may have co-transferred with the *tatABC* operon.

RIs in fGRs
Because RIs are composed of IS elements, composite transposons, and integrons, which are by definition mobile and therefore "flexible", we predicted that our algorithm would identify them as fGIs, but it was unclear where they would insert into the core pan-chromosome.

Table 2 Analysis of select fGIs from the A. baumannii pan-chromosome

fGR Region number+	End5	End3	Span (bp)	Number of fGIs	RI	GI	Phage	Metabolic	House-keeping	Extracellular polysaccharide	Description of largest fGI-encoded functions£	pA_ICU¶	Flanking+ core ACICU loci	fGR id‡	Largest fGI assemblies§
K	68497	82812	14316	17						X	K-antigen	1	00074/00087	CL_INS_4	105
N	152292	155346	2955	3	X						Novel; acetyltransferase, fragment of composite IS26 transposon	-	00139 (acylCS)/00147	CL_INS_12	791*
1	243163	350187	107025	38		X					comM, aminoglycoside/hydroxyurea antibiotic resistance kinase, streptomycin 3"-kinase, transporter, major facilitator family protein	3	00219/00242	CL_INS_20	58*
2	702940	747393	44454	7	X						Copper/heavy metal resistance	-	00567/00568	CL_INS_49	16
3	906910	938373	31464	9	X	X					Phage 1 in ACICU, but no core phage genes	6	00684/00702	CL_INS_65	64
4	1103071	1189920	86850	62		X					Toxin/anti-toxin system, large terminase, methylase	-	00861/00869	CL_INS_74	9
5	1401709	1425417	23709	43		X					phage protein F-like	-	01048/01056	CL_INS_93	29
6	1425814	1449657	23844	31		X					Arc-like protein, lysozyme	-		CL_INS_94	76
7	1472644	1510578	37935	16		X	X				Major capsid, prohead protease, portal, large protein, lysozyme, antitermination protein Q, integrase	-		CL_INS_97	14
8	1561693	1595358	33666	11	X						Zeta toxin, phage/plasmid-like protein, recombinase	-	01106/01110	CL_INS_101	52
9	1603966	1638890	35925	2			X				bla, hlyD, phenylpropanoid catabolism, porin, acetaldehyde dehydrogenase; ompA-like, yadA-like	-	01115/01116	CL_INS_104	38, 260*
10	1666240	1704336	38097	7			X				Aldehyde dehydrogenase, vanillin dehydrogenase, porins, transporters	-	01136 (astA)/01153	CL_INS_107	28
11	1818532	1852125	33594	12		X					Lysis protein, tail assembly, tape measure protein, acetaldehyde dehydrogenase	-	01222/01224	CL_INS_120	50
12	1928539	1956234	27696	2			X				bla, hlyD, phenylpropanoid catabolism, porin, acetaldehyde dehydrogenase	-	01256/01257	CL_INS_128	38
13	2402650	2440626	37977	32		X					Major capsid, prohead protease, portal, large and small terminase, head-tail adaptor, tail protein, lysozyme, antitermination protein Q, integrase	-	01626/01627	CL_INS_164	14
14	2664622	2705871	41250	11	X						Inovirus-like; zonula occludens toxin, coat protein B, replication protein	-	01813/01815	CL_INS_180	110
15	2716186	2754267	38082	6		X			X		tatABC, TonB receptors, ABC transporters	-	01824/01827	CL_INS_182	33
16	2802271	2828589	26319	15			X				Phage-associated protein, phage protein F-like, site-specific recombinase	-	01849/01864	CL_INS_187	40
17	2850997	2872608	21612	2				X			Oxidoreductase, aldehyde dehydrogenase	-	01886/01887	CL_INS_190	62

33

Chan et al. Genome Biology (2015) 16:143

Page 10 of 28

Table 2 Analysis of select fGIs from the *A. baumannii* pan-chromosome *(Continued)*

fGR Region number[+]	End5	End3	Span (bp)	Number of fGIs	RI	GI	Phage	Metabolic	House-keeping	Extracellular polysaccharide	Description of largest fGI-encoded functions£	pA$_{ICU}$¶	Flanking[+] core ACICU loci	fGR id‡	Largest fGI assemblies§
18	2874184	2898845	25662	2			X		X		tRNA ligase, aldehyde dehydrogenases, Homoprotocatechuate/hydroxyphenylacetate degradation, transporter	-	01887/01888	CL_INS_191	37
19	2990911	3011439	20529	4				X			Medium chain fatty acid ligase, transporter, oxidoreductase	-	01936/01949	CL_INS_199	121
20	3143872	3176853	32982	7			X				Mu-like; Gam-like protein, terminase, methylase, Mu protein F-like, Mu-like major head, tail sheath-like, Mu Gp45, baseplate J-like	-	02064/02066	CL_INS_211	15
21	3250042	3277383	27342	12			X				lysozyme, baseplate, phage protein F-like, phage-associated protein	-	02139/02236	CL_INS_216	25
22	3465244	3487854	22611	3		X*					Novel 7.8 kb region; salicylate monooxygenase	-	02398/02399 (acetylT)	CL_INS_237	338*
23	3569029	3597828	28800	6			X				Phage	-	02457/02470	CL_INS_246	19
24	3790117	3828819	38703	12				X			Rubredoxin, MFS transporter, prevent host death, aldehyde dehydrogenase, methylmalonate-semialdehyde dehydrogenase	29	02595/02624	CL_INS_259	35
25	4223758	4247211	23454	6			X				Integrase, CII, large and small terminase, portal, prohead protease, major capsid, head-tail connector, head-tail joining, tail	-	03014/03015	CL_INS_287	59
O	4387696	4395870	8175	5						X	O-antigen	-	03146/03149	CL_INS_297	168
26	4420246	4450038	29793	6			X				P2-like; integrase, tape measure, tail proteins, baseplate J-like, lysozyme, baseplate assembly, large and small terminase, major capsid, capsid scaffolding protein, portal	-	03157/03161	CL_INS_299	17
27	4818799	4844895	26097	2		X			X		Novel; *bla*, Tn7, sulfur transport, *fur*, tRNA ligase	-	03502/03503	CL_INS_334	39
28	4960555	4989495	28941	5	X						*ompA*-like protein, Tnp	-	03594/03595	CL_INS_346	148

Functional categories

[+] Cross reference with Fig. 4B

£ Only functions from select fGIs are listed. Other elements and functions may be encoded within selected fGRs

† Not all fGIs are present in ACICU

¶ Largest fGI in fGR similar in composition to the "alien islands" reported by Iacono et al. [38]

‡ Cross reference Additional files 5 and 21

§ Cross reference Additional files 18 and 21

*Not largest fGI in region

Chan *et al. Genome Biology* (2015) 16:143

Page 11 of 28

There are four known hot spots for insertion, including *comM* [26, 68–70], *pho* [37, 71], *astA* [69], and an acetyltransferase (acetylT) gene (a.k.a. HPA2 in [40]). Three fGRs (1, 10, and 22; Table 2) were discovered, corresponding to the known locations within or adjacent to *comM*, *astA*, and acetylT, respectively; however, we did not observe an fGR/fGI near *pho*. Drug resistance (DR) genes in RI-associated fGRs were only observed at the *comM* (fGR 1) locus, which comprised 13 of the 38 fGIs and 31 drug resistance genes (Additional file 10). In addition to the known RIs, a putative novel RI was discovered in an fGI 26,097 bp in length, encoding a metallo-beta-lactamase (ACIN5143_A3078 and ACIN-NAV18_0027) and located within fGR 27 (Table 2, Fig. 2b), residing in two military isolates sequenced in this study (OIFC143 and Naval-18).

Identification of RI signatures

As RIs are made up of one or more transposable elements and most of the sequenced *A. baumannii* genomes are not finished and are, therefore, represented as multiple genomic contigs, RIs are often difficult to characterize. Even with the use of the novel pan-chromosome consensus-building algorithm described above, RIs appear to be fragmented and represented as multiple fGIs. Therefore, to better identify RI insertion events in draft genomes, a high-throughput bioinformatics approach was developed and implemented. This approach characterized RI signatures rather than complete RI structures. RI signatures are defined as both the genomic location and the type of RI insertion identified in an individual isolate. The approach searches for insertions within known RI insertion hot spots *comM*, *pho*, *astA*, and acetylT, and identifies homology with a group of carefully selected representative RIs to minimize redundancy from among those previously reported in *A. baumannii*, including AbaR3 [37], AbaR4 [70], AbGRI1 and AbGRI2 [69], and Tn*1548* [72] (Additional file 11).

Using this bioinformatics approach, a total of 173 out of 247 (70 %) *A. baumannii* genomes analyzed were scored as RI-positive and assigned RI signatures (Additional file 12A–G). Individual clone types showed insertion site preferences and carried specific RI signatures (Fig. 3a–c). While RI insertions in *comM* were common among multiple clone types, insertions outside of *comM* were only detected at the *pho* locus in clonal complex 1 (CC1) isolates, and only at the *astA* or acetylT loci in CC2 isolates (Fig. 3a; Additional file 12b–d). Two distinct types of RIs were identified at the *comM* locus of RI-positive isolates: AbaR3 or AbaR4 in CC1 (22 out of 26 isolates) and predominantly AbGRI1 in CC2 (101 out of 105 isolates) (Fig. 3a; Additional file 12a, b). At non-*comM* loci, only a single type of RI insertion was detected; either AbaR4 at *pho* in CC1 isolates, or in CC2 isolates, AbGRI2 at *astA* or

Tn*1548* at acetylT (Fig. 3a; Additional file 12b-d). Among the group of 123 CC1 and CC2 isolates identified to carry major RI signatures, 67 isolates (54 %) carried more than one RI insertion in the genome versus 56 (46 %) carrying single RI insertions (Additional file 12b).

To determine the mechanism of RI inheritance (i.e., vertical or horizontal) and to understand their evolution in individual clonal lineages, a whole genome single nucleotide polymorphism (SNP) tree was constructed for all isolates analyzed (including four non-*baumannii* outgroups) (Additional file 13). The SNP tree was defined by ~150,000 variant positions located on the backbone of the genomes by excluding regions with unusually high SNP density (Additional file 14).

Phylogenetic relationships of the isolates as shown by the SNP tree were similar to those in the BSR tree in that *A. baumannii* isolates were grouped by MLST type with exceptions for certain allelic differences within CC2. Many of the genomes that cluster between strains of the major STs were off by one allele from the major ST, making them a member of a CC [73]. However, MRSN 4106, 3405 and 3942 (i.e., ST94) differed from ST 1 by two alleles, suggesting possible horizontal gene transfer of MLST markers in these strains. It is clear from both the BSR tree and the SNP tree that the military isolates cover a spectrum of genome diversity, confirming the observed diversity via PFGE (Additional file 1).

When the RI signatures were superimposed onto the SNP tree, specific patterns of RI distribution were observed across different sequence types (Additional file 13). For example, the distribution of AbGRI1, which is predominantly found in CC2 isolates, appeared largely to be the result of vertical inheritance. It is interesting to note that an entire clade does not carry the AbGRI1 RI (triangle, Additional file 13). In contrast AbaR3, which is mostly found in CC1 strains, showed a more scattered pattern of inheritance with seemingly equal numbers with and without this RI. However, it should be noted that the absence of a detectable RI signature in this approach could be due to the incompleteness of the draft genome assemblies. Additional examples of apparent clonal or vertical inheritance were insertions in *pho* in a subgroup of CC1 isolates, two novel insertions discussed in the next section, including a 7.8 kb non-RI gene insertion in acetylT in the entire group of ST 25 isolates and a composite IS26 insertion in acyl-CoA synthase (acylCS) in the entire group of CC3 isolates (Additional file 13).

Identification of novel RIs and GIs

During the analysis of RI signatures, we identified a novel RI insertion detected at a genomic region (ACICU positions 157,224–165,463 nucleotides) flanked by acylCS (ACICU_00319) and a predicted transporter protein
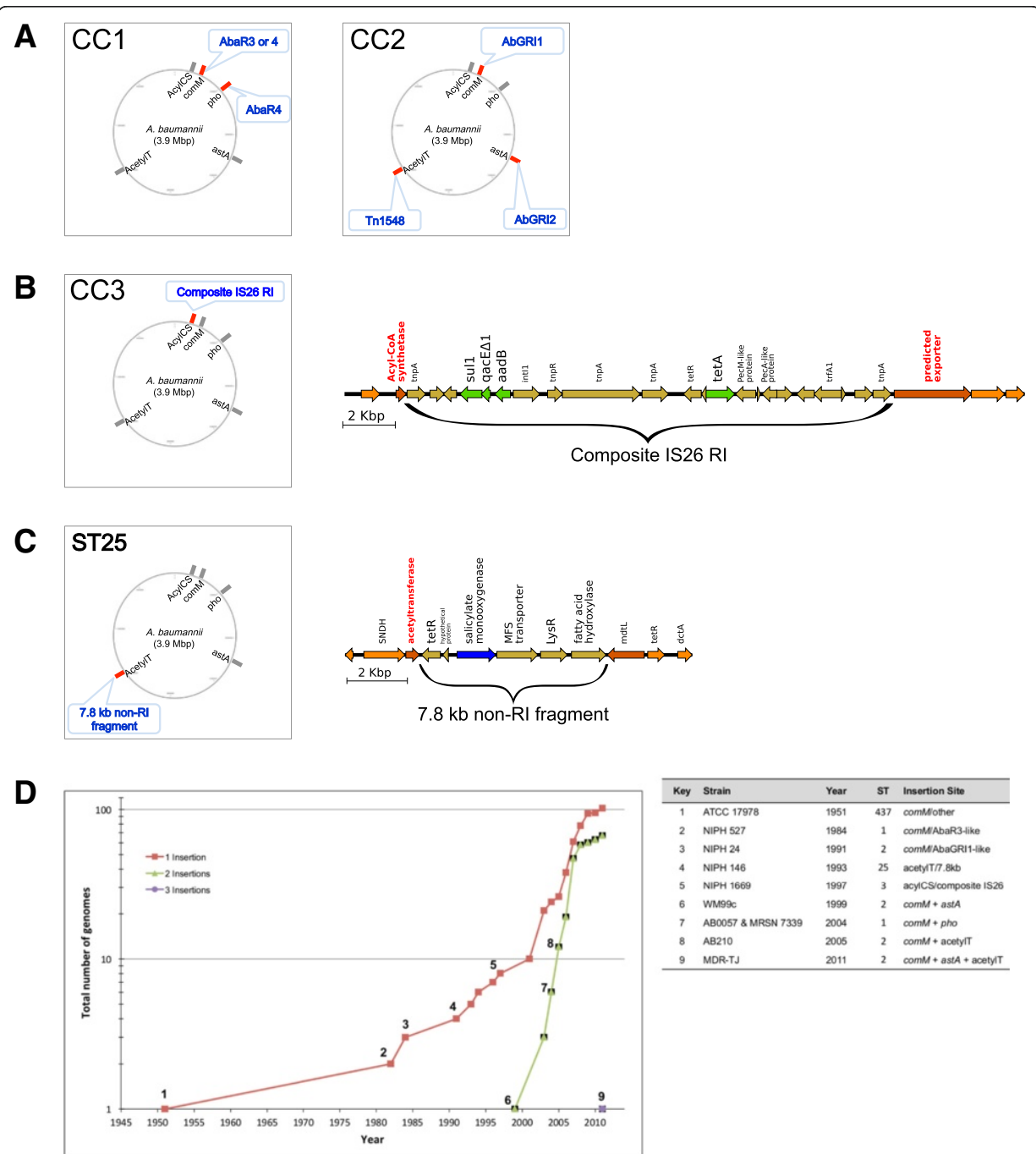
Fig. 3 Clone-type specific RI signatures and RI insertion frequencies over time. **a–c** Genomic locations of RI signatures specific to clonal complexes (CCs) 1–3 and ST 25. In CC1 isolates, RI insertions are detected in the *comM* and/or *pho* loci (**a**). In CC2 isolates, RI insertions are found in the *comM* locus, and in addition the *astA*, or acetylT locus. A novel RI insertion (composite IS26) was identified in CC3 isolates at the acyl-CoA synthase (acylCS) locus (**b**). Gene annotation of the composite IS26 RI is shown to the right. Drug resistance genes (*green*); immediate flanking genes acylCS and a transporter protein (*dark orange*). A novel GI was identified in ST 25 isolates at the acetylT locus (**c**). Gene annotation of the 7.8 kb GI is shown to the right. Salicylate monooxygenase (*blue*); immediate flanking genes acetylT and *mdtL* (*dark orange*). A cumulative frequency graph showing the number of RI-positive isolates carrying single, double, or triple RI insertions collected between 1950 and 2011 (**d**). Isolates that represent the first occurrence of a given RI signature are labeled on the graph (numbered 1–9)

Chan *et al. Genome Biology* (2015) 16:143

Page 13 of 28

(ACICU_00143). The novel RI replaces an 8 kb genomic region with an 18 kb RI identical to a previously reported composite IS26 transposon carrying a class I integron (GenBank accession JX041889) [74]. The composite RI carries two antibiotic resistance gene cassettes, including *sulI-qacEdelta1-aadB-intI1* (resistance to sulfonamides and gentamycin) and *tetR-tetA* (resistance to tetracycline). The gene structure of this novel RI is shown in Fig. 3b. A fragment of the RI was also detected within fGR "N" (Fig. 2b, Table 2). This composite IS26 RI was detected exclusively in all eight of the CC3 isolates analyzed, including six sequenced in this study (Additional file 12b, e). Seven of these isolates were MDR strains collected from the military healthcare system between 2003 and 2009 from wound, blood, catheter, or unknown sources. The earliest sequenced CC3 isolate was collected in the Netherlands in 1997 and contained only the 5′ fragment of the composite IS26 RI, which carried only one resistance gene cassette, *sulI-qacEdelta1-aadB-intI1*, rather than the full length version (Additional file 15).

In addition to the composite IS26 RI, we also identified a novel non-RI 7.8 kb genomic island (GI) juxtaposed to the acetylT locus in the absence of the Tn*1548* RI insertion commonly found at this location (Fig. 3c; Additional file 16). This novel non-RI insertion was also detected within fGR 22 (Fig. 2b, Table 2). The 7.8 kb GI shared over 90 % identity at the nucleotide level with *A. calcoaceticus* PHEA-2 and carried six annotated open reading frames (ORFs), including genes encoding a fatty acid hydroxylase and a salicylate monooxygenase. Salicylate monooxygenase, normally absent from the *A. baumannii* genome, is involved in the conversion of salicylate to catechol, which could possibly be used as a building block for the construction of catecholate-type siderophores. The acetylT/7.8 kb insertion was detected among all seven isolates of the non-major sequence type ST 25 (Additional file 12b, f). Two of these isolates, OIFC143 and Naval-18, were sequenced in this study.

Evolution of RI insertion site usage from single to multiple RI insertions

To provide insight into how RI signatures and insertion site usage have evolved over time, insertion site usage was plotted by cumulative frequency (Fig. 3d). Three phases of site usage were observed, with a single RI insertion site in 1951, double insertions in 1999, and more recently, triple insertions in 2011 (Fig. 3d). During the first phase, single insertions were detected either at the *comM*, acetylT (7.8 kb) or acylCS loci. During the second phase, RI insertions were detected at *comM* in conjunction with a second insertion at *pho*, *astA* or acetylT. Finally, triple insertions were observed at *comM*, *astA*, and acetylT in the MDR-TJ isolate.

These results showed a rapid increase in the number of RI insertions during the course of evolution of *A. baumannii* for antibiotic resistance. Analysis of additional genome sequences will help to further confirm the above observations.

The gain and loss of virulence gene content

To better determine the presence or absence of specific gene clusters associated with virulence and survival, we studied the distribution and conservation of known virulence genes across all isolates. We detected the gain and loss of gene clusters at both the protein and nucleotide levels based on centroid-to-ortholog derived BSR analysis followed by whole genome sequence alignments. Among the ten classes of known virulence/survival mechanisms analyzed, including a collection of 178 genes (Additional file 17), three classes of genes (type I pili, siderophores, and efflux pumps) showed distinct gain/loss variations among the isolates. A heat map generated based on centroid-to-ortholog derived BSR is shown in Additional file 18 (BSR values in Additional file 19). A summary of the diversity of three virulence properties (i.e., adhesion, iron acquisition, and efflux) among the isolates analyzed is shown in Table 3 and Additional file 20.

The *csuAB-E* gene cluster has been shown to encode a chaperone-usher type I pili system [75] and is functionally characterized [76, 77]. *A. baumannii* also encodes two additional related type I pili clusters [78]. The presence of the *csuAB-E* gene cluster has been shown to be variable among relatively smaller subsets of *A. baumannii* genomes studied [31, 40, 78]. We observed the deletion of the *csu* gene cluster (i.e., type I pili cluster 1) only in certain ST 2 and ST 10 isolates as 42 and 17 kb deletions, respectively (Table 3, Fig. 4). Deletions of the *csu* gene cluster in ST 2 strains have been previously reported [40, 79], but the 17 kb deletion is a novel discovery. These *csu* deletions appeared to be the result of independent molecular events based on observations that the deletions occurred in different lineages as shown on the SNP tree (Additional file 13), and the distinct sizes of the deletions (Fig. 5a). Furthermore, type I pili cluster 2 was detected across all isolates except two strains, NIPH 60 and SDF. Type I pili cluster 3 was present among CC1 and CC3 isolates but absent from all ST 2, ST 25, ST 79, ST 113, and ST 215 isolates (Additional files 20 and 21; total = 113 isolates) as shown in the centroid-ortholog BSR-derived heat map (Additional file 18). It should be noted that by taking into account the overall genomic content of type I pili, strain MDR-ZJ06 and nine UH clade B isolates encoded a single type I pilus represented by cluster 2. The functional significance for type I pili expressed from different clusters is yet to be determined. Interestingly, six out of

Chan *et al. Genome Biology* (2015) 16:143

Page 14 of 28

Table 3 Diversity of virulence gene content across *A. baumannii* isolates

Isolates	Genome category	Source	Year	ST	Allele summary	Country	Gene clusters			
							1	2	3	4
Type I pili										
AYE	Global	Urinary	2001	1	1-1-1-1-5-1-1	France	+	+	+	
ACICU	Global	Internal	2005	2	2-2-2-2-2-2-2	Italy	+	+	-	
SDF	Global	Miscellaneous	2000	17	3-29-30-1-9-1-4	France	-	-	-	
NIPH 335	Global	Respiratory	1994	10	1-3-2-1-4-4-4	Czech Republic	-	+	+	
*OIFC098**	WRAIR	Miscellaneous	2003	10	1-3-2-1-4-4-4	Germany	-	+	+	
MDR-ZJ06	Global	Blood	2006	2	2-2-2-2-2-2-2	China	-[1]	+	-	
UH clade B[2]	US hospital	Respiratory[3]	2007	2	2-2-2-2-2-2-2	USA	-[1]	+	-	
NIPH 60	Global	Respiratory	1992	34	8-1-14-3-12-1-13	Czech Republic	+	-	+	
NIPH 528	Global	Unknown	1982	2	2-2-2-2-2-2-2	Netherlands	+	+	-[4]	
MDR-TJ	Global	Miscellaneous	Before 2011	2	2-2-2-2-2-2-2	China	+	+	-[4]	
*OIFC143**	WRAIR	Wound	2003	25	3-3-2-4-7-2-4	USA	+	+	-[4]	
Siderophores										
AYE	Global	Urinary	2001	1	1-1-1-1-5-1-1	France	+	-	+	-
ACICU	Global	Internal	2005	2	2-2-2-2-2-2-2	Italy	+	-	+	-
SDF	Global	Miscellaneous	2000	17	3-29-30-1-9-1-4	France	-	-	-	-
NIPH 190	Global	Unknown	1993	9	3-1-5-3-6-1-3	Czech Republic	-	-	+	-
NIPH 410[5]	Global	Blood	1996	39	10-4-3-2-13-1-2	Czech Republic	-	-	+	-
*OIFC0162**	WRAIR	Respiratory	2003	412	1-52-2-2-67-4-5	USA	-	-	+	-
OIFC047[5]	WRAIR	Miscellaneous	2003	Novel	1-75-2-2-67-1-2	USA	-	-	+	-
*Naval-82**	WRAIR	Blood	2006	410	3-1-2-3-6-1-16	USA	-	-	+	-
*WC-348**	WRAIR	Skin	2008	412	1-52-2-2-67-4-5	Iraq	-	-	+	-
ATCC 17978	Global	Miscellaneous	1951	437	3-2-2-2-30-4-28	NA	+	+[6]	+	-
6013113	Global	Skin	2007	81	1-1-1-1-5-1-2	England	+	+	+	-
6013150	Global	Skin	2007	81	1-1-1-1-5-1-2	England	+	+	+	-
*MRSN 3527**	MRSN	Wound	2011	81	1-1-1-1-5-1-2	USA	+	+	+	-
*MRSN 3405**	MRSN	Wound	2011	94	1-2-2-1-5-1-1	USA	+	+	+	-
*MRSN 3942**	MRSN	Wound	2011	94	1-2-2-1-5-1-1	USA	+	+	+	-
*MRSN 4106**	MRSN	Wound	2011	94	1-2-2-1-5-1-1	USA	+	+	+	-
WC-487[7]	WRAIR	Skin	2008	410	20-26-26-14-26-16-23	Iraq	-	-	-	+[8]
Efflux pumps										
AYE	Global	Urinary	2001	1	1-1-1-1-5-1-1	France	+	+	+	
ACICU	Global	Internal	2005	2	2-2-2-2-2-2-2	Italy	+	+	+	
SDF	Global	Miscellaneous	2000	17	3-29-30-1-9-1-4	France	-	+	+	
NIPH 60	Global	Respiratory	1992	34	8-1-14-3-12-1-13	Czech Republic	-	+	+	
NIPH 80	Global	Blood	1993	37	3-2-2-2-7-1-2	Czech Republic	-	+	+	
NIPH 615	Global	Respiratory	1994	12	3-5-7-1-7-2-6	Czech Republic	-	+	+	
NIPH 410[5]	Global	Blood	1996	39	10-4-3-2-13-1-2	Czech Republic	-	+	+	
OIFC047[5]	WRAIR	Miscellaneous	2003	Novel	1-75-2-2-67-1-2	USA	-	+	+	
*OIFC111**	WRAIR	Miscellaneous	2003	49	3-3-6-2-3-1-5	USA	-	+	+	
AB900	WRAIR	Skin	2003	49	3-3-6-2-3-1-5	USA	-	+	+	
AB_TG27343	Global	Wound	2005	422	26-72-2-2-29-4-5	USA	-	+	+	

Chan *et al. Genome Biology* (2015) 16:143

Page 15 of 28

Table 3 Diversity of virulence gene content across *A. baumannii* isolates *(Continued)*

Isolates	Genome category	Source	Year	ST	Allele summary	Country	Gene clusters 1	2	3	4
AB_1536-8	Global	Unknown	2006	413	1-3-2-2-5-8-12	USA	-	+	+	
AB_1583-8	Global	Unknown	2006	422	26-72-2-2-29-4-5	USA	-	+	+	
*Naval-72**	WRAIR	Wound	2006	405	5-3-16-4-29-1-60	USA	-	+	+	
ZWS1122	Global	Blood	2011	2	2-2-2-2-2-2-2	China	-	+	+	
ZWS1219	Global	Blood	2011	2	2-2-2-2-2-2-2	China	-	+	+	
BJAB0715	Global	Miscellaneous	5/2007–4/2008	23	1-3-10-1-4-4-4	China	-	+	+	

Isolate name: finished genomes (bold), pre-2000 isolates (underline), sequenced in this study (italics with asterisk)
Specific gain or loss of gene clusters with respect to majority of isolates analyzed and reference genomes AYE, ACICU, SDF shown as "+" and "-" signs, respectively
(1) A 42 kb deletion was detected in ST2 strain MDR-ZJ06 and the UH clade B isolates, in contrast to the 17 kb deletion observed in ST10 strains NIPH 335 and OIFC098
(2) Nine UH clade B isolates carry a deletion of the type I pili *csu* gene cluster [40]
(3) Six out of nine UH clade B isolates which showed a loss of the type I pili *csu* gene cluster are of respiratory origin
(4) Loss of type I pili cluster 3 was detected in 133 isolates, including ST2, ST25, ST79, ST113, and ST215. Only three isolates are shown. Similar gene loss was not detected in ST1 or ST3 isolates
(5) Two isolates (NIPH 410, OIFC047) had a dual loss of siderophore cluster 1 and efflux cluster 1 (AdeABC)
(6) Insertion of siderophore cluster 2 was detected at 3 Mb in ATCC 17978, which differed from the location identified in ST81 and ST94 isolates at 3.8 Mb (coordinates based on ACICU genome)
(7) WC-487 is a non-baumannii *Acinetobacter* sp. isolate
(8) Siderophore cluster 4 was also detected in *A. baumannii* 8399 [78, 80]
ATCC American Type Culture Collection, *NA* not available, *WRAIR* Walter Reed Army Institute of Research

nine UH clade B isolates originated from respiratory samples, and all have been reported to be MDR (Table 3).

Siderophores are iron uptake machinery for bacterial survival and virulence under limiting iron conditions and are encoded in five known clusters/genomic islands in *A. baumannii* [78, 80]. We observed that ST 1 (e.g., AYE), ST 2 (e.g., ACICU) and most isolates analyzed in general carried siderophore cluster 1 (A1S_1647 to A1S_1657) and cluster 3 (A1S_2372 to A1S_2392) (Table 3; Additional file 18), which were also part of the core pan-genome. However, siderophore cluster 1 was missing in four US military Walter Reed Army Institute of Research (WRAIR) isolates sequenced in this study (strains OIFC0162, OIFC047, Naval-82, and WC-348) and two additional isolates (NIPH 190 and NIPH 410) (Table 3; Additional file 22). Despite belonging to different sequence types, all six isolates shared close phylogenetic distances as shown on the SNP tree (Additional file 13). We showed that siderophore cluster 3, encoding the key *A. baumannii* siderophore acinetobactin, was detected among all isolates analyzed except SDF (from body louse) and the non-*A. baumannii* isolate WC-487.

In addition, we also observed the acquisition of a siderophore gene cluster among specific isolates. Siderophore cluster 2 was rarely found in *A. baumannii* and only previously reported in two isolates: ATCC 17978 (Figs. 4 and 5b) collected in 1951 and *A. baylyi* ADP1 [78]. Siderophore cluster 2 was also found on an fGI (Assembly_fGI 41, Additional file 8). In our analysis, we detected cluster 2 in six additional isolates belonging to ST 81 and ST 94 collected between 2007 and 2011 (Table 3, Figs. 4 and 5c). The six isolates shared a common insertion site for siderophore cluster 2 at 3.8 Mbp different from that of ATCC 17978 at 3.0 Mbp (reference genomic

coordinates were based on the ACICU genome, which does not carry the insertion). The six isolates are also phylogenetically distinct from ATCC 17978 as shown on the SNP tree (Additional file 13). Among the six isolates, four were isolated from wound samples of the US military MRSN collection sequenced in this study. Further studies are needed to determine if siderophore cluster 2 is associated with different iron availability in military wound samples. Lastly, siderophore cluster 4, which was previously identified in *A. baumannii* isolate 8399 [78, 80], was only identified in one isolate in this study, the non-*A. baumannii* isolate WC-487 (Table 3).

Efflux pumps are outer membrane proteins that drive the expulsion of antimicrobials leading to resistance against aminoglycosides, β-lactams, chloramphenicol, erythromycin and tetracycline [81]. We noted that the AdeABC efflux (A1S_1823 to A1S_1825) gene cluster was deleted in a small set of isolates across multiple strain types (Table 3). Similar to SDF, two isolates, OIFC047 and NIPH 410, which are phylogenetically closely related as shown on the SNP tree (Additional file 13), showed a dual loss of the AdeABC efflux cluster and the siderophore cluster 1 (Table 3). Determining the functional consequence of the gene loss will aid in the characterization of the significance of these specific virulence determinants.

Discussion

In this study, the draft genome sequences of 50 *A. baumannii* isolates from the military healthcare system were determined and analyzed within the framework of a 249 isolate pan-genome, to identify the genetic determinants underlying MDR and virulence properties in
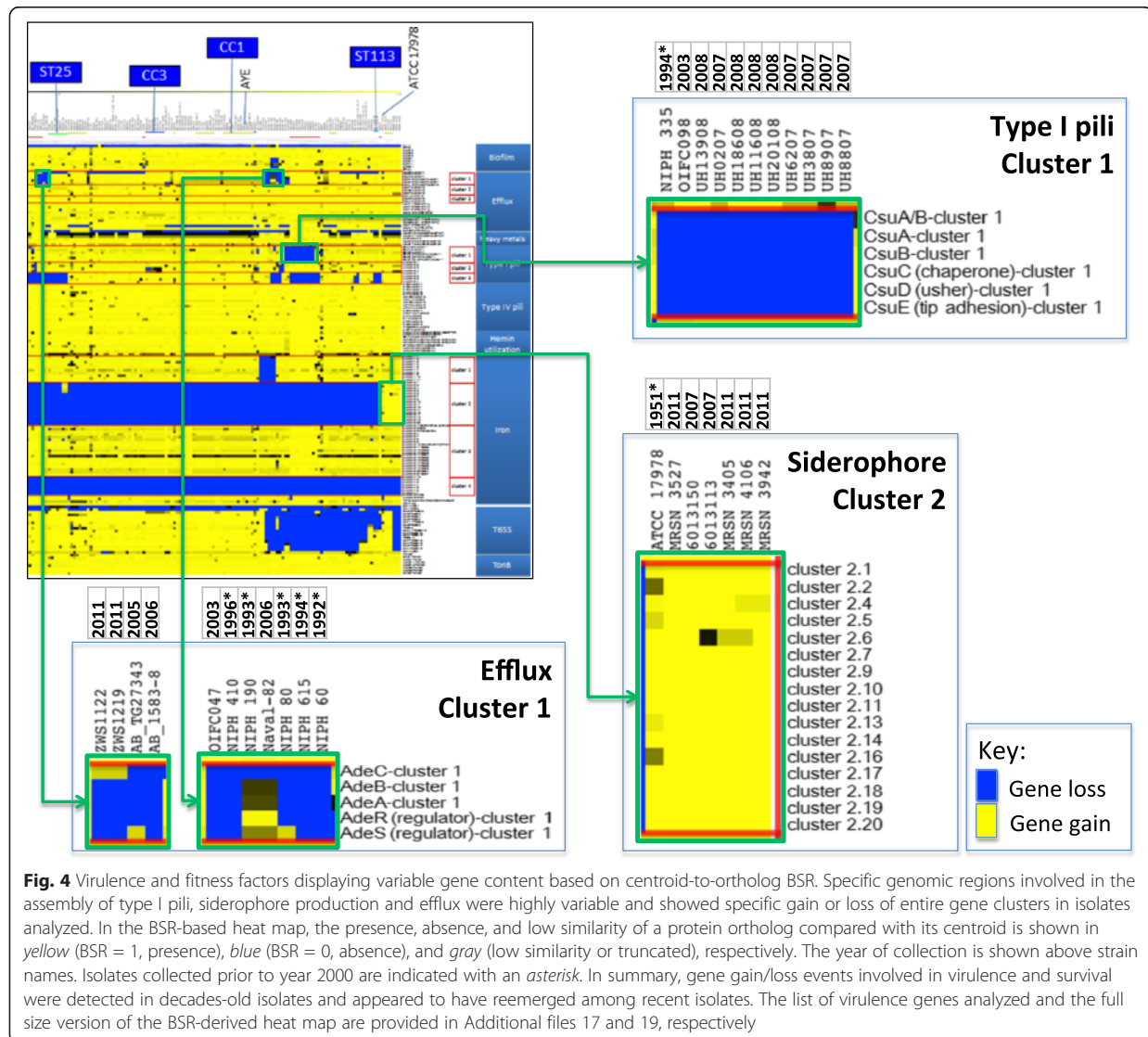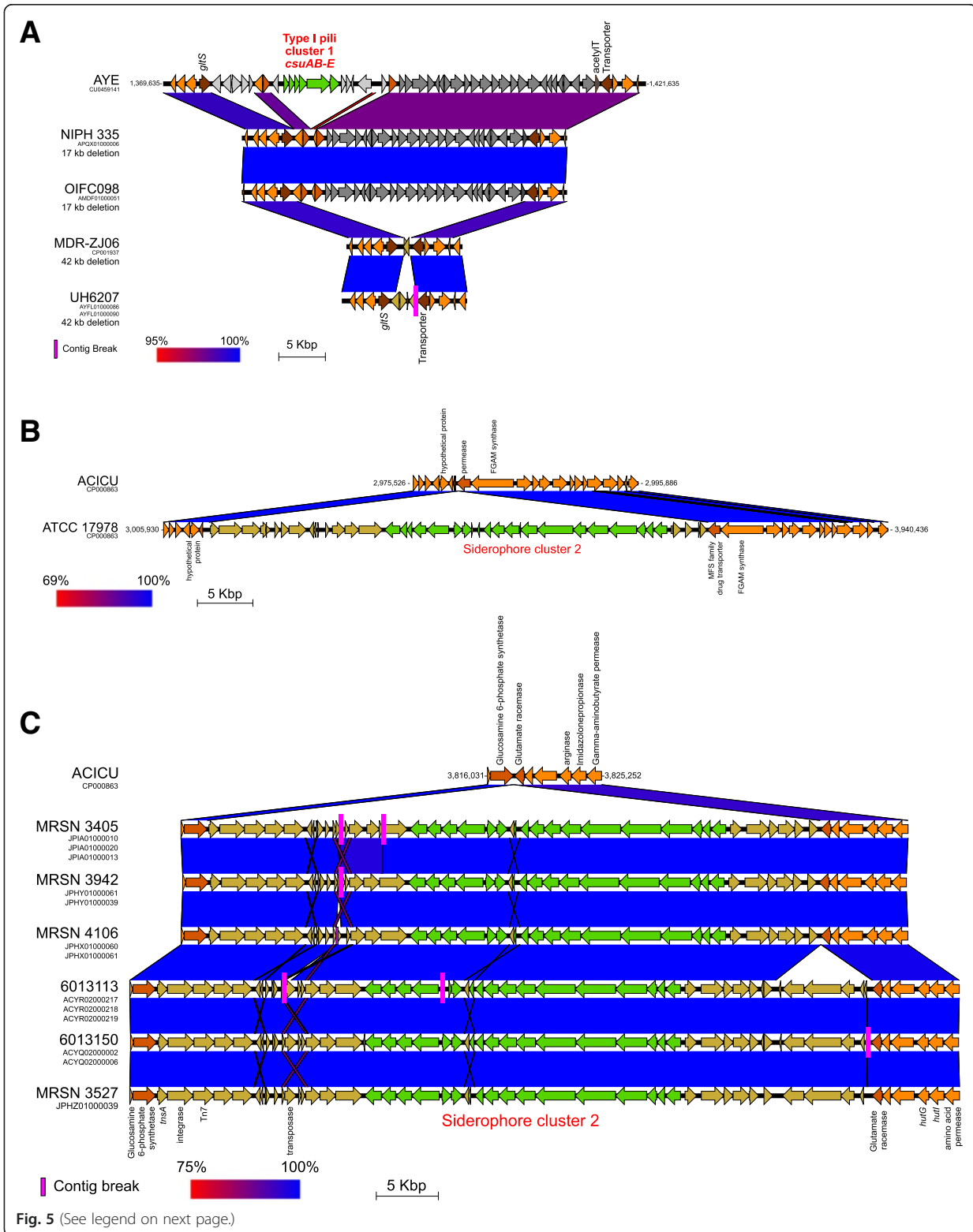
Chan *et al. Genome Biology* (2015) 16:143

Page 16 of 28

Fig. 4 Virulence and fitness factors displaying variable gene content based on centroid-to-ortholog BSR. Specific genomic regions involved in the assembly of type I pili, siderophore production and efflux were highly variable and showed specific gain or loss of entire gene clusters in isolates analyzed. In the BSR-based heat map, the presence, absence, and low similarity of a protein ortholog compared with its centroid is shown in *yellow* (BSR = 1, presence), *blue* (BSR = 0, absence), and *gray* (low similarity or truncated), respectively. The year of collection is shown above strain names. Isolates collected prior to year 2000 are indicated with an *asterisk*. In summary, gene gain/loss events involved in virulence and survival were detected in decades-old isolates and appeared to have reemerged among recent isolates. The list of virulence genes analyzed and the full size version of the BSR-derived heat map are provided in Additional files 17 and 19, respectively

the context of strain diversity and evolution. Using a novel graph-based approach, we identified highly variable and dynamic genomic content of the *A. baumannii* genome, which may be the result of its rapid adaption and survival in both biotic and abiotic environments through the gain and loss of gene clusters controlling fitness. Importantly, our results show that some of the adaptation mechanisms (e.g., gain/loss of pili and siderophore gene clusters) existed in decades-old isolates and appeared to have reemerged among recent isolates. This study will provide a valuable framework and genetic landmarks for surveillance, prediction of outbreaks, and understanding the epidemiology of globally distributed isolates.

A. baumannii pan-genome

To determine whether the genomic diversity of *A. baumannii* has been captured among all sequenced isolates (i.e., a closed pan-genome) and to understand how the 50 selected military isolates were evolutionarily related to previously sequenced isolates, we conducted, to our knowledge, the first *A. baumannii* pan-genome analysis on the most expansive set of isolates, including 249 genomes. We observed 1867 core (100 % membership), 2833 core (95 % membership) protein clusters and a paralog-collapsed pan-genome cluster size of 11,694 proteins. For comparison, in a pan-genome study of 186 *E. coli* strains (~1 Mbp larger than *A. baumannii* and ~1000 more genes per genome), there were 1702 core

Chan *et al. Genome Biology* (2015) 16:143

Page 17 of 28

Fig. 5 (See legend on next page.)

Chan *et al. Genome Biology* (2015) 16:143

Page 18 of 28

(See figure on previous page.)
Fig. 5 Loss of pili cluster 1 (*csu* gene cluster) and gain of siderophore cluster 2 in specific isolates. **a** Two types of deletion were observed which led to a complete loss of the type I pilus *csuAB-E* gene cluster. A novel 17 kb deletion was detected in NIPH 335 and OIFC098, whereas a previously reported 42 kb deletion was found in MDR-ZJ06 and nine UH clade B isolates (e.g., UH6207). **b** Siderophore cluster 2 was detected only in a small subset of isolates across all 249 analyzed. Two apparently independent molecular events were observed among the siderophore cluster 2-positive isolates. In decades-old isolate ATCC 17978, insertion of the gene cluster was detected at a genomic position corresponding to 3.0 Mbp of the ACICU reference genome. **c** In the remaining siderophore cluster 2-positive modern isolates (e.g., MRSN 3405), insertion was detected at a different location, which corresponds to 3.8 Mbp of the ACICU reference genome. Since ATCC 17978 was isolated in 1951 while other isolates were isolated more recently between 2007 and 2011, the acquiring of siderophore cluster 2 among modern isolates could be an example of the reemergence of a survival mechanism of *A. baumannii*. The functional significance of siderophore cluster 2 is yet to be determined. Key: pairwise nucleotide identity shown in *red* to *blue* (100 % identity) color scale; contig breaks (*pink vertical bars*); open reading-frames (*thick arrows*); type I pilus cluster 1 and siderophore cluster 2 genes (*green*); deleted genes (*gray scale*); genes bordering insertions/deletions (*dark orange* and *brown*); other flanking genes (*orange*); other genes (*light brown*)

(100 %), 3051 core (95 %), and a pan-genome cluster size of 16,373 proteins [82]. This shows that even though the average genome size of *E. coli* is larger by ~1 Mbp, the core pan-genome cluster size is similar to *A. baumannii*. However, the larger pan-genome cluster size observed in *E. coli* (by ~5000 proteins) may reflect a higher proportion of variable/flexible regions within the pan-genome of *E. coli* compared with *A. baumannii*.

Pan-genome open or closed?
Our initial analysis of all 249 genomes suggested that the pan-genome was closed; however, after determining that around half of the genomes were from highly related strains of MLST CC2, we tested whether inclusion of highly similar strains can alter the pan-genome state (e.g., open versus closed). We used hierarchical clustering to normalize the diversity of strains chosen for inclusion and showed that the pan-genome was open when restricting to a diverse set of 100 genomes. To test whether this was the result of undersampling rather than removal of highly similar genomes, we conducted a parallel analysis on about 100 CC2 isolates and showed that the pan-genome was closed. These results suggest that the inclusion of the entire set of 249 strains in the pan-genome state calculation can bias the outcome, resulting in a closed pan-genome. We concluded that including many closely related strains (i.e., from an outbreak) in a pan-genome study could bias the results of the pan-genome state (open versus closed). We suggest using a normalization step to choose strains for inclusion in the study or taking a bootstrapping approach as we did: first run all genomes to identify ortholog/paralog clusters, build a BSR tree, normalize isolate collection for diversity, then re-run the analysis a second time using the final strain list. The bootstrap approach may also be useful in situations where a non-target contaminant strain has been sequenced or an isolate has been misidentified, thus also serving as a quality control step.

Assembly of core proteins and fGIs into a pan-chromosome
To facilitate analysis and interpretation of this large pan-genome dataset, an unsupervised approach was developed and implemented through a novel graph-based algorithm to assemble ortholog clusters of core proteins (75 % core definition) into the first reference-independent consensus core "pan-chromosome" of a bacterial species. This formed the foundation for the identification and placement along the core pan-chromosome of fGIs that are highly flexible and variable across the group of isolates. Both circular and linear "assemblies" were produced, where the core pan-chromosome clusters assembled into a circle of 3126 genes, which is roughly the size estimated for the 95 % core definition. The linear cluster assemblies were the fGIs that can be placed on the core pan-chromosome, making up fGRs, while the non-core circular cluster assemblies were identified as plasmids and circular phage genomes. There is increased interest in these extra-chromosomal prophages as sources of virulence factors [83] and as vehicles for rapid adaptation to changing environments in a "carrier state" [84]. The circular nature of these extra-chromosomal phage genomes is often not observed; however, our novel assembly algorithm can distinguish both circular and linear forms of prophages as circular and linear fGIs, respectively.

Overall, analysis of genes encoded on fGIs confirms previously identified catabolic diversity and reiterates the versatility and adaptation of *A. baumannii* to survive and thrive in a variety of environments where nutrients are scarce. The occurrence of alcohol and aldehyde dehydrogenase genes in fGIs of hospital-isolated strains could be an indication of the ability of *Acinetobacter* to thrive in the presence of ethanol disinfectant reagents. With regard to the unexpected finding of additional copies of essential housekeeping genes such as the tRNA synthetases, we do not know the function of these additional copies or the purpose for having additional copies. Experiments will have to be conducted to determine whether these fGIs carrying the aaRS genes can complement the core aaRS genes and under what conditions they may be expressed.

Chan *et al. Genome Biology* (2015) 16:143

Page 19 of 28

Virulence factor diversity and strain fitness for host survival

It is noteworthy that among the ten classes of genes and gene clusters previously shown to be associated with virulence and fitness, to our surprise, a high genomic diversity was observed in genes involved in adhesion (type I pili assembly), iron acquisition (siderophore production), and efflux pumps among the 249 isolates studied.

Functional characterization of type I pili cluster 1 (*csuAB-E*, A1S_2213 to A1S_2218) has shown that its expression is required for biofilm formation and attachment to abiotic surfaces such as plastic medical devices (e.g., ventilator tubes and catheters). Interestingly, a *csu*-deficient strain showed a loss of long appendages while retaining short pili on the cell surface and also enhanced attachment to an increased number of bronchial epithelial cells [75]. As previously reported [36], we also observed a relatively higher incidence of *csu*-deleted isolates in respiratory samples among the UH clade B isolates which belong to CC2. It is tempting to hypothesize that the loss of the *csu*-encoded pili is related to niche specialization for increased invasiveness or enhanced survival at specific sites of infection, such as the respiratory epithelium.

Siderophores are iron-scavenging systems utilized by pathogens to survive in mammalian host environments. Besides siderophore gene cluster 3 (which encodes the well characterized acinetobactin system), it is unclear what types of siderophores (e.g., catecholate, phenolate, hyroxamate, carboxylate or mixed) are produced from the other three siderophore clusters in the *A. baumannii* genome. It is conceivable that the acquisition of cluster 2, specifically among the four US military MRSN wound-isolates, is to produce a novel or stealth type of iron scavenger to circumvent host iron defense systems (e.g., catechol-type siderophore inhibitor siderocalin [85]) or outcompete other bacteria.

Also potentially pertinent to iron scavenging, a novel 7.8 kb non-RI GI with a best match to the environmental isolate *A. calcoaceticus* PHEA-2 was identified at the acetylT hot spot among all seven ST 25 isolates analyzed. One of the ORFs located on the 7.8 kb GI encodes salicylate monooxygenase, which converts salicylate to catechol. In principle, catechol can directly serve as an iron carrier or building block for siderophore synthesis. Functional analysis will be necessary to determine whether the specific acquisition of this salicylate monooxygenase can increase the capacity for iron acquisition, making it a novel mechanism that can reinforce and diversify siderophore production in this pathogen.

WC-487 is one of the strains sequenced in this study and originally thought to be *A. baumannii*. Both WC-487 and SDF showed a general loss or absence of genes for the virulence factors analyzed. The lack of key virulence factors in the human louse strain SDF supports the idea that although currently classified as *A. baumannii*, SDF has adapted to a life style different from that of a human pathogen. For WC-487, multiple lines of evidence, such as placement on both the BSR and SNP trees and the absence of key virulence determinants, suggest that WC-487 is truly not *A. baumannii*. Indeed, matrix assisted laser desorption ionization time-of-flight (MALDI-TOF) mass spectrometry results suggest that WC-487 instead belongs to *Acinetobacter nosocomialis* (X-Z Huang, manuscript in preparation).

Dynamics of drug resistance genes and RIs

Drug resistance genes are acquired via IS elements and small composite transposons. The association with IS elements, which are repetitive and classically result in the misassembly of sequence data, are also problematic during the assembly of protein clusters. Using the fGI approach, we only detected drug resistance genes associated with an RI in the *comM* hot spot, but not the other three hot spots. Even with this limitation, we were able to identify three of the four known RI insertional hot spots as fGRs. Our algorithm was also able to identify a potentially novel RI, encoding a putative metallo-beta-lactamase in two of our sequenced military isolates. We identified a ~38 kb fGI within the *astA* region that is similar in size to the ~40 kb deletion that is known to have occurred in some strains [40], which highlights the point that fGIs can be insertions or deletions.

Interestingly, analysis of the drug resistance profiles and genome sequences of the military isolates revealed a potentially novel *parC* mutation (Glu88Lys) in strain Naval-83, which could be associated with quinolone resistance in *A. baumannii*. This mutation has been shown to confer resistance to a third generation quinolone (levofloxacin) in *Haemophilus influenzae* [36] and may, therefore, by analogy also do so in *A. baumannii*. Incidentally, we also observed this same mutation in *A. baumannii* 1656-2 [86]; however, its resistance to levofloxacin was not communicated, stressing the need to publish antibiotic drug resistance profiles alongside genomic data.

Vertical and horizontal transmission of RIs

Two major questions of RI transmission are whether they are vertically or horizontally acquired and in how many genomic locations they can reside. Since the presence of IS elements resulted in fragmented genomic and pan-chromosome assemblies, we developed a high-throughput three-step bioinformatics approach to define the type and location of RIs in individual isolates to answer these questions. The approach included the identification of gene fragments at insertion hot spots, recruitment of genomic contigs using RI references and confirmation for the

Chan *et al. Genome Biology* (2015) 16:143

Page 20 of 28

presence of antibiotic resistance gene cassettes. Based on the classification of isolates by RI signatures and phylogenetic distance defined by a SNP tree, our results revealed that clonal expansion and vertical inheritance of specific RI signatures are commonly observed (e.g., CC1, CC2, CC3, ST 25). Additionally, the accumulation of RIs at multiple hot spots within an isolate also suggested a combined dual mode of transmission that includes both vertical transmission of the *comM*-RI and horizontal acquirement of RIs at secondary locations.

Dynamics of RI insertions and virulence/fitness determinants

Since the *A. baumannii* isolates analyzed in this study were collected throughout several decades between 1951 and 2011, we had an opportunity to follow the evolution of genomic determinants such as RIs and virulence factors during this timeframe. Comparing single to multi-RI existence in an individual genome, the ratio is 6:1 (n = 7) in pre-2000 isolates versus 0.9:1 (n = 125) in post-2000 isolates. Despite the limited sample size within the pre-2000 group, there is a prevalence of multi-RI insertions among modern isolates. Specifically, by considering the same set of insertional hot spots among pre-2000 and post-2000 isolates, the post-2000 isolates have a higher prevalence of these sites occupied, which likely resulted from selective pressure from the increased use of antibiotics in recent years and possibly higher sampling rates post-2000. There were also strains with no RI insertion detected. Considering the draft status of most genomes analyzed, more isolates need to be finished, particularly for older isolates that are not well represented.

It is interesting to note that the earliest gain or loss events can be traced back to isolates collected from two or more decades ago. For example, the lack of different type I pili clusters were first observed in strains NIPH 528 (ca. 1982), NIPH 60 (ca. 1992), and NIPH 335 (ca. 1994), which are among the oldest strains in this dataset (Additional file 20). Similarly, the earliest isolates showing the presence of siderophore cluster 2 and the absence of siderophore cluster 1 were ATCC 17978 (ca. 1951) and NIPH 190 (ca. 1993), respectively. These results suggest the early existence of genetic determinants controlling virulence and pathogenesis in decades-old isolates and their recent reemergence amongst modern isolates as shown in this study.

Conclusions

We conducted the largest bacterial pan-genome analysis (249 genomes) of *A. baumannii* and determined that this pan-genome is open when the input genomes are normalized for diversity. A novel graph-based algorithm was developed and implemented to assemble ortholog clusters of core proteins into the first reference-

independent "pan-chromosome" of a bacterial species, which was essential for mapping fGIs to fGRs. We concluded that the observed PFGE diversity of the 50 selected military isolates was mostly due to differences in fGI content rather than chromosomal rearrangements as no rearrangements of large contigs were detected; however, our ability to detect rearrangements is limited due to the fragmented nature of the genome assemblies.

We utilized a comparative genomics approach to analyze the diversity of RIs and virulence factors of *A. baumannii*. We demonstrated the existence of novel RIs and isolates with an increased number of RI insertions over time. Clusters of genes for carbon utilization, siderophore production, and pili assembly were highly variable, which may contribute to the success of *A. baumannii* in surviving and adapting to different and changing environments. A vast collection of genetic determinants and mechanisms to control antibiotic resistance and survival adaptations existed in decades-old isolates, and these genetic mechanisms appear to have reemerged among modern isolates, sometimes in different genomic locations. The comprehensive comparisons of the highly variable and flexible genomic features in the context of whole genome phylogeny will serve as genetic landmarks for surveillance and prediction of outbreaks, understanding the epidemiology of globally distributed isolates and identifying clonal origins of nosocomial infections of *A. baumannii* across healthcare institutions.

Materials and methods

Ethical statement

Per WRAIR Policy 12-09, the use of bacterial isolates without associated human data does not require a determination from the institutional review board or Human Subjects Protection Branch, the corresponding regulatory office.

Strain isolation and verification

All 50 strains sequenced in this study were isolated at US military healthcare facilities [15, 87, 88] and identified as *A. baumannii* by standard automated biochemical analysis as described previously [8]. PFGE and 16S rRNA typing was also used to further validate species-level classification from genomic DNA prepared as described [20].

Antimicrobial susceptibility tests

Antimicrobial susceptibility tests were performed on all isolates at the Walter Reed Army Medical Center clinical laboratory using the commercially available BD Phoenix NMIC/ID133 panel (Becton, Dickinson and Company, Franklin Lakes, NJ, USA). Susceptibility was determined according to Phoenix criteria and CLSI M-100-S-19, Vol.29, No.3 2009. For MRSN 58, antimicrobial

Chan *et al. Genome Biology* (2015) 16:143

Page 21 of 28

susceptibility tests were performed using the commercially available Siemens MicroScan panel.

Genome sequencing

The genomes of 50 *A. baumannii* isolates were sequenced at JCVI by Illumina HiSeq (2 × 100 bp), or a combination of Illumina HiSeq and 454 FLX Titanium. Additionally, MiSeq (2 × 150 bp), IonTorrent PGM, 454 libraries, and OpGen optical restriction maps generated by WRAIR were available to aid in gap closure for certain MRSN strains. Briefly, paired-end libraries were constructed for each sequencing technology from randomly nebulized genomic DNA in the 300–800 bp (Illumina) and 2–3 kb (454) size ranges following manufacturer recommendations. Sequence reads were generated with a target average read depth of ~20–30 fold (454) and ~60 fold (Illumina) coverage.

Draft genome assembly

Sequences for the non-MRSN isolates were assembled using the Celera Assembler version 6.1 [89]. Assembled contigs undergoing further genome finishing (n = 10) and automated gap closure (n = 7) were ordered based on alignment against the best-matching complete *A. baumannii* reference genome using NUCmer [90]. Mapped contigs were never broken even if the contig matched different regions of the reference genome — the longest match was used for placement. Mapping merely entailed ordering and orienting the contigs with small spacers inserted between the contigs. As a result, all core gene adjacency information within the contigs was retained. Ten of the 42 genomes underwent manual gap closure to elevate the genome status to IHQD (Table 1).

For the seven MRSN isolates, we explored several assembly strategies to integrate the JCVI Illumina HiSeq data with data generated through various sequencing platforms by WRAIR. We decided to employ a pipeline that combined *de novo* assembly followed by automated reference-guided gap closure to resolve short and uncomplicated gaps <3.5 kb in length. JCVI sequence reads were assembled with Velvet version 1.0.19 [91] and optimized using the VelvetOptimiser 2.2.0 [92]. The Velvet assembly served as the backbone while other *de novo* assemblies of the WRAIR libraries built with Celera assembler version 7.0 or Velvet version 1.0.19 served as references from which the gap sequences would be predicted. In the first round of gap closure, optical maps (OpGen) were used to validate the assembly as well as to order and orient the backbone contigs using SOMA [93]. Automated gap closure consisted of the following processes: 1) to determine gap regions, consecutive contig ends were identified by alignment against the consensus sequence generated from various *de novo* assemblies using NUCmer [90]; 2) the identified contig ends were used to recruit reads from the

JCVI Illumina paired-end library using Burrows-Wheeler Aligner (BWA) 0.7.3 [94]; 3) the recruited reads were assembled using the CLC command line tool *clc_mapper* from *clc-assembly-cell* v.4.0.11 [95] by mapping the recruited reads from step 2 to the gap regions from step 1 to generate a new consensus sequence for each of the gaps; 4) the contigs, and if available, the new gap sequences from step 3, were stitched together to resolve the gaps; 5) the CLC *clc_find_variations* command line tool, also from *clc-assembly-cell* v.4.0.11, was run to validate the new consensus sequence by determining the existence of any 0× coverage regions. If any 0× regions were found, the original gap remained. BLAST v.2.2.28 [96] was then used to select the closest matching complete *A. baumannii* genome in GenBank to serve as the reference for scaffolding the resulting contigs from the first round of the automated gap closure, using NUCmer [90] alignments. The contigs then proceeded through a second round of the automated gap closure process.

Annotation

Contigs were annotated for protein- and RNA-encoding features using the JCVI automated annotation pipeline essentially as described previously [44, 47, 97, 98] except hidden Markov models were run using HMMER3 [99].

Identification of antibiotic resistance genes

Genes conferring drug resistance were identified using the RGI (Resistance Gene Identifier, version 2) tool in CARD (Comprehensive Antibiotic Resistance Database) [100]. For each genome in this study (Table 1) a multi-FASTA composite file was loaded into RGI and the output saved for further parsing. Results were filtered by selecting the highest percent identity match for each ORF. Genes that were regulators or modulators were filtered out. Genes identified were classified by their antibiotic resistance ontology assigned by CARD; ontologies are based on resistance mechanisms, determinants and targets.

Several other genes were identified by BLAST analysis. A database of additional drug resistance genes was compiled from the GenBank accessions of previously curated lists [17, 101]. Genomes were searched against this database using BLASTP and unique ORFs not already identified by RGI were examined. Matches with >90 % amino acid identity were assigned a classification.

MLST analysis

MLST was determined using an in-house automated pipeline that first searches for homologs of each gene of the typing schema (*cpn60:fusA:gltA:pyrG:recA:rplB:rpoB*) from [73, 102], using BLASTN [96]. MLST homologs were extracted from the genome sequence and

Chan *et al. Genome Biology* (2015) 16:143

Page 22 of 28

compared with an MLST allele database to generate the allele number and ST for each genome.

Pan-genome analysis

Clusters of orthologous proteins were generated (Additional file 5) by version 3.18 of PanOCT [35] using default parameters (Additional file 23). In order to plot "power law and exponential regressions for new genes discovered with the availability of additional genome sequences", as defined by Tettelin et al. [41], we adapted the R scripts, *compute_pangenome.R* and *plot_pangenome.R*, from Park et al. [103] and developed a Perl script, *paralog_matchtable.pl*. Since PanOCT does not place paralogs into its ortholog clusters, but does produce a *paralogs.txt* file that specifies which clusters are paralogs, an in-house PERL script, *paralogs_matchtable.pl*, was created to merge paralogous clusters (Additional file 23). This is necessary because analysis of core and novel genes has historically been defined for clusters containing all paralogs [42, 103–107]. In the past, core and novel pan-genome plots were computed from all possible combinations in genome order, but this is computationally prohibitive when the number of genomes is over 100. To overcome this limitation, *compute_pangenome.R* was modified to randomly sample without replacement a subset of 500 combinations in genome order of addition. The output of this script is a set of data where each row contains columns for core, dispensable, unique, and genes novel for the last genome added. The *plot_pangenome.R* script computes the medians of the *compute_pangeome.R* output and uses the nonlinear least squares, *nls*, function in R to find power law and exponential models to fit the medians.

Consensus assemblies of the core and the flexible parts of the *A. baumannii* pan-genome were calculated using outputs from PanOCT. The consensus core pan-chromosome was computed by running an in-house PERL script, *gene_order.pl*, using the PanOCT *75_core_adjacency_vector.txt*, *0_core_adjacency_vector.txt*, and the centroids.fasta output files as input (Additional file 23). The *75_core_adjacency_vector.txt* file lists the set of adjacent core gene clusters (called "adjacencies") and specifies which genomes contain them. Core gene clusters are defined as gene clusters conserved in at least some threshold number of genomes (e.g., 75 %). A core gene cluster is adjacent to another core gene cluster in a given genome if the representative cluster members for that genome are adjacent (i.e., they are on the same contig and have no other core genes between them). The consensus assembly of the core gene clusters is the set of adjacencies supported by the largest number of genomes (Additional file 8).

Conceptually, the order and orientation of these clusters can be depicted as linear or circular arrangements, analogous to sequence assembly. The linear paths can result from contig breaks, linear chromosomes or plasmids, or because there is a disagreement in the juxtaposition of neighboring core clusters between two or more genomes. The circular paths can represent circular chromosomes, plasmids or occasionally small elements that are inverted in different genomes.

fGIs were defined in [50] as GIs encoding similar types of functions (e.g., O-antigen, phage, pili), having the same genomic location, but a variable gene content. We define fGIs more loosely to be variable (i.e., "flexible") linear assemblies of noncore genes present between core gene clusters. These assemblies were constructed and the fGIs identified using the same *gene_order.pl* script; however, the PanOCT output file *0_core_adjacency_vector.txt* is used (0 % threshold) as input so that all gene clusters are considered, not just core gene clusters (Additional file 9). The fGIs are not allowed to extend into core gene clusters already in the core pan-genome; rather, they are terminated at a core gene cluster and the core gene cluster is labeled as an fGI insertion site.

Pan-genome tree

A UPGMA (unweighted pair group method with arithmetic mean) tree was constructed using the mean of the BSR as described previously [108]. The PanOCT output file *100_pairwise_BSR_distance_matrix_phylip.txt* was used as input for Neighbor [109, 110] to build an unrooted tree. This PanOCT output file is a Phylip-style distance matrix derived from the pairwise mean BSR of core proteins present in 100 % of genomes where a single value is presented for each pair of genomes in the pan-genome.

SNP tree

A phylogenetic tree was inferred from SNPs identified among 253 *Acinetobacter* genomes. SNPs were identified by kSNP [111] with a requirement that at least 80 % of the genomes (i.e., 203 genomes) have a nucleotide at a given SNP position in order for the SNP to be considered for inclusion in downstream analysis. A total of 207,619 identified SNP positions were further filtered to remove SNPs in regions likely undergoing recombination by detecting regions with unusually highly SNP density. For this filtering step, a set of pairwise SNPs was identified between the finished genome of *A. baumannii* ACICU and related ST 2 genomes using the SNP export functionality within progressiveMauve [112]. The pairwise SNP density was computed based on ACICU positions shared among a subset of genomes with the fewest total number of pairwise SNPs. Any regions with higher than 10 SNPs/kb for any strain were considered as potential recombination regions. After filtering out these regions there were 152,995 presumed non-recombinant SNPs. These SNPs were used to generate

Chan *et al. Genome Biology* (2015) 16:143

Page 23 of 28

a maximum-likelihood tree using RAxML [113] with 100 bootstrap replicates.

Identification of RI signatures

A high-throughput approach was developed to identify RI signatures for 249 isolates, including draft genome assemblies. In draft genomes, RIs are often poorly assembled due to repetitive elements. In this approach, the RI signatures were determined based on: (i) junction fragments of target genes, (ii) sequence similarities to previously reported RIs and homology to antibiotic resistance cassettes within individual RIs. First, the presence of target gene junction fragments was identified using a BLASTN search against five target genes known to harbor RIs in *A. baumannii* (Additional file 11). A summary of target gene lengths when intact or carrying junction fragments in the presence of RI insertion is shown in Additional file 12h. Second, contigs identified to carry the target gene and junction fragments were searched against a collection of carefully selected RIs, which captures the diversity of RIs identified to-date (Additional file 11), using BLAST and NUCmer [90]. RI signature assignments were performed based on BLAST similarity and mummerplot alignments to the set of reference RIs. An example RI signature assignment for *comM* is shown in Additional file 12i.

Gain/loss of virulence factor gene clusters

For every gene of interest, the average BSR value between the centroid protein of the ortholog cluster and the ortholog protein identified in each isolate were obtained from the PanOCT output (e.g., *pairwise_in_cluster.txt* and *centroids.fasta*). We use the term "centroid", which is technically the medoid, to be a representative protein sequence of a cluster whose average dissimilarity to all the sequences in the cluster is minimal [114]. An average BSR value close to 1 indicates identical sequences, a value near 0 indicates absence of the protein in the given isolate, and a value around 0.5 suggests a truncation of the protein with respect to the centroid. A matrix of averaged BSR values between centroid-ortholog pairs was constructed with genes as rows and isolates as columns (Additional file 19).

To identify initial evidence of gain or loss of gene clusters at the ortholog protein level, the centroid-to-ortholog BSR matrix was analyzed using hierarchical clustering in MeV version 4.9.0 [115]. Additionally, regions of gene cluster gain/loss and flanking genomics sequences were then examined at the genomic contig level using pairwise sequence alignments by MUMmer version 3.0 [116]. Alignments of genome contigs comparing selected reference genomes and isolates of interest to show gain/loss of gene clusters were plotted using EasyFig [117]. The set of *A. baumannii* virulence genes analyzed is shown in Additional file 17. The genomic

locations of virulence genes and RI insertions studied are summarized in Additional file 24.

Software, genome sequences, and raw data availability

The pan-genome analysis software developed and implemented in this study, including *panoct.pl* version 3.18, *paralog_matchtable.pl*, and *gene_order.pl* are publicly available in the code section of the PanOCT SourceForge page [118], under the GNU General Public License.

GenBank accession numbers for the 50 genomes that were sequenced, assembled and annotated in this study are listed in Table 1 and Additional file 2. The whole genome sequencing data are available at [119] under the following accession numbers: AFCZ00000000, AFDA00000000, AFDB00000000, AFDK00000000, AFDL00000000, AFDM00000000, AFDN00000000, AFDO00000000, ALAL00000000, ALII00000000, AMDE00000000, AMDF00000000, AMDQ00000000, AMDR00000000, AMEI00000000, AMEJ00000000, AMFH00000000, AMFI00000000, AMFK00000000, AMFL00000000, AMFP00000000, AMFS00000000, AMFT00000000, AMFU00000000, AMFV00000000, AMFW00000000, AMFX00000000, AMFY00000000, AMFZ00000000, AMGA00000000, AMGE00000000, AMGF00000000, AMGG00000000, AMGH00000000, AMSW00000000, AMSX00000000, AMSY00000000, AMSZ00000000, AMTA00000000, AMTB00000000, AMZR00000000, AMZT00000000, AMZU01000000, JPHV00000000, JPHW00000000, JPHX00000000, JPHY00000000, JPHZ00000000, JPIA00000000, JPIB00000000. The raw sequence reads generated at JCVI are available at [120] under the following accession numbers: SRR1945422, SRR1945425, SRR1945426, SRR1945427, SRR1945428, SRR1945430, SRR1946597, SRX027591, SRX027592, SRX027593, SRX027595, SRX027596, SRX027597, SRX031272, SRX031273, SRX031275, SRX032336, SRX101596, SRX101598, SRX101601, SRX101602, SRX101603, SRX101604, SRX101606, SRX101793, SRX101794, SRX101795, SRX101796, SRX101797, SRX101798, SRX101800, SRX110040, SRX110090, SRX110091, SRX110092, SRX110095, SRX110096, SRX110097, SRX110098, SRX110099, SRX110100, SRX110101, SRX110102, SRX110103, SRX110104, SRX110105, SRX110106, SRX110107, SRX110109, SRX110110, SRX110111, SRX110112, SRX110113, SRX110114, SRX110115, SRX110118, SRX110119, SRX110120, SRX110121, SRX110122, SRX110123, SRX110124, SRX110125, SRX110126.

The combined JCVI-annotated fasta-formatted amino acid sequences and combined attribute files required for *panoct.pl* are available as Additional files 25 and 26, respectively. An essential set of raw output files from

Chan *et al. Genome Biology* (2015) 16:143

Page 24 of 28

panoct.pl and *gene_order.pl* is also available in Additional file 27.

Additional files

Additional file 1: Figure S1. Pulse field gel electrophoresis (PFGE) of *A. baumannii* isolates collected from the Military healthcare system. A dendrogram was produced based on the analysis of PFGE banding patterns. Genomic DNA was digested with ApaI, separated by clamped homogenous electric fields (CHEF) gel electrophoresis and analyzed with the Dice coefficient as described previously [15]. Isolates with greater than or equal to 90 % similarity are considered to be the same strain. Strain names are noted at the right and their corresponding MLST sequence types in parentheses.

Additional file 2: Table S1. GenBank identifiers for *A. baumannii* genomes sequenced at JCVI in this study.

Additional file 3: Table S2. Antibiotic resistance susceptibility profiles and predicted resistance mechanisms for *A. baumannii* genomes sequenced in this study.

Additional file 4: Table S3. All *A. baumannii* isolates used in this study.

Additional file 5: Text file of all PanOCT clusters.

Additional file 6: Figure S2. Phylogenetic tree of the *A. baumannii* pan-genome. A dendrogram was constructed based on the mean of the pairwise BLASTP score ratios (BSRs) of core protein clusters that were present in 100 % of all 249 *A. baumannii* isolates constituting the pan-genome. The BSR tree was generated from the PanOCT-derived BSR distance matrix using the Interactive Tree of Life (iTOL). The five most abundant MLST sequence types with available genome sequence are illustrated by color highlights (see inset key). The 50 isolates sequenced in this study are noted with a *red bar* on the outside of the tree. Genomes chosen for sub-sampling of the pan-genome by hierarchical clustering are marked with a *gold bar* on the outside of the tree.

Additional file 7: Figure S3. *A. baumannii* pan-genome of ST 2 genomes. The pan-genome size (*left column*) and the number of novel genes discovered with the addition of each new genome (*right column*) were estimated for 111 ST 2 genomes using a pan-genome model based on the original Tettelin et al. model [42]. *Purple circles* are the median of each distribution (*gray circles*). Power law (*red lines*) and exponential (*blue lines*) regressions were plotted to determine α (open/closed status) and tg(θ), the average extrapolated number of strain-specific/novel genes, respectively.

Additional file 8: Text file of cluster assembly composition.

Additional file 9: Text file of the location and composition of fGRs.

Additional file 10: Table S4. Chromosomally encoded antibiotic resistance genes found within fGIs and fGRs.

Additional file 11: Table S5. Resistance island target sites.

Additional file 12: Table S6. a Distribution of RI-positive isolates among *A. baumannii* genomes analyzed. **b** Summary of major RI signatures identified among CC1, CC2, CC3, and ST 25 isolates. All RI signatures identified in (**c**) CC1, (**d**) CC2, (**e**) CC3, (**f**) ST25, and (**g**) other isolates. **h** A list of RI target genes showing total gene length detected when intact and having no RI insertion, or carrying a RI insertion with junction fragments. **i** Total gene length of the *comM* target gene detected in a collection of finished *A. baumannii* genomes.

Additional file 13: Figure S4. *A. baumannii* whole genome SNP tree. A whole genome SNP tree was constructed for 249 *A. baumannii* genomes and four *Acinetobacter* spp. genomes. Major clonal complexes (CC1, CC2, and CC3), ST 25, and US hospital isolates forming CC2 UH clades A-E are highlighted with a colored background (see key) [40]. A colored box following the strain name marks the 50 isolates sequenced in this study (*red*) and the finished public reference genomes (*blue*). The annotation table (*right*) summarizes (i) RI signatures and (ii) virulence factor diversity reported in this study. See main text for a more detailed description. Briefly, (i) RI insertions were examined at the following gene loci: *comM*, *pho*, *astA*, acetylT, acylCS, and a hypothetical protein (Additional file 11). Specific RI

insertion types detected at individual insertion loci were reported. A colored cell in the RI section of the annotation table represents the presence of an RI feature for a given isolate. For example, AbaR3 and AbaR4 type RIs are found at *comM* in CC1 isolates, whereas AbGRI1 type RIs instead are detected at *comM* in CC2 isolates. "*P*" was used to indicate that the Tn*1548* RI was detected on a plasmid in three finished genomes instead of the acetylT locus located on the chromosome (this study) [79]. "#" RI was previously reported at the *astA* locus but not in this study [71]. "***", "**", and "*S*" represent extreme antibiotic resistance, strong resistance, and susceptible to antibiotics as determined in this study, respectively (Additional file 3). The *black triangle* indicates a branch node where the loss of AbGRI1 insertion at the *comM* locus is suspected. Previously reported Aba-type RIs are listed in black bold to the right of the annotation table. (ii) Virulence factor diversity was detected as specific gain or loss of gene clusters involved in type I pili assembly, siderophore production, or efflux. In general, a colored cell in the virulence section of the annotation table represents the detection of a genomic variation, which in most cases indicates the loss of a gene cluster in a given isolate; the only exception is for siderophore cluster 2 in which a colored cell represents the specific gain of the gene cluster in the isolate. For example, type I pilus cluster 1 (*csu*) was lost in two ST 10 isolates, and also a subset of ST 2 isolates including the entire group of nine UH clade B strains and also the multi-drug resistant strain MDR-ZJ06. In contrast, across all 249 isolates analyzed, siderophore cluster 2 was only detected and thus specifically gained in ATCC 17978, and also six isolates belonging to strain types ST 81 and ST 94. A SNP matrix file containing 150,000 genomic variants for SNP tree construction is provided as Additional file 14.

Additional file 14: Text file of SNP variants identified across 150,000 genomic positions (ACICU reference coordinates) and 249 *A. baumannii* isolates analyzed. This file was compressed using tar and 7-Zip (a).

Additional file 15: Figure S5. Novel composite IS26 RI inserted into the acylCS gene locus. ACICU was used as a reference to show that an 18 kb composite IS26 RI replaced the original 8 kb genomic region in RI-positive isolates. The composite RI contains two resistance gene cassettes. The oldest isolate was NIPH 1669 (1997), which only carried the 5′ fragment of the composite IS26 RI including one resistance gene cassette. Pairwise nucleotide identity shown in a *red* to *blue* (100 % identity) color scale. Key: ORFs (*arrows*); drug resistance genes located on RI (*green*); deleted genes (*gray*); immediate RI flanking genes acylCS and a predicted exporter (*dark orange*); other flanking genes (*orange*).

Additional file 16: Figure S6. Novel genomic fragment inserted into the acetylT gene locus. AB307-0294 was used as a reference to show the RI and non-RI type insertions found at the acetylT locus. **a** A 7.8 kb non-RI fragment was detected juxtaposed to the acetylT locus across all ST 25 isolates analyzed. The annotated salicylate monooxygenase gene located on the genomic fragment could be involved in catechol production. **b** A Tn*1548* RI insertion was detected at the acetylT locus in other isolates (e.g., multi-drug resistance MDR-TJ isolate). Pairwise nucleotide identity shown in a *red* to *blue* (100 % identity) color scale. Key: open reading-frames (*thick arrows*); drug resistance genes located on RI (*green*); RI insertion target acetylT (*dark green*); RI flanking genes (*orange*).

Additional file 17: Table S7. Virulence and fitness factors used in this study.

Additional file 18: Figure S7. Diversity of virulence and fitness factors based on centroid-to-ortholog BSR. Genomic regions involved in assembly of type I pili, siderophore production, and efflux were highly variable and showed specific gain or loss of the entire gene clusters in isolates analyzed. In the heat map, the presence, absence, and low similarity of a protein ortholog compared with its centroid is shown in *yellow* (BSR = 1), *blue* (BSR = 0), and *gray*, respectively. The list of virulence genes analyzed and the BSR-derived heat map file are provided in Additional files 17 and 19, respectively.

Additional file 19: Excel file containing the distance matrix of centroid-ortholog pairs based on BSR.

Additional file 20: Table S8. Diversity of type I pili gene clusters in isolates analyzed.

Additional file 21: Figure S8. Loss of type I pili cluster 3 gene cluster. A complete loss of the type I pilus cluster 3 was observed in all ST 2 isolates

Chan *et al. Genome Biology* (2015) 16:143

Page 25 of 28

(e.g., ACICU, Naval-78, NIPH 528) and additional strain types including ST 25 (e.g., Naval-18, NIPH 146), ST 79 (e.g., UH7907), ST 113, ST 215, and others. Pairwise nucleotide identity shown in a *red* to *blue* (100 % identity) color scale. Key: open reading-frames (*thick arrows*); type I pilus cluster 3 (*green*); genes immediately flanking deletion (*dark orange*); other flanking genes (*orange*).

Additional file 22: Figure S9. Loss of siderophore cluster 1 gene cluster. A complete loss of siderophore cluster 1 was observed in six isolates of mixed strain types, but within short phylogenetic distance as shown on the whole genome SNP tree. Pairwise nucleotide identity shown in a *red* to *blue* (100 % identity) color scale. Key: open reading-frames (*thick arrows*); siderophore cluster 1 (*green*); genes immediately flanking deletion (*dark orange*); other flanking genes (*orange*).

Additional file 23: Command line arguments used for running NCBI. *blastall, panoct.pl, paralog_matchtable.pl, and gene_order.pl.*

Additional file 24: Figure S10. Genomic locations of RIs and virulence factors analyzed in this study. The ACICU genome was used as a reference backbone to show genomic features analyzed in this study. Note that not all features were detected in the ACICU genome.

Additional file 25: The JCVI-annotated combined amino acid fasta file used as input to *panoct.pl*. This file was compressed using tar and 7-Zip (a).

Additional file 26: The combined genome attribute file required to run *panoct.pl*, which contains contig identifiers, protein identifiers, coordinates of protein coding regions, protein annotation, and genome identifiers. This file was compressed using tar and 7-Zip (a).

Additional file 27: A minimal set of output files generated by *panoct.pl* and *gene_order.pl*. Also included are look-up tables to cross reference JCVI internal genome identifiers with GenBank identifiers as well as to cross-reference JCVI internal locus names with GenBank locus names. Note that many more output files were generated, which are informative, but not required to interpret the results of pan-genome analysis, except the output file of paralog_matchtable.pl, which was too large and easily made from the provided files. This file was compressed using tar and 7-Zip (a).

Abbreviations
aaRS: aminoacyl tRNA synthetase; acetylT: acetyltransferase; acylCS: acyl-CoA synthase; ATCC: American Type Culture Collection; bp: base pair; BSR: BLAST score ratio; BWA: Burrows-Wheeler Aligner; CARD: Comprehensive Antibiotic Resistance Database; CC: clonal complex; CDC: Centers for Disease Control and Prevention; cGC: core gene cluster; fGI: flexible genomic island; fGR: flexible genomic region; GI: genomic island; HQD: high-quality draft; IHQD: improved high-quality draft; IS: insertion sequence; JCVI: J. Craig Venter Institute; kb: kilobase; Mbp: megabase pair; MDR: multidrug-resistant; MLST: multilocus sequence typing; MRSN: Multidrug-resistant Organism and Surveillance Network; ORF: open reading frame; PCR: polymerase chain reaction; PFGE: pulsed-field gel electrophoresis; RGI: Resistance Gene Identifier; RI: resistance island; SNP: single nucleotide polymorphism; ST: sequence type; Tat: twin-arginine translocation; WRAIR: Walter Reed Army Institute of Research.

Competing interests
The authors declare that they have no competing interests.

Authors' contributions
APC, GS, and DEF designed and coordinated studies; XZH, MPN and EPL performed analysis and interpretation of PFGE data; MPN and EPL selected isolates for genome sequencing; XZH, MPN and EPL provided genomic DNA for genome sequencing; APC and DEF organized and led the sequencing studies; MK and DMH assembled and annotated the genomes. APC, GS, JD, RK, YC, EB, and DEF analyzed the genomic data; and APC, GS, JD, RK, YC, XZH, DMH, and DEF prepared the manuscript. All authors read and approved the final manuscript.

Author details
[1]J. Craig Venter Institute (JCVI), Rockville, MD, USA. [2]Department of Emerging Bacterial Infections, Bacterial Diseases Branch, Walter Reed Army Institute of Research, Silver Spring, MD, USA. [3]Multidrug-resistant organism Repository and Surveillance Network, Bacterial Diseases Branch, Walter Reed Army Institute of Research, Silver Spring, MD, USA.

Published online: 21 July 2015

References
1. Roca I, Espinal P, Vila-Farres X, Vila J. The *Acinetobacter baumannii* oxymoron: commensal hospital dweller turned Pan-drug-resistant menace. Front Microbiol. 2012;3:148. doi:10.3389/fmicb.2012.00148.
2. Peleg AY, Seifert H, Paterson DL. *Acinetobacter baumannii*: emergence of a successful pathogen. Clin Microbiol Rev. 2008;21:538–82. doi:10.1128/CMR.00058-07.
3. Sebeny PJ, Riddle MS, Petersen K. *Acinetobacter baumannii* skin and soft-tissue infection associated with war trauma. Clin Infect Dis. 2008;47:444–9. doi:10.1086/590568.
4. Mihu MR, Martinez LR. Novel therapies for treatment of multi-drug resistant *Acinetobacter baumannii* skin infections. Virulence. 2011;2:97–102.
5. Howard A, O'Donoghue M, Feeney A, Sleator RD. *Acinetobacter baumannii*: an emerging opportunistic pathogen. Virulence. 2012;3:243–50. doi:10.4161/viru.19700.
6. CDC. Antibiotic resistance threats in the United States: US Department of Health and Human Services Centers for Disease Control and Prevention. 2013.
7. Beaumier CM, Gomez-Rubio AM, Hotez PJ, Weina PJ. United States military tropical medicine: extraordinary legacy, uncertain future. PLoS Neglect Trop Dis. 2013;7:e2448. doi:10.1371/journal.pntd.0002448.
8. Scott P, Deye G, Srinivasan A, Murray C, Moran K, Hulten E, et al. An outbreak of multidrug-resistant *Acinetobacter baumannii-calcoaceticus* complex infection in the US military health care system associated with military operations in Iraq. Clin Infect Dis. 2007;44:1577–84. doi:10.1086/518170.
9. Hujer KM, Hujer AM, Hulten EA, Bajaksouzian S, Adams JM, Donskey CJ, et al. Analysis of antibiotic resistance genes in multidrug-resistant *Acinetobacter* sp. isolates from military and civilian patients treated at the Walter Reed Army Medical Center. Antimicrob Agents Chemother. 2006;50:4114–23. doi:10.1128/AAC.00778-06.
10. Weintrob AC, Murray CK, Lloyd B, Li P, Lu D, Miao Z, et al. Active surveillance for asymptomatic colonization with multidrug-resistant gram negative bacilli among injured service members–a three year evaluation. MSMR. 2013;20:17–22.
11. Taitt CR, Leski TA, Stockelman MG, Craft DW, Zurawski DV, Kirkup BC, et al. Antimicrobial resistance determinants in *Acinetobacter baumannii* isolates taken from military treatment facilities. Antimicrob Agents Chemother. 2014;58:767–81. doi:10.1128/AAC.01897-13.
12. Vila J, Marti S, Sanchez-Cespedes J. Porins, efflux pumps and multidrug resistance in *Acinetobacter baumannii*. J Antimicrob Chemother. 2007;59:1210–5. doi:10.1093/jac/dkl509.
13. Adams MD, Nickel GC, Bajaksouzian S, Lavender H, Murthy AR, Jacobs MR, et al. Resistance to colistin in *Acinetobacter baumannii* associated with mutations in the PmrAB two-component system. Antimicrob Agents Chemother. 2009;53:3628–34. doi:10.1128/AAC.00284-09.
14. Vila J, Ruiz J, Goni P, Marcos A, Jimenez de Anta T. Mutation in the *gyrA* gene of quinolone-resistant clinical isolates of *Acinetobacter baumannii*. Antimicrob Agents Chemother. 1995;39:1201–3.

Chan *et al. Genome Biology* (2015) 16:143

Page 26 of 28

15. Lesho E, Yoon EJ, McGann P, Snesrud E, Kwak Y, Milillo M, et al. Emergence of colistin-resistance in extremely drug-resistant *Acinetobacter baumannii* containing a novel *pmrCAB* operon during colistin therapy of wound infections. J Infect Dis. 2013;208:1142–51. doi:10.1093/infdis/jit293.

16. Yoon EJ, Courvalin P, Grillot-Courvalin C. RND-type efflux pumps in multidrug-resistant clinical isolates of *Acinetobacter baumannii*: major role for AdeABC overexpression and AdeRS mutations. Antimicrob Agents Chemother. 2013;57:2989–95. doi:10.1128/AAC.02556-12.

17. Zhao WH, Hu ZQ. *Acinetobacter*: a potential reservoir and dispenser for beta-lactamases. Crit Rev Microbiol. 2012;38:30–51. doi:10.3109/1040841X.2011.621064.

18. Rumbo C, Gato E, Lopez M, Ruiz de Alegria C, Fernandez-Cuenca F, Martinez-Martinez L, et al. Contribution of efflux pumps, porins, and beta-lactamases to multidrug resistance in clinical isolates of *Acinetobacter baumannii*. Antimicrob Agents Chemother. 2013;57:5247–57. doi:10.1128/AAC.00730-13.

19. Ruzin A, Keeney D, Bradford PA. AdeABC multidrug efflux pump is associated with decreased susceptibility to tigecycline in *Acinetobacter calcoaceticus-Acinetobacter baumannii* complex. J Antimicrob Chemother. 2007;59:1001–4. doi:10.1093/jac/dkm058.

20. McGann P, Courvalin P, Snesrud E, Clifford RJ, Yoon EJ, Onmus-Leone F, et al. Amplification of aminoglycoside resistance gene *aphA1* in *Acinetobacter baumannii* results in tobramycin therapy failure. MBio. 2014;5:e00915. doi:10.1128/mBio.00915-14.

21. Corvec S, Caroff N, Espaze E, Giraudeau C, Drugeon H, Reynaud A. AmpC cephalosporinase hyperproduction in *Acinetobacter baumannii* clinical strains. J Antimicrob Chemother. 2003;52:629–35. doi:10.1093/jac/dkg407.

22. Corvec S, Poirel L, Naas T, Drugeon H, Nordmann P. Genetics and expression of the carbapenem-hydrolyzing oxacillinase gene *bla*$_{OXA-23}$ in *Acinetobacter baumannii*. Antimicrob Agents Chemother. 2007;51:1530–3. doi:10.1128/AAC.01132-06.

23. Héritier C, Poirel L, Nordmann P. Cephalosporinase over-expression resulting from insertion of ISAba1 in *Acinetobacter baumannii*. Clin Microbiol Infect. 2006;12:123–30. doi:10.1111/j.1469-0691.2005.01320.x.

24. Turton JF, Ward ME, Woodford N, Kaufmann ME, Pike R, Livermore DM, et al. The role of ISAba1 in expression of OXA carbapenemase genes in *Acinetobacter baumannii*. FEMS Microbiol Lett. 2006;258:72–7. doi:10.1111/j.1574-6968.2006.00195.x.

25. Schmidt H, Hensel M. Pathogenicity islands in bacterial pathogenesis. Clin Microbiol Rev. 2004;17:14–56.

26. Fournier PE, Vallenet D, Barbe V, Audic S, Ogata H, Poirel L, et al. Comparative genomics of multidrug resistance in *Acinetobacter baumannii*. PLoS Genet. 2006;2:e7. doi:10.1371/journal.pgen.0020007.

27. Di Nocera PP, Rocco F, Giannouli M, Triassi M, Zarrilli R. Genome organization of epidemic *Acinetobacter baumannii* strains. BMC Microbiol. 2011;11:224. doi:10.1186/1471-2180-11-224.

28. Sahl JW, Johnson JK, Harris AD, Phillippy AM, Hsiao WW, Thom KA, et al. Genomic comparison of multi-drug resistant invasive and colonizing *Acinetobacter baumannii* isolated from diverse human body sites reveals genomic plasticity. BMC Genomics. 2011;12:291. doi:10.1186/1471-2164-12-291.

29. Sahl JW, Gillece JD, Schupp JM, Waddell VG, Driebe EM, Engelthaler DM, et al. Evolution of a pathogen: a comparative genomics analysis identifies a genetic pathway to pathogenesis in *Acinetobacter*. PLoS One. 2013;8:e54287. doi:10.1371/journal.pone.0054287.

30. Touchon M, Cury J, Yoon EJ, Krizova L, Cerqueira GC, Murphy C, et al. The genomic diversification of the whole *Acinetobacter* genus: origins, mechanisms, and consequences. Genome Biol Evol. 2014;6:2866–82. doi:10.1093/gbe/evu225.

31. Li H, Liu F, Zhang Y, Wang X, Zhao C, Chen H, et al. Evolution of carbapenem-resistant *Acinetobacter baumannii* through whole genome sequencing and comparative genomic analysis. Antimicrob Agents Chemother. 2014. doi:10.1128/AAC.04609-14.

32. Bourque G, Pevzner PA. Genome-scale evolution: reconstructing gene orders in the ancestral species. Genome Res. 2002;12:26–36.

33. Ma J, Zhang L, Suh BB, Raney BJ, Burhans RC, Kent WJ, et al. Reconstructing contiguous regions of an ancestral genome. Genome Res. 2006;16:1557–65. doi:10.1101/gr.5383506.

34. Gagnon Y, Blanchette M, El-Mabrouk N. A flexible ancestral genome reconstruction method based on gapped adjacencies. BMC Bioinformatics. 2012;13:S4. doi:10.1186/1471-2105-13-S19-S4.

35. Fouts DE, Brinkac L, Beck E, Inman J, Sutton G. PanOCT: automated clustering of orthologs using conserved gene neighborhood for

36. Pan-genomic analysis of bacterial strains and closely related species. Nucleic Acids Res. 2012;40:e172. doi:10.1093/nar/gks757.

36. Kuo SC, Chen PC, Shiau YR, Wang HY, Lai JF, Huang W, et al. Levofloxacin-resistant *Haemophilus influenzae*, Taiwan, 2004-2010. Emerg Infect Dis. 2014;20:1386–90. doi:10.3201/eid2008.140341.

37. Adams MD, Goglin K, Molyneaux N, Hujer KM, Lavender H, Jamison JJ, et al. Comparative genome sequence analysis of multidrug-resistant *Acinetobacter baumannii*. J Bacteriol. 2008;190:8053–64. doi:10.1128/JB.00834-08.

38. Iacono M, Villa L, Fortini D, Bordoni R, Imperi F, Bonnal RJ, et al. Whole-genome pyrosequencing of an epidemic multidrug-resistant *Acinetobacter baumannii* strain belonging to the European clone II group. Antimicrob Agents Chemother. 2008;52:2616–25. doi:10.1128/AAC.01643-07.

39. Snitkin ES, Zelazny AM, Montero CI, Stock F, Mijares L, Murray PR, et al. Genome-wide recombination drives diversification of epidemic strains of *Acinetobacter baumannii*. Proc Natl Acad Sci U S A. 2011;108:13758–63. doi:10.1073/pnas.1104404108.

40. Wright MS, Haft DH, Harkins DM, Perez F, Hujer KM, Bajaksouzian S, et al. New insights into dissemination and variation of the health care-associated pathogen *Acinetobacter baumannii* from genomic analysis. MBio. 2014;5:e00963–13. doi:10.1128/mBio.00963-13.

41. Tettelin H, Riley D, Cattuto C, Medini D. Comparative genomics: the bacterial pan-genome. Curr Opin Microbiol. 2008;11:472–7.

42. Tettelin H, Masignani V, Cieslewicz MJ, Donati C, Medini D, Ward NL, et al. Genome analysis of multiple pathogenic isolates of *Streptococcus agalactiae*: implications for the microbial "pan-genome". Proc Natl Acad Sci U S A. 2005;102:13950–5. doi:10.1073/pnas.0506758102.

43. Vernikos G, Medini D, Riley DR, Tettelin H. Ten years of pan-genome analyses. Curr Opin Microbiol. 2014;23C:148–54. doi:10.1016/j.mib.2014.11.016.

44. Fouts DE, Mongodin EF, Mandrell RE, Miller WG, Rasko DA, Ravel J, et al. Major structural differences and novel potential virulence mechanisms from the genomes of multiple *Campylobacter* species. PLoS Biol. 2005;3:e15.

45. Gill SR, Fouts DE, Archer GL, Mongodin EF, Deboy RT, Ravel J, et al. Insights on evolution of virulence and resistance from the complete genome analysis of an early methicillin-resistant *Staphylococcus aureus* strain and a biofilm-producing methicillin-resistant *Staphylococcus epidermidis* strain. J Bacteriol. 2005;187:2426–38.

46. Nelson KE, Fouts DE, Mongodin EF, Ravel J, DeBoy RT, Kolonay JF, et al. Whole genome comparisons of serotype 4b and 1/2a strains of the food-borne pathogen *Listeria monocytogenes* reveal new insights into the core genome components of this species. Nucleic Acids Res. 2004;32:2386–95.

47. Chen Y, Stine OC, Badger JH, Gil AI, Nair GB, Nishibuchi M, et al. Comparative genomic analysis of *Vibrio parahaemolyticus*: serotype conversion and virulence. BMC Genomics. 2011;12:294. doi:10.1186/1471-2164-12-294.

48. Aydanian A, Tang L, Morris JG, Johnson JA, Stine OC. Genetic diversity of O-antigen biosynthesis regions in *Vibrio cholerae*. Appl Environ Microbiol. 2011;77:2247–53. doi:10.1128/AEM.01663-10.

49. Jacobsen A, Hendriksen RS, Aaresturp FM, Ussery DW, Friis C. The *Salmonella enterica* pan-genome. Microb Ecol. 2011;62:487–504. doi:10.1007/s00248-011-9880-1.

50. Rodriguez-Valera F, Ussery DW. Is the pan-genome also a pan-seletome? F1000 Res. 2012;1:16. doi:10.3410/f1000research.1-16.v1.

51. Huang H, Dong Y, Yang ZL, Luo H, Zhang X, Gao F. Complete sequence of pABTJ2, a plasmid from *Acinetobacter baumannii* MDR-TJ, carrying many phage-like elements. Genomics Proteomics Bioinformatics. 2014;12:172–7. doi:10.1016/j.gpb.2014.05.001.

52. Smith MG, Gianoulis TA, Pukatzki S, Mekalanos JJ, Ornston LN, Gerstein M, et al. New insights into *Acinetobacter baumannii* pathogenesis revealed by high-density pyrosequencing and transposon mutagenesis. Gene Dev. 2007;21:601–14. doi:10.1101/gad.1510307.

53. Segal H, Elisha BG. Characterization of the *Acinetobacter* plasmid, pRAY, and the identification of regulatory sequences upstream of an *aadB* gene cassette on this plasmid. Plasmid. 1999;42:60–6. doi:10.1006/plas.1999.1403.

54. Vallenet D, Nordmann P, Barbe V, Poirel L, Mangenot S, Bataille E, et al. Comparative analysis of Acinetobacters: three genomes for three lifestyles. PLoS One. 2008;3:e1805. doi:10.1371/journal.pone.0001805.

55. Gaddy JA, Tomaras AP, Actis LA. The *Acinetobacter baumannii* 19606 OmpA protein plays a role in biofilm formation on abiotic surfaces and in

Chan *et al. Genome Biology* (2015) 16:143

Page 27 of 28

the interaction of this pathogen with eukaryotic cells. Infect Immun. 2009;77:3150–60. doi:10.1128/IAI.00096-09.

56. Smani Y, Fabrega A, Roca I, Sanchez-Encinales V, Vila J, Pachon J. Role of OmpA in the multidrug resistance phenotype of *Acinetobacter baumannii*. Antimicrob Agents Chemother. 2014;58:1806–8. doi:10.1128/AAC.02101-13.

57. Jin JS, Kwon SO, Moon DC, Gurung M, Lee JH, Kim SI, et al. *Acinetobacter baumannii* secretes cytotoxic outer membrane protein A via outer membrane vesicles. PLoS One. 2011;6:e17027. doi:10.1371/journal.pone.0017027.

58. Schindler MK, Schutz MS, Muhlenkamp MC, Rooijakkers SH, Hallstrom T, Zipfel PF, et al. *Yersinia enterocolitica* YadA mediates complement evasion by recruitment and inactivation of C3 products. J Immunol. 2012;189:4900–8. doi:10.4049/jimmunol.1201383.

59. Troxell B, Hassan HM. Transcriptional regulation by Ferric Uptake Regulator (Fur) in pathogenic bacteria. Front Cell Infect Microbiol. 2013;3:59. doi:10.3389/fcimb.2013.00059.

60. Noinaj N, Guillier M, Barnard TJ, Buchanan SK. TonB-dependent transporters: regulation, structure, and function. Annu Rev Microbiol. 2010;64:43–60. doi:10.1146/annurev.micro.112408.134247.

61. Zimbler DL, Arivett BA, Beckett AC, Menke SM, Actis LA. Functional features of TonB energy transduction systems of *Acinetobacter baumannii*. Infect Immun. 2013;81:3382–94. doi:10.1128/IAI.00540-13.

62. Smith MG, Des Etages SG, Snyder M. Microbial synergy via an ethanol-triggered pathway. Mol Cell Biol. 2004;24:3874–84.

63. Sparnins VL, Chapman PJ, Dagley S. Bacterial degradation of 4-hydroxyphenylacetic acid and homoprotocatechuic acid. J Bacteriol. 1974;120:159–67.

64. Brevet A, Chen J, Leveque F, Blanquet S, Plateau P. Comparison of the enzymatic properties of the two *Escherichia coli* lysyl-tRNA synthetase species. J Biol Chem. 1995;270:14439–44.

65. Putzer H, Brakhage AA, Grunberg-Manago M. Independent genes for two threonyl-tRNA synthetases in *Bacillus subtilis*. J Bacteriol. 1990;172:4593–602.

66. Henkin TM, Glass BL, Grundy FJ. Analysis of the *Bacillus subtilis tyrS* gene: conservation of a regulatory sequence in multiple tRNA synthetase genes. J Bacteriol. 1992;174:1299–306.

67. Palmer T, Berks BC. The twin-arginine translocation (Tat) protein export pathway. Nat Rev Microbiol. 2012;10:483–96. doi:10.1038/nrmicro2814.

68. Krizova L, Dijkshoorn L, Nemec A. Diversity and evolution of AbaR genomic resistance islands in *Acinetobacter baumannii* strains of European clone I. Antimicrob Agents Chemother. 2011;55:3201–6. doi:10.1128/AAC.00221-11.

69. Nigro SJ, Farrugia DN, Paulsen IT, Hall RM. A novel family of genomic resistance islands, AbGRI2, contributing to aminoglycoside resistance in *Acinetobacter baumannii* isolates belonging to global clone 2. J Antimicrob Chemother. 2013;68:554–7. doi:10.1093/jac/dks459.

70. Hamidian M, Hall RM. AbaR4 replaces AbaR3 in a carbapenem-resistant *Acinetobacter baumannii* isolate belonging to global clone 1 from an Australian hospital. J Antimicrob Chemother. 2011;66:2484–91. doi:10.1093/jac/dkr356.

71. Seputiene V, Povilonis J, Suziedeliene E. Novel variants of AbaR resistance islands with a common backbone in *Acinetobacter baumannii* isolates of European clone II. Antimicrob Agents Chemother. 2012;56:1969–73. doi:10.1128/AAC.05678-11.

72. Galimand M, Sabtcheva S, Courvalin P, Lambert T. Worldwide disseminated *armA* aminoglycoside resistance methylase gene is borne by composite transposon Tn*1548*. Antimicrob Agents Chemother. 2005;49:2949–53. doi:10.1128/AAC.49.7.2949-2953.2005.

73. Diancourt L, Passet V, Nemec A, Dijkshoorn L, Brisse S. The population structure of *Acinetobacter baumannii*: expanding multiresistant clones from an ancestral susceptible genetic pool. PLoS One. 2010;5:e10034. doi:10.1371/journal.pone.0010034.

74. Domingues S, Harms K, Fricke WF, Johnsen PJ, da Silva GJ, Nielsen KM. Natural transformation facilitates transfer of transposons, integrons and gene cassettes between bacterial species. PLoS Pathog. 2012;8:e1002837. doi:10.1371/journal.ppat.1002837.

75. Tomaras AP, Dorsey CW, Edelmann RE, Actis LA. Attachment to and biofilm formation on abiotic surfaces by *Acinetobacter baumannii*: involvement of a novel chaperone-usher pili assembly system. Microbiology. 2003;149:3473–84.

76. de Breij A, Gaddy J, van der Meer J, Koning R, Koster A, van den Broek P, et al. CsuA/BABCDE-dependent pili are not involved in the adherence of *Acinetobacter baumannii* ATCC19606(T) to human airway epithelial cells and their inflammatory response. Res Microbiol. 2009;160:213–8. doi:10.1016/j.resmic.2009.01.002.

77. McQueary CN, Actis LA. *Acinetobacter baumannii* biofilms: variations among strains and correlations with other cell properties. J Microbiol. 2011;49:243–50. doi:10.1007/s12275-011-0343-7.

78. Eijkelkamp BA, Hassan KA, Paulsen IT, Brown MH. Investigation of the human pathogen *Acinetobacter baumannii* under iron limiting conditions. BMC Genomics. 2011;12:126. doi:10.1186/1471-2164-12-126.

79. Zhou H, Zhang T, Yu D, Pi B, Yang Q, Zhou J, et al. Genomic analysis of the multidrug-resistant *Acinetobacter baumannii* strain MDR-ZJ06 widely spread in China. Antimicrob Agents Chemother. 2011;55:4506–12. doi:10.1128/AAC.01134-10.

80. Dorsey CW, Tolmasky ME, Crosa JH, Actis LA. Genetic organization of an *Acinetobacter baumannii* chromosomal region harbouring genes related to siderophore biosynthesis and transport. Microbiology. 2003;149:1227–38.

81. Soto SM. Role of efflux pumps in the antibiotic resistance of bacteria embedded in a biofilm. Virulence. 2013;4:223–9. doi:10.4161/viru.23724.

82. Kaas RS, Friis C, Ussery DW, Aarestrup FM. Estimating variation within the genes and inferring the phylogeny of 186 sequenced diverse *Escherichia coli* genomes. BMC Genomics. 2012;13:577. doi:10.1186/1471-2164-13-577.

83. Utter B, Deutsch DR, Schuch R, Winer BY, Verratti K, Bishop-Lilly K, et al. Beyond the chromosome: the prevalence of unique extra-chromosomal bacteriophages with integrated virulence genes in pathogenic *Staphylococcus aureus*. PLoS One. 2014;9:e100502. doi:10.1371/journal.pone.0100502.

84. Siringan P, Connerton PL, Cummings NJ, Connerton IF. Alternative bacteriophage life cycles: the carrier state of *Campylobacter jejuni*. Open Biol. 2014;4:130200. doi:10.1098/rsob.130200.

85. Sia AK, Allred BE, Raymond KN. Siderocalins: Siderophore binding proteins evolved for primary pathogen host defense. Curr Opin Chem Biol. 2013;17:150–7. doi:10.1016/j.cbpa.2012.11.014.

86. Park JY, Kim S, Kim SM, Cha SH, Lim SK, Kim J. Complete genome sequence of multidrug-resistant *Acinetobacter baumannii* strain 1656-2, which forms sturdy biofilm. J Bacteriol. 2011;193:6393–4. doi:10.1128/JB.06109-11.

87. Huang XZ, Frye JG, Chahine MA, Cash DM, Barber MG, Babel BS, et al. Genotypic and phenotypic correlations of multidrug-resistant *Acinetobacter baumannii-A. calcoaceticus* complex strains isolated from patients at the National Naval Medical Center. J Clin Microbiol. 2010;48:4333–6. doi:10.1128/JCM.01585-10.

88. Huang XZ, Chahine MA, Frye JG, Cash DM, Lesho EP, Craft DW, et al. Molecular analysis of imipenem-resistant *Acinetobacter baumannii* isolated from US service members wounded in Iraq, 2003-2008. Epidemiol Infect. 2012;140:2302–7. doi:10.1017/S0950268811002871.

89. Myers EW, Sutton GG, Delcher AL, Dew IM, Fasulo DP, Flanigan MJ, et al. A whole-genome assembly of *Drosophila*. Science. 2000;287:2196–204.

90. Delcher AL, Phillippy A, Carlton J, Salzberg SL. Fast algorithms for large-scale genome alignment and comparison. Nucleic Acids Res. 2002;30:2478–83.

91. Zerbino DR, Birney E. Velvet: algorithms for *de novo* short read assembly using de Bruijn graphs. Genome Res. 2008;18:821–9. doi:10.1101/gr.074492.107.

92. Gladman S, Torsten S. VelvetOptimiser - a wrapper script for the Velvet assembler. http://www.vicbioinformatics.com/software.velvetoptimiser.shtml. Accessed 2015.

93. Nagarajan N, Read TD, Pop M. Scaffolding and validation of bacterial genome assemblies using optical restriction maps. Bioinformatics. 2008;24:1229–35. doi:10.1093/bioinformatics/btn102.

94. Li H. Aligning sequence reads, clone sequences and assembly contigs with BWA-MEM. 2013. http://arxiv.org/abs/1303.3997v2.

95. White Paper on CLC Read Mapping. http://www.clcbio.com/files/whitepapers/whitepaper-on-CLC-read-mapper.pdf.

96. Altschul SF, Gish W, Miller W, Myers EW, Lipman DJ. Basic local alignment search tool. J Mol Biol. 1990;215:403–10.

97. Fouts DE, Tyler HL, DeBoy RT, Daugherty S, Ren Q, Badger JH, et al. Complete genome sequence of the N_2-fixing broad host range endophyte *Klebsiella pneumoniae* 342 and virulence predictions verified in mice. PLoS Genet. 2008;4:e1000141. PMCID: PMC2453333.

98. Davidsen T, Beck E, Ganapathy A, Montgomery R, Zafar N, Yang Q, et al. The comprehensive microbial resource. Nucleic Acids Res. 2010;38:D340–5. doi:10.1093/nar/gkp912.

99. Finn RD, Clements J, Eddy SR. HMMER web server: interactive sequence similarity searching. Nucleic Acids Res. 2011;39:W29–37. doi:10.1093/nar/gkr367.

100. McArthur AG, Waglechner N, Nizam F, Yan A, Azad MA, Baylay AJ, et al. The comprehensive antibiotic resistance database. Antimicrob Agents Chemother. 2013;57:3348–57. doi:10.1128/AAC.00419-13.

101. van Hoek AH, Mevius D, Guerra B, Mullany P, Roberts AP, Aarts HJ. Acquired antibiotic resistance genes: an overview. Front Microbiol. 2011;2:203. doi:10.3389/fmicb.2011.00203.
102. Institut Pasteur: *Acinetobacter baumannii* MLST Database. http://www.pasteur.fr/recherche/genopole/PF8/mlst/Abaumannii.html. Accessed 22 Jan 2015.
103. Park J, Zhang Y, Buboltz AM, Zhang X, Schuster SC, Ahuja U, et al. Comparative genomics of the classical *Bordetella* subspecies: the evolution and exchange of virulence-associated diversity amongst closely related pathogens. BMC Genomics. 2012;13:545. doi:10.1186/1471-2164-13-545.
104. Hogg JS, Hu FZ, Janto B, Boissy R, Hayes J, Keefe R, et al. Characterization and modeling of the *Haemophilus influenzae* core and supragenomes based on the complete genomic sequences of Rd and 12 clinical nontypeable strains. Genome Biol. 2007;8:R103. doi:10.1186/gb-2007-8-6-r103.
105. Rasko DA, Rosovitz MJ, Myers GS, Mongodin EF, Fricke WF, Gajer P, et al. The pangenome structure of *Escherichia coli*: comparative genomic analysis of *E. coli* commensal and pathogenic isolates. J Bacteriol. 2008;190:6881–93. doi:10.1128/JB.00619-08.
106. Davie JJ, Earl J, de Vries SP, Ahmed A, Hu FZ, Bootsma HJ, et al. Comparative analysis and supragenome modeling of twelve *Moraxella catarrhalis* clinical isolates. BMC Genomics. 2011;12:70. doi:10.1186/1471-2164-12-70.
107. Gordienko EN, Kazanov MD, Gelfand MS. Evolution of pan-genomes of *Escherichia coli*, *Shigella* spp., and *Salmonella enterica*. J Bacteriol. 2013;195:2786–92. doi:10.1128/JB.02285-12.
108. Fouts DE. Phage_Finder: automated identification and classification of prophage regions in complete bacterial genome sequences. Nucleic Acids Res. 2006;34:5839–51.
109. Felsenstein J. PHYLIP - Phylogeny Inference Package (Version 3.2). Cladistics. 1989;5:164–6.
110. Felsenstein J. PHYLIP version 3.69. http://evolution.genetics.washington.edu/phylip.html. 2009.
111. Gardner SN, Hall BG. When whole-genome alignments just won't work: kSNP v2 software for alignment-free SNP discovery and phylogenetics of hundreds of microbial genomes. PLoS One. 2013;8:e81760. doi:10.1371/journal.pone.0081760.
112. Darling AE, Mau B, Perna NT. progressiveMauve: multiple genome alignment with gene gain, loss and rearrangement. PLoS One. 2010;5:e11147. doi:10.1371/journal.pone.0011147.
113. Stamatakis A. RAxML version 8: a tool for phylogenetic analysis and post-analysis of large phylogenies. Bioinformatics. 2014;30:1312–3. doi:10.1093/bioinformatics/btu033.
114. Struyf A, Hubert M, Rousseeuw P. Clustering in an object-oriented environment. J Stat Softw. 1997;1:1–30.
115. Saeed AI, Sharov V, White J, Li J, Liang W, Bhagabati N, et al. TM4: a free, open-source system for microarray data management and analysis. BioTechniques. 2003;34:374–8.
116. Kurtz S, Phillippy A, Delcher AL, Smoot M, Shumway M, Antonescu C, et al. Versatile and open software for comparing large genomes. Genome Biol. 2004;5:R12. doi:10.1186/gb-2004-5-2-r12.
117. Sullivan MJ, Petty NK, Beatson SA. Easyfig: a genome comparison visualizer. Bioinformatics. 2011;27:1009–10. doi:10.1093/bioinformatics/btr039.
118. PanOCT - Pan-genome Ortholog Clustering Tool. http://sourceforge.net/projects/panoct/.
119. NCBI Nucleotide database. http://www.ncbi.nlm.nih.gov/nuccore/.
120. NCBI Sequence Read Archive (SRA). http://www.ncbi.nlm.nih.gov/sra/.

Appendix II. Select differentially expressed genes in *A. baumannii* confrontations. LogFC values are only shown if the corresponding FDR was < 0.05.

Annotation	MRSN 7339 Locus ID	LogFC of *A. baumannii* confronted with:		
		E. hormaechei	*K. pneumoniae*	*C. jeikeium*
Biofilm				
pgaD.2	T634_1013	0.81		
BfmS-two-component system sensor kinase protein	T634_0792			-0.56
Type I pili				
Type I pili cluster 2.4	T634_1729			0.79
Type I pili cluster 3.4	T634_2348			-0.86
CsuA - type I pili cluster 1	T634_2492			-3.05
CsuA/B - type I pili cluster 1	T634_2493			-3.09
CsuB - type I pili cluster 1	T634_2491		1.74	-3.02
CsuC - type I pili cluster 1 - chaperone	T634_2490			-2.45
CsuD - type I pili cluster 1 - usher	T634_2489			-2.69
CsuE - type I pili cluster 1 - tip adhesion	T634_2488			-2.14
Type IV pili				
pilB - type IV pili cluster 1	T634_0406			1.19
pilC - type IV pili cluster 1	T634_0405			1.80
pilT - type IV pili cluster 2	T634_0943			1.18
pilU - type IV pili cluster 2	T634_0942			0.98
comL - type IV pili cluster 3	T634_3583			2.04
comM - type IV pili cluster 3	T634_3586			1.80
comN - type IV pili cluster 3	T634_3585			2.12
comO - type IV pili cluster 3	T634_3584			1.87
comQ - type IV pili cluster 3	T634_3582			1.94
pilZ - type IV pili cluster 4	T634_1785			0.74
pilG - type IV pili cluster 5	T634_3239			1.59
pilH - type IV pili cluster 5	T634_3238			1.14
pilI - type IV pili cluster 5	T634_3237			1.34
pilJ - type IV pili cluster 5	T634_3236	0.76	0.86	2.41
chpA-like - type IV pili cluster 5	T634_3235			2.23
A1S0232 - type IV pili cluster 6	T634_0311			0.69
Iron				
siderophore cluster 1.3 - MFS superfamily MDR protein	T634_1851			-0.65
siderophore cluster 1.11	T634_1860	1.02		
siderophore cluster 3.1 - acinetobactin-isochorismate synthase	T634_2721	1.22		-0.65
siderophore cluster 3.2 - acinetobactin - BasI	T634_2722	1.49		
siderophore cluster 3.3 - acinetobactin - thioesterase	T634_2723	1.61		
siderophore cluster 3.4 - acinetobactin	T634_2724	1.66	0.73	-0.58
siderophore cluster 3.7 - acinetobactin	T634_2725	1.72	0.71	-0.63
siderophore cluster 3.8 - acinetobactin	T634_2726	1.79		
siderophore cluster 3.9 - acinetobactin-bifunctional isochorismate lyase / aryl carrier protein	T634_2727	1.65	0.76	-0.56
siderophore cluster 3.10 - acinetobactin-enterobactin synthase subunit E	T634_2728	1.55	0.58	
siderophore cluster 3.11 - acinetobactin - BasE	T634_2729	1.73	0.64	-0.83
siderophore cluster 3.12 - acinetobactin - BasD	T634_2730	1.92	0.82	-0.54
siderophore cluster 3.13 - acinetobactin - BasC-acinetobactin siderophore biosynthesis protein	T634_2731	1.73	0.72	-0.79
siderophore cluster 3.14 - acinetobactin - BauA-ferric acinetobactin receptor	T634_2732	1.53	0.78	
siderophore cluster 3.15 - acinetobactin - BauB-ferric acinetobactin binding protein	T634_2733	1.48		
siderophore cluster 3.16 - acinetobactin - BauE-ferric acinetobactin transport system ATP-binding protein	T634_2734	1.18		
siderophore cluster 3.17 - acinetobactin - BauC-ferric acinetobactin transport system permease	T634_2735	1.21		
siderophore cluster 3.18 - acinetobactin - BauD-ferric acinetobactin transport system permease	T634_2736	1.22		
siderophore cluster 3.19 - acinetobactin - BasB-non-ribosomal peptide synthase	T634_2738	1.47	0.69	
siderophore cluster 3.20 - acinetobactin - BasA-acinetobactin biosynthesis protein	T634_2739	0.62		
siderophore cluster 3.21 - acinetobactin - BauF-acinetobactin utilization protein	T634_2741	0.64		
entA - siderophore cluster 5 - 2,3-dihydro-2,3-dihydroxybenzoate dehydrogenase	T634_1961	1.00	0.53	
TonB dependent ferrisiderophore receptor protein	T634_2182		0.64	
entB - siderophore cluster 5 - isochorismatase	T634_1962	1.01	0.67	
Heavy metals				
acr3-arsenical resistance protein	T634_1670			-1.18
czcB/A.1-cobalt–zinc–cadmium resistance	T634_3607	-0.75		
Efflux				
AdeA - efflux cluster 1	T634_2009		0.55	
AdeC - efflux cluster 1	T634_2007		0.56	
abeM.3-MATE family efflux pump	T634_3767			-0.65
adeT.2-RND family efflux pump	T634_0006	-0.67	-0.54	
K antigen				
KL2.20	T634_0109			-0.59
KL2.21	T634_0110			-0.55
beta-lactamase				
AmpC/ADC.1	T634_2715		0.55	
OXA-51.3	T634_1739			-0.79
TEM-1	T634_0270		0.88	
Cell-cell interaction				
Type VI secretion system.11	T634_1371	-2.13	-2.14	
Type VI secretion system.12	T634_1372			-1.14
Type VI secretion system.13	T634_1373			-1.11
hemin utilization				
biopolymer transport protein ExbD/TolR	T634_1146		-0.48	
Other				
class A beta-lactamase	T634_0314			-0.52
AMP-binding enzyme	T634_0689	1.40	1.54	
transporter, major facilitator family protein	T634_0763	1.12	1.87	
hypothetical protein	T634_1278		1.27	
cold shock-like protein CspE	T634_1351			1.42
universal stress family protein	T634_1403			-0.67
ABC transporter, ATP-binding protein	T634_1657	1.41	1.68	
taurine dioxygenase	T634_1659	1.10	1.67	
hypothetical protein	T634_1935		1.68	
universal stress family protein	T634_2216			-0.94
bacterial transmembrane pair family protein	T634_2308	1.11	1.65	
hypothetical protein	T634_2339		1.69	
lipocalin-like protein	T634_2472		1.05	
beta-alinine-pyruvate transaminase	T634_2517	1.17	1.76	0.84
PF04328 family protein	T634_2789		0.74	
carbon starvation protein CstA	T634_2790		0.59	
CRISPR type I-F/YPEST-associated protein Csy3	T634_2844		0.52	0.56
CRISPR-associated endonuclease Cas1, subtype I-F/YPEST	T634_2848		0.56	0.91
serine hydrolase	T634_2916		1.54	
phage protein F-like protein	T634_3147		0.91	
DNA-binding transcriptional regulator Cro	T634_3172		1.03	
hypothetical protein	T634_3179		0.78	

Appendix III. Select differentially expressed genes in *K. pneumoniae* confrontations. LogFC values are only shown if the corresponding FDR was < 0.05.

Annotation	MRSN 1319 Locus ID	LogFC of *K. pneumoniae* confronted with:		
		A. baumannii	*E. hormaechei*	*C. jeikeium*
Transporter				
ABC transporter, ATP-binding protein	T643_A0984	-1.36		
ABC transporter, permease protein	T643_A2983		-1.40	
Cell metabolism				
diacetyl reductase ((S)-acetoin forming)	T643_A2465	0.92		
cytochrome d ubiquinol oxidase, subunit II	T643_A1048	-1.07		-0.73
spermidine export protein MdtI	T643_A1929	-0.71		
pyruvate, water dikinase	T643_A2572	-1.19		
hydroxylamine reductase	T643_A1263	0.85		
Iron				
ferrienterobactin receptor	T643_A0904		-2.73	-0.95
Transcription				
DNA gyrase, A subunit	T643_A3091	-1.00		
HTH-type transcriptional regulator TdcA	T643_A2708	1.52		
Other				
PF07256 family protein	T643_A0102	2.20		
PF09209 domain protein	T643_A1131	1.38		
conserved hypothetical protein	T643_A0625	0.84		
biofilm formation regulatory protein BssS	T643_A0534	1.09		
transcriptional regulator, LuxR family	T643_A0769	1.45		
putative PQQ-like domain protein	T643_A0825	2.02		-1.74
plasmid stabilization system protein, RelE/ParE family	T643_A0921	1.13		
universal stress family protein	T643_A0955	0.82		
universal stress family protein	T643_A1096	0.81		
putative multiple stress resistance protein BhsA	T643_A1141	1.22		
universal stress family protein	T643_A1798			0.68
universal stress family protein	T643_A1952			1.62
multiple antibiotic resistance protein MarR	T643_A1998	0.81		
coenzyme PQQ biosynthesis protein A	T643_A2194	1.52		
universal stress family protein	T643_A2817	0.91		
O-antigen biosynthesis protein WbnF	T643_A2936			0.68
transcriptional regulator, LuxR family	T643_A3863	1.14		
putative multiple stress resistance protein BhsA	T643_A4136	1.81		
universal stress protein B	T643_A4389	1.06		
quaternary ammonium compound-resistance protein SugE	T643_A5092	1.08		
toxin RelE	T643_A5190	0.94		
antirestriction protein ArdA	T643_A5522	2.21		

Appendix IV. Bibliography of all publications and meeting abstracts (reverse chronological order).

Chan AP, Sutton G, DePew J, Krishnakumar R, Choi Y, Huang XZ, Beck E, Harkins DM, Kim M, Lesho EP, Nikolich, M. P., and Fouts, D. E. **A novel method of consensus pan-chromosome assembly and large-scale comparative analysis reveal the highly flexible pan-genome of *Acinetobacter baumannii.*** *Genome Biol* 2015, **16:**143.

Chan, A. P., DePew, J., Choi, Y., and **Fouts, D. E.** "An Informatics Approach to Identify *A. baumannii* Resistance Island Signatures" A poster presented at the Military Health System Research Symposium, Fort Lauderdale, FL, August 18-21, 2014.

Oliver-Kozup, H. A., DePew, J., Chan, A., Fouts, D. E. "Genomic and Transcriptomic Characterization of Multi-Drug Resistant Bacteria Associated with Combat Wound Infections" A poster presented at the 2nd Annual Host Pathogen Interactions in Biodefense and Emerging Infectious Diseases Conference, George Mason University, Manassas, VA, November 21, 2013.

Appendix V. List of personnel receiving pay.

Dr. Derrick E. Fouts, Ph.D.
Dr. Agnes P. Chan, Ph.D.
Dr. Mark Adams, Ph.D.
Dr. Karen E. Nelson, Ph.D.
Dr. Yongwook Choi, Ph.D.
Dr. Radha Krishnakumar, Ph.D.
Dr. Heaven Oliver-Kozup, Ph.D.
Jessica DePew
Maria Kim
Derek Harkins
Anthony Durkin

Appendix VI. Quad Chart.

Characterization and Expression of Drug Resistance Genes in MDRO*s Originating from Combat Wound Infections
DM110352 Final Report
W81XWH-12-2-0106

PI: Dr. Derrick E. Fouts, Ph.D. & Dr. Agnes Chan, Ph.D.   **Org:** J. Craig Venter Institute   Award Amount: $ 968,624.00

Study/Product Aim(s)

• Aim 1: Characterize the regulatory gene network of MDROs when challenged in co-culture with other bacteria.

• Aim 2: To understand the interaction of MDROs with human cells in a cell culture model.

Approach

This study uses advanced genomic and bioinformatics approaches coupled to cell culturing to identify and characterize factors that influence virulence (including antibiotic resistance, and biofilm formation) in multidrug-resistant organisms (MDROs). Deep next-generation cDNA sequencing is being used as a tool to dissect the regulatory networks altered during these organismal-level confrontations. Cell-cell challenges include: MDROs versus human microbiome organisms, MDROs versus other MDROs and MDROs versus the human host via cell culture.
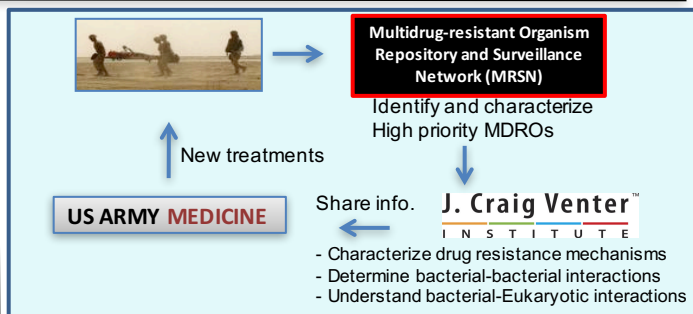
Accomplishments: 1) Manuscript published on pan-genome comparison of *A. baumannii* in Genome BIology; 2) Bacterial-Bacterial co-culture experiments are completed. Statistical analysis of RNA-seq data was performed, biological interpretation and manuscript were initiated; 3) MDRO:Human HDF cell confrontations experiments are completed. Boinformatic analysis of MDRO:Human HDF cell confrontation data has been completed.

Timeline and Cost

Activities CY	12	13	14+
1. Transcriptome profiling of MDRO-bacteria interaction			
2. Confrontation assays to monitor interaction of MDROs with human cells			
Estimated Budget ($968K)	$162K	$485K	$321K

Updated: September 9, 2016

Goals/Milestones

CY12/13 Goals – Sequence 25 MDROs from MRSN & perform bacterial-bacterial confrontation assays
☑MDRO bacterial isolate selection
☑Genomic library construction and whole genome sequencing
☑Sequence assembly and mapping
☑Genome annotation and analysis
☑Bacterial-bacterial confrontation assay
☑Bacterial RNA-Seq and gene expression analysis

CY13/14+ Goal - Perform bacterial-eukaryotic confrontation assays
☑Primary human skin cell culture
☑Bacterial-eukaryotic confrontation assay
☑Deposit raw sequence data from confrontation assays in NCBI SRA
☑Bacterial-host RNA-Seq and gene expression analysis

Comments/Challenges/Issues/Concerns
• Administrative delays noted in technical report.

Budget Expenditure to Date
Projected Expenditure: $968K
Actual Expenditure: $968K